PURIFICATION OF POLYPHENOLIC COMPOUNDS FROM CRUDE OLIVE LEAF EXTRACT

A Thesis Submitted to
the Graduate School of Engineering and Sciences of
İzmir Institute of Technology
in Partial Fulfillment of the Requirements for the Degree of

MASTER OF SCIENCE

in Chemical Engineering

by
Alihan KARAKAYA

May 2011
İZMİR

We approve the thesis of **Alihan KARAKAYA**

_____
Assoc. Prof. Dr. Oğuz BAYRAKTAR
Supervisor

_____
Assist. Prof. Dr. Ayşegül BATIGÜN
Committee Member

_____
Assist. Prof. Dr. Çağatay CEYLAN
Committee Member

22 May 2011

_____
Prof. Dr. Mehmet POLAT
Head of the Department of
Chemical Engineering

_____
Prof. Dr. Durmuş Ali DEMİR
Dean of the Graduate School of
Engineering and Sciences

ACKNOWLEDGEMENTS

This study was carried on in the Department of Chemical Engineering, Izmir Institute of Technology during the years 2009-2011.

First of all I would like to express my gratitude to my advisor Assoc. Prof. Dr. Oğuz Bayraktar for his supervision, guidance, support and encouragement during my study.

I present my deepest thanks to Ali Bora Balta for not only her friendship but also her kind efforts, help and endless support.

I also wish to thank to Evren Altıok, Hale Oğuzlu, İpek Erdoğan, Zelal Polat, Çisem Bulut, Ali Emrah Çetin, Mehmet Emin Uslu, Dilek Yalçın Tuncalı, Taner Erdoğan for their help and friendship.

Finally, my thanks go to my family for their help and encouragement during this thesis.

The technical and financial support from DÜAG Natural Compounds Research and Development Company in this study is gratefully acknowledged.

ABSTRACT

PURIFICATION OF POLYPHENOLIC COMPOUNDS FROM CRUDE OLIVE LEAF EXTRACT

Study was carried out to investigate the adsorption characteristics of olive leaf extract on the macroporous adsorption resins and the efficiency of the adsorption column for the separation and purification of oleuropein and rutin from the crude plant extract. Both static and dynamic experiments were performed.

In static studies, the performances of three macroporous Amberlite resins namely XAD4, XAD 16 and XAD7HP for the adsorption of polyphenols were evaluated. XAD7HP was chosen as an adsorbent for further adsorption study. XAD7HP was selected for the studies of isotherms, kinetics of adsorption. In conventional alcohol extraction, crude feedstock is mixed with solvent which is alcohol for most cases, and then extract is distilled to remove ethanol. This process ends with a certain amount of residual ethanol because of complication in separation process for ethanol and water makes an azeotropic binary system. The results showed that adsorption capacity of an alcoholic solution with 10 % ethanol content is better than aqueous solution which contained no ethanol.

In dynamic studies, the adsorption and desorption experiments were carried out on a glass column packed with XAD7HP resin. The flow velocity 122 cm/h operated as a fixed bed while operation was in an expanded bed mode at 367 cm/h and 611 cm/h, respectively. The effectiveness of the packed bed adsorption and the fluidized bed adsorption were compared. The results show the breakthrough occurred earlier when the feed flow velocity increased. In the elution step, elution program with 2,000 ml for 0 %, 4,000 ml for 40 % and 3,000 ml for 90 % aqueous ethanol was used to achieve an efficient separation. Total phenol content and antioxidant capacity of olive leaf crude extract and effluent fractions were analyzed in order to find the difference between before and after separation.

Consequently, fluidized bed adsorption is a promising alternative for the packed bed adsorption in order to isolate oleuropein and rutin from the olive leaf extract.

ÖZET

ZEYTİN YAPRAĞI HAM ÖZÜTÜNDEN POLİFENOLİK BİLEŞİKLERİN SAFLAŞTIRILMASI

Oleuropein ve rutin bileşikleri, zeytin yaprağı ham ekstraktından adsorpsiyon yöntemiyle ayrılarak ve saflaştırıldı. Bu amaçla makroporoz adsorbsiyon reçinesinin zeytin ekstraktı adsorplama özellikleri ve adsorpsiyon kolonunun verimi incelendi. Deneyler statik ve dinamik ortamda gerçekleştirildi.

Statik adsorpsiyon çalışmasında üç farklı makroporoz Amberlit reçinesi olan XAD4, XAD 16 ve XAD7HP'ün polifenol adsorplama kapasiteleri araştırıldı. Sonraki çalışmalar için XAD7HP'nin kullanılmasına karar verildi. XAD7HP ile yapılan deneylerde izotermler belirlendi ve adsorpsiyon kinetiği çalışıldı. Alkol ekstraksiyonu ile elde edilen ham özütte, su ve alkol karışımı azeotrop oluşturduğu için ayırma işleminde karşılaşılan güçlükler nedeniyle bir miktar alkol kalıntısının kaldığı gözlendi. Deneyler sonucunda 10% alkol içeren özüt çözeltilerinin adsorpsiyon kapasitelerinin, alkol içermeyen sulu özüt çözeltilerinden yüksek olduğu saptandı.

Dinamik adsorpsiyon çalışmasında XAD7HP dolgulu bir cam yatak kolon hazırlanarak, adsorpsiyon ve desorpsiyon deneyleri gerçekleştirildi. 122 cm/sa'lik hızda kolon sabit yatak özelliği gösterirken, 367 cm/sa ve 611 cm/sa hızlarında akışkan yatak özelliği gözlendi. Sabit ve akışkan yatak işlemlerinde adsorpsiyon kapasiteleri ölçülerek karşılaştırıldı. Sisteme beslenen akışın hızı arttıkça adsorpsiyon eşik değerine daha erken ulaşıldığı gözlendi. Yıkama aşamasında sırasıyla 2.000 ml için 0%, 4.000 ml için 40% ve 3.000 ml için 90% su içinde alkol çözeltileri kullanılarak, etkin bir yıkama sağlandı. Ham zeytin ekstraktında bulunan toplam fenol miktarı, antioksidan kapasitesi ve fraksiyonları belirlenerek, ayırma işleminin verimi hesaplandı.

Sonuç olarak, zeytin yaprağı ektraktından oleuropein ve rutin ayırma işlemi için akışkan yatak adsorpsiyonu, etkili bir dolgulu yatak uygulaması olarak önerildi.

TABLE OF CONTENTS

LIST OF FIGURES

Figure **Page**

LIST OF TABLES

LIST OF ABBREVIATIONS

$ABTS^+$	2,2'-Azinobis 3-Ethylbenzothiazoline-6-Sulphonic Acid
BHA	Butylated hydroxyanisole
BHT	Butylated hydroxytoluene
C	Concentration (mg/mL)
C_e	Concentration of solute in solution at equilibrium (mg/mL)
C_t	Solute concentration at instant time t (mg/mL)
C_i	Initial concentration (mg/mL)
F-C	Folic-Ciocalteu
GAE	Gallic acid equivalent
HPLC	High Performance Liquid Chromotography
K_d	Langmuir constants (mg/mL)
nm	Nanometer
Q_e	Adsorption capacity at equilibrium (mg/g)
Q_m	maximum adsorption capacity (mg/g)
Q	Adsorbed amount on adsorbent,
S/L	Solid-liquid ratio
TEAC	Trolox equivalent antioxidant capacity
G_a	Gallileo number
H_0	Initial bed height (cm)
Hexp	Expanded bed height (cm)
Re_t	Terminal Reynolds number
$U_{t\text{-stoke}}$	Terminal velocity of a single adsorbent particle calculated by the Stokes' law (cm/h)
d_c	Column diameter (m)
d_p	Mean diameter of the adsorbent beads (m)
n	Richardson–Zakai parameter
u	Superficial liquid velocity (cm/h)
u_t	Terminal velocity of a single adsorbent particle in a volume of stagnant liquid (cm/h)

CHAPTER 1

INTRODUCTION

Phytochemicals are non-nutritive plant chemicals that have preventive or disease protective properties. They are nonessential nutrients, meaning that they are not required by the human body for sustaining life. Clinical studies prove that the active components of plant polyphenols, which have been used to treat many important diseases for centuries. The components are known as secondary metabolites and have higher anti-oxidative, antimicrobial, antiviral, anti-inflammatory, and anti-carcinogenic effects (Omar, 2010).

Polyphenols show a complex class of phytochemicals that they include flavonoids such as rutin, oleuropein, aglycon quercetin, verbascoside, teupolioside, isoflavonoids, coumarins, and lignanes. These substances behave as potent antioxidants by direct scavenging of reactive oxygen and nitrogen species and by acting as chain-breaking peroxyl radical scavengers. Antioxidants prevent the oxidative damage to biomolecules such as DNA, lipids and proteins that cause cancer and cardiovascular diseases (Yang et al., 2009; Russo et al., 2010).

Olive leaf is one of the potent plant polyphenols having anti-oxidative, antimicrobial, anti-inflammatory and antiviral properties due to its components. The mostly abundant and bioactive components of olive leaf are oleuropein and rutin. In order to use these components effectively in the industry, they should be recovered from the olive leaf (Lee and Lee, 2010; Visioli et al., 2002).

Olive leaves are abundant in polyphenols, especially in oleuropein, rutin, verbacoside, apigenin-7-glucoside and luteolin-7-glucoside (Altiok et al., 2008; Baycin et al., 2007; Garcia et al., 2000). Recent studies indicated that olive leaf extract has anti-HIV activity effect (Zhao et al., 2009; Omar, 2010), antioxidant, antimicrobial (Lee and Lee, 2010), anti-inflammatory (Süntar et al., 2010; Kim et al., 2010). Oleuropein is the major phenolic compound in olive leaves, which has been used for diseases. Besides, rutin is one of the most bioactive flavonoids and the second abundant component in olive leaves (Garcia et al., 2000).

The aim of this study was to selectively isolate biologically active compounds from olive leaves. After obtaining the highest yields in extraction (Altiok et al., 2008; Baycin et al., 2007), adsorption studies were performed using XAD7HP. Main phenolic compounds in these extracts were determined by HPLC analysis. Both static and dynamic experiments were carried out, as well as the design of adsorption column for separating and purifying active components of the crude plant material. Besides, the efficiency of the adsorption column for separation and purification were investigated.

In static experiments, the effects of the resin structures and different initial olive leaf extract concentration and initial alcohol content on adsorption performance were investigated. In addition, adsorption isotherms and kinetics were also investigated.

In dynamic experiments, the effects of operating parameters such as feed concentration on the adsorption performance of the column were determined. Besides, a proper step-gradient elution program was developed to achieve an efficient separation.

CHAPTER 2

LITERATURE REVIEW

2.1. Free Radicals

Unstable atom or molecules with unpaired electrons are called free radicals; these unpaired electrons tend to be highly reactive, resulting in chemical reactions such as oxidation. Oxidative metabolism is important for the well being of the cells in living organisms. If it does not work well, the radicals may have side effects (Shilin, 2010). Free radicals are naturally occurring; however, air pollution, stress, smoking, alcohol, radiation, light, heavy exercising and aging all contribute to the creation of harmful free radicals in the body. Environmental influences that can contribute to the formation of free radicals include UV radiation, smoking, pollution and diet (Halliwell, 2009; Stahl 2010). Figure 2.1 shows how formations of free radicals occur.

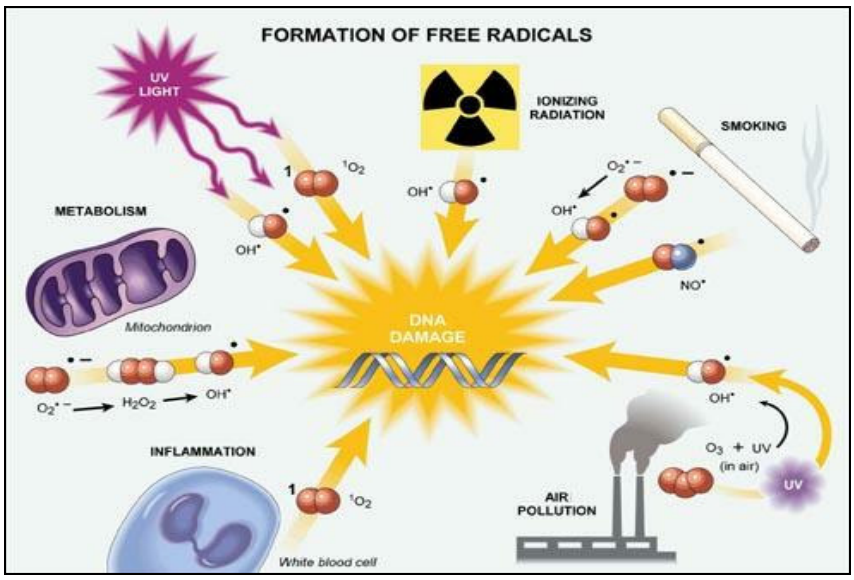

Figure 2.1. Formation of free radicals
(Source: healthfruit, 2011).

Free radicals can cause oxidative damage to the body, potentially leading to serious health problems. Normally the body is able to protect itself from the damaging effects of free radicals, but if antioxidants are unavailable in the medium, or if free radical production becomes excessive, damage can occur. They oxidize membrane lipids, cellular proteins, DNA, enzymes and prevent the cellular respiration (Shılın, 2010; Wiseman and Halliwell, 1996).

On the other hand, various free radicals are generated by aerobic metabolism and they are necessary to sustain life. Our immune system needs free radicals to fight invading bacteria and viruses. In biological system, the main free radicals or precursors of free radicals include reactive oxygen species (ROS) such as singlet oxygen (O_2), superoxide ($O_2^{\bullet -}$), peroxide(O_2^{2-}), hydrogen peroxide (H_2O_2), hydroxyl radical (HO•), and reactive nitrogen species (RNS) (Ahmad et al., 2010; Halliwell, 2011). They are generally built by ionizing radiation, reduction of oxygen molecule, reactive metals, enzymes and other endogenous and environmental initiators. Superoxide and hydroxyl radicals are the most common radicals existing in the human body (Halliwell, 2009; Halliwell, 2011). A superoxide radical is created when one electron is added to an oxygen molecule. This free radical can be made by accident in the body involving the different reactions with oxygen, or it can be made deliberately by phagocytes which are cells in the blood that are capable of destroying bacteria. The hydroxyl radical may be the most reactive oxygen radical known in chemistry. It can be formed when water is exposed to X-rays, or when a reduced metal catalyses the breaking of the oxygen bond of hydrogen peroxide. The hydroxyl radical attacks all biological molecules as soon as it comes into contact with them. Peroxynitrite (ONOO-) is reactive nitrogen species formed at sites of inflammation by the rapid reaction of superoxide with nitrogen monoxide. It is a highly oxidizing species capable of damaging lipids, protein, carbohydrate and DNA (Halliwell, 2009). Despite the fact that the immune system needs free radicals to fight penetrating bacteria and viruses, excess amounts of free radicals are harmful since their reactivity. Radicals can damage lipids, proteins, and DNA (Pietta, 2000; Chandrasekara and Shahıdı, 2011; Halliwell, 2009) and by doing so, they change biochemical compounds, damage cell membrane and kill cells completely. Many researches suggest that they play a major role in the development of many diseases, like cancer, cataracts, heart diseases and aging in general (Lua and Finkel, 2008). Increased levels of oxidative damage to DNA, proteins and lipids have been detected, using a wide range of biomarkers, in post-mortem central nervous system

(CNS) tissue sampled from patients who died with Alzheimer's disease, Parkinson's disease (Seet et al., 2010; Smith et al., 2010). Although all cells have some ability of repairing oxidative damage to proteins and DNA, they are not able to deal with excess damage.

Antioxidants are capable of neutralizing some of the free radicals that are generated internally in mitochondria. Antioxidants are largely found in nature especially in plants. Free radicals may react with other free radicals and lose their capability to initiate further reactions; the free radical can also be terminated by antioxidants, scavengers and enzymes. Figure 2.2. demonstrates in what ways free radicals may react within living metabolisms.

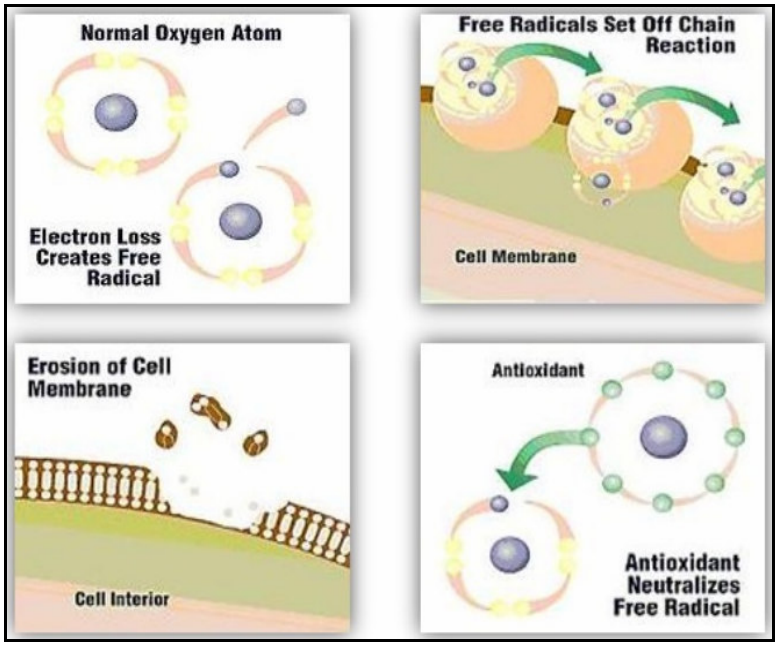

Figure 2.2. Reactions initiated by free radicals in living organisms
(Source: Antioxidants-Health-Guide, 2011).

The other way for the production of new radicals (hydroperoxides and different peroxidases) is the interplay of oxygen free radicals with lipid molecules and molecules alike. They can influence biological systems and have cytotoxic, mutagenic, carcinogenic, atheragenic and antitoxic effects (Benavente-Garcia et al., 2000; Xin et al., 2010).

The direct reaction of a lipid molecule with a molecule of oxygen, referred as autoxidation, is a chain reaction initiated by free-radicals. The mechanism of

autoxidation can be classified in three main steps: initiation, propagation, and termination (Madhavi, 1996).

Unsaturated lipid contact with oxygen and free radicals are formed as a result of the initiation process. Substrate molecule (LH) reacts with the oxidizing radical ($R^{\bullet}$), this process creates reactive allyl radical ($L^{\bullet}$), which can interact with oxygen to create lipid peroxyl radical ($LOO^{\bullet}$). Peroxyl radicals are the chain carriers of the reaction and they can break down into various compounds (alcohols, aldehydes, alkyl formates, ketones).

During propagation, branching may also occur which includes breakdown of a lipid hydro peroxides and can also have transition metal ion catalysis to create peroxyl and lipid alkoxyl radicals. Radicals interact with one another to form non-radical products, when there is a reduction in the fatty acids. This is called termination reaction (Madhavi, 1996; Antolovich and Prenzler, 2002). Mechanisms of those reactions are as follows:

Initiation Reaction:

$$LH + R^{\bullet} \rightarrow L^{\bullet} + RH \quad (2.1)$$

Propagation Reaction:

$$L^{\bullet} + O_2 \rightarrow LOO^{\bullet} \quad (2.2)$$

$$LOO^{\bullet} + LH \rightarrow L^{\bullet} + LOOH \quad (2.3)$$

Branching:

$$LOOH \rightarrow LO^{\bullet} + HO^{\bullet} \quad (2.4)$$

$$2LOOH \rightarrow LOO^{\bullet} + LO^{\bullet} + H_2O \quad (2.5)$$

$$LOOH + M^{n+} + H^{+} \rightarrow LO^{\bullet} + M^{(n+1)+} + H_2O \quad (2.6)$$

$$LOOH + M^{(n+1)+} + OH^- \rightarrow LOO^{\bullet} + M^{n+} + H_2O \quad (2.7)$$

Termination Reaction:

$$\left.\begin{array}{ll} LO^{\bullet} + LO^{\bullet} \rightarrow & (2.8) \\ LOO^{\bullet} + LOO^{\bullet} \rightarrow & (2.9) \\ LO^{\bullet} + LOO^{\bullet} \rightarrow & (2.10) \end{array}\right\} \text{non-radical products}$$

2.2. Phytochemicals

Phytochemicals are non-nutritive plant chemicals that have preventive or protective properties. They are nonessential nutrients, meaning that they are not required by the human body for sustaining life. The word phytochemicals is derived from the Greek word phyto, which means plant (Lui, 2004; Sharma et al., 2011). Plants produce these chemicals to protect themselves but several recent studies show that phytochemicals prevent many undesirable health conditions, like cancer, heart disease, diabetes, and high blood pressure. Fruits and vegetables are important for a healthy and well balanced diet required for a healthy living. Besides their useful characteristics, most fruits and vegetables are excellent sources of fibre, starch, vitamins and minerals. These protective effects are generally considered to be related to the various phytonutrients, especially antioxidants contained in such products.

Antioxidants are compounds that are proved to reduce free radical activity. They protect the components of cells and bio molecules from oxidation by scavenging an electron from reactive oxygen species (ROS) such as superoxide, peroxy and hydroxyl radicals.Many recent studies reported that people can reduce the risk for cancer and cardiovascular diseases significantly by eating more fruits, vegetables, and other foods from plants that contain phytochemicals (Yang et al., 2009; Russo et al., 2010; Tung and Chang, 2010; Subhashini et al., 2010).

Fruits and vegetables consist of several classes of compounds which can contribute to antioxidant activity. Most of the plant extracts exhibit some antioxidant properties. L-ascorbic acid (vitamin C) is one of the most widely studied antioxidant that can be taken from fruits and vegetables. L-Ascorbic acid has many biological

functions, which include the synthesis of collagen, some hormones and certain neurotransmitters. It is known that the role of L-ascorbic acid in disease prevention is due to its ability to scavenge free radicals in the biological systems. Cancer is a kind of disease where a cell or cells display uncontrolled growth, invasion and sometimes metastasis. It may be initiated by oxidative reactivity of free radicals or their damage to DNA and cells. L-ascorbic acid may act as an effective antioxidant and is able to slow down or prevent such a damage (Hsieh and Wu, 2009; Telang et al., 2007; Michels et al., 2010).

Carotenoids, another big family of compounds with antioxidant activities, are the most common and most important natural pigments in fruits and vegetables. They are responsible for many of the red, orange, and yellow hues of plant leaves, fruits, and flowers. Only about 50 of the approximately 600 carotenoids are identified to have provitamin A activity. The most widely studied carotenoid is β-carotene. Others, however, like lycopene, lutein, and zeaxantin, may offer health protection equal to or better than β-carotene (Rao and Rao, 2007; Voutilainen et al., 2006; Rodriguez-Amaya, 2010).

A large body of the study supports that one of the most important antioxidants in fruits and vegetables might be phenolic compounds. Because of their redox properties, phenolic compounds exhibit strong antioxidant activity. Besides antioxidant properties, phenolic compounds have some biological effects, such as antibacterial, antiviral and antithrombotic activity (Vaquero et al., 2010; Ho et al., 2010).

There are more than thousand known phytochemicals. Phytochemicals can be classified as carotenoids, phenolics, alkaloids, nitrogen-containing compounds, and organosulfur compounds. The most studied of the phytochemicals are the phenolics and carotenoids (Lui, 2004). These groups have several subgroups and these are showed in Figure 2.3.

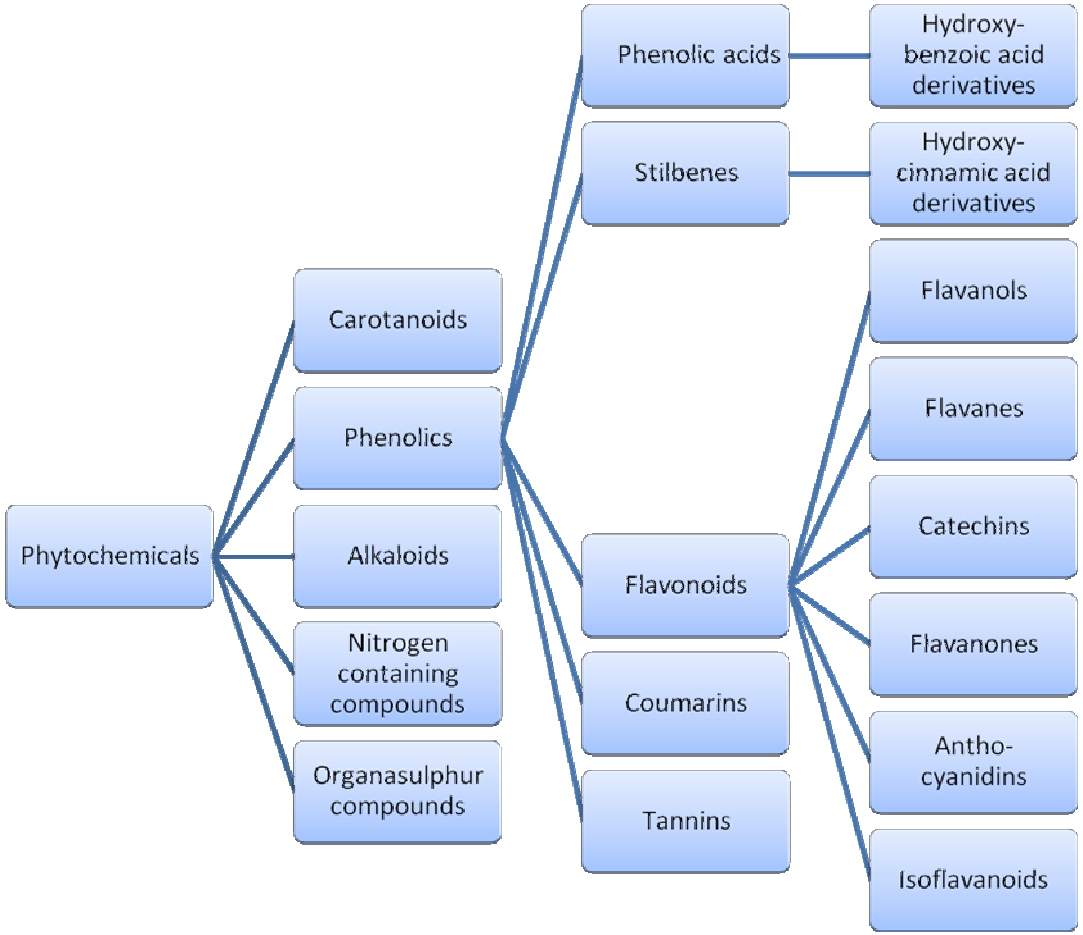

Figure 2.3. Phytochemical groups
(Source: Liu, 2004).

2.3. Classification Antioxidants Based on Their Sources

Antioxidants can be classified into two classes as natural or synthetic antioxidants. Natural antioxidants are extracted from plant and animal sources while synthetic antioxidants are prepared synthetically.

2.3.1. Natural Antioxidants

Natural antioxidants like tocopherols and ascorbic acid can behave as primary antioxidants and are efficient radical scavengers, other natural antioxidants such as thiols, sulfides, free amino groups of proteins, carotenoids act as secondary antioxidants (Svilaas et al., 2004). Primary Antioxidants, mostly acting as chain-breaking antioxidants, react rapidly with peroxy radicals (ROO*). Secondary Antioxidants,reacting with hydroperoxides (ROOH) to yield non-radical, non-reactive products, are generally named hydroperoxide decomposers (SpecialChem, 2011). Organic acids may work as chelating agents by binding metal atoms and prevent them from initiating radicals; citric acid and phytic acid are two examples that are both naturally and synthetically available (Mahoney and Graf, 1986). Table 2.1.summarize the some natural antioxidants and sources.

Table 2.1. Some natural antioxidants and sources
(Source: Pokorny, 1991).

Natural antioxidants	**Sources**
Tocopherols, Tocotrienols,Sesamol, Phospholipids, Olive oil resins	Oils and Seeds
Several lignin-derived compounds	Oats and Rice bran
Ascorbic acid, Hydroxycarboxylic acids, Flavonoids, Carotenoids	Fruits and Vegetables
Phenolic compounds	Spices, Herbs, Tea, Cocoa
Amino acids, Dihydropyridines, Maillard reaction products.	Proteins and Protein hydrolysates
Catechin, Epicatechin, Myricetin, Quercetin, Kaempferol	Teas

The chemical structures of tocopherols, vitamin C, citric and phytic acid are shown in Figure 2.4. (Rajalakshmi and Narasimhan, 1996).

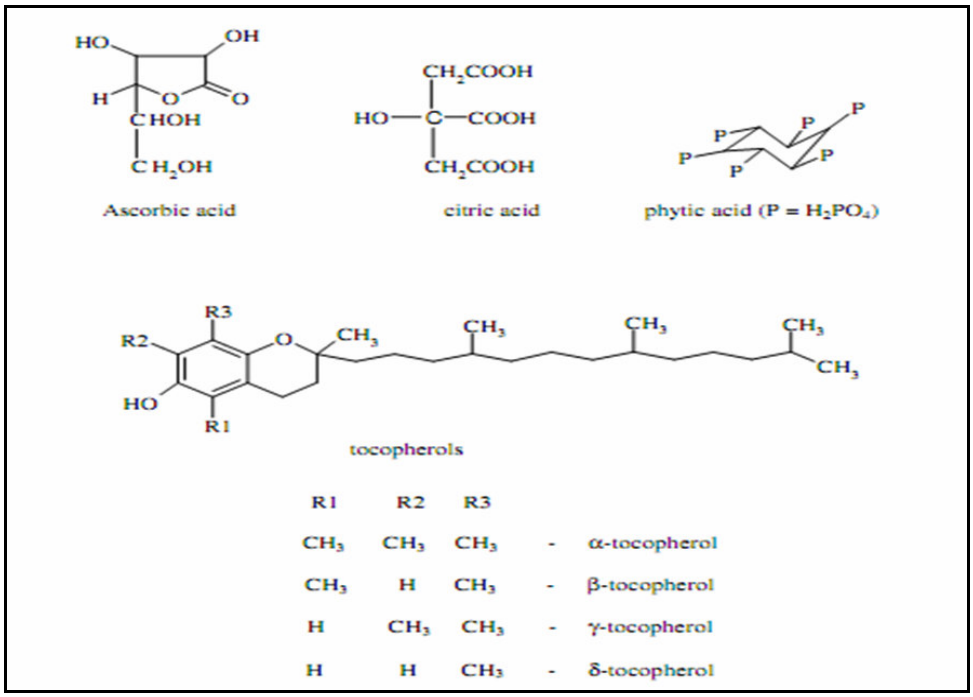

Figure 2.4. The chemical structures of tocopherols, vitamin C, citric and phytic acid

2.3.2. Synthetic Antioxidants

Synthetic antioxidants are prepared synthetically in the laboratory. They are mostly phenolic compounds. Hence the mechanism of their reaction with radicals is similar as that of phenolic antioxidant compounds, i.e. they behave as chain breaking antioxidants and include transfer of a hydrogen atom or an electron to radicals. Antioxidants of this category such as butylated hydroxyanisole (BHA) and butylated hydroxytoluene (BHT) stabilize by delocalization of electrons after the donation of a hydrogen atom .

Many synthetic antioxidants are accepted to be safe and used as food additives to prevent oxidative destruction and increase shelf life. Figure 2.5. shows

some of synthetic antioxidants which are butylated hydroxyanisole, butylated hydroxytoluene, and tert-butyl hydroquinone (Rajalakshmi and Narasimhan, 1996).

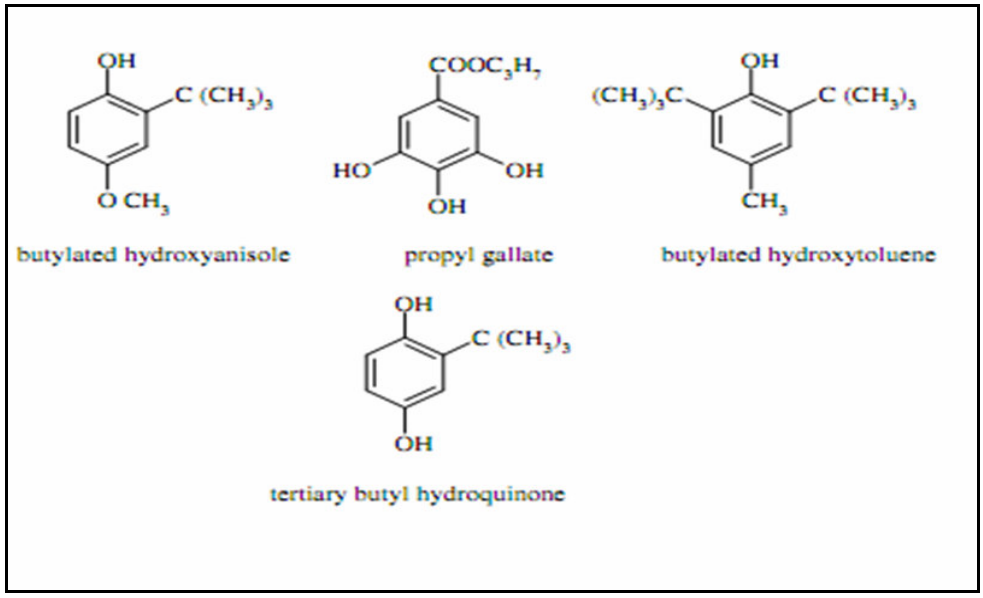

Figure 2.5. Some of synthetic antioxidants

2.4. Antioxidant Properties of Plant Phenolics

Polyphenolic compounds are one of the most paramount groups of natural antioxidants. Polyphenols contain more than one aromatic ring with each containing one or more hydroxyl group (Lazarus et al., 2001; Farrazzano et al., 2009). On the other hand, phenols made up of one aromatic ring, which has at least one hydroxyl group. Hydroxyl groups displays 'acidic' characteristics, this makes phenolic compounds excellent antioxidants due to the electron donating activity of the 'acidic' phenolic hydroxyl group (Simirnoff, 2005). Flavonoids are one of the most copious groups in polyphenols. The groups of flavonoids are presented subsequently;

Flavonoids: Most plants have flavonoids which are polyphenolic compounds. Flavonoids have C_6 - C_3 - C_6 form which contains of 15 carbon atoms arranged in three rings (Pietta, 2000). The main chemical structure is displayed in Figure 2.6.

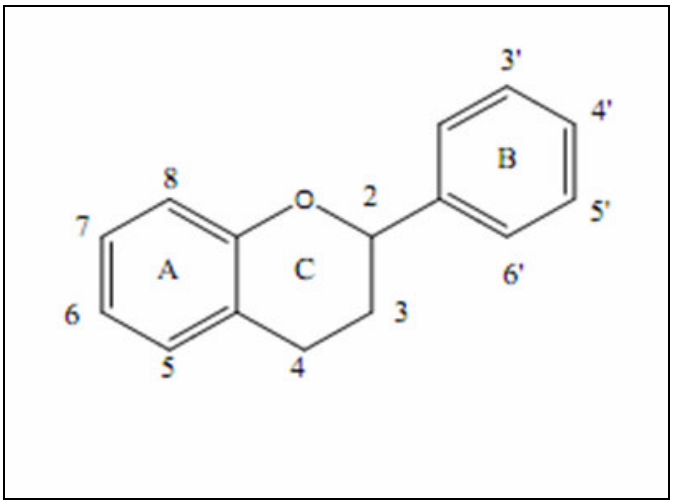

Figure 2.6. The basic chemical structure of Flavonoids.

Flavonoids can be organized into several subgroups among other things, flavones, flavanones, isoflavones, flavonols, flavanols, and anthocyanins (Rice-Evans et al., 1997). 3, 4-dihydroxychalcones such as okanin , butein , flanones such as isovitexin, luteolin , anthocyanins such as malvidin-3-glucoside , cyanidin-3-glucoside, isoflavones such as genistein, daidzein , dihydroflavonols dihydroquercetin, flavonols gossypetin, cinnamic acids, ferulic acid, caffeic acid, procyanidine B-1 are examples of natural antioxidants belonging to flavonoids (Hodgson and Croft, 2010). Table 2.2 presents subgroups of flavonoids in food sources.

Table 2.2. Subclasses of flavonoids in food sources

Flavonoids Subgroups	Major Flavonoids	Fruits/Vegetables
Flavones	Apigenin, Luteolin, Tangeretin, Nobiletin	Beets, Bell peppers, Brussels sprouts, Cabbage, Cauliflower, Celery, Chives, Kale, Lettuces, Spinach, Peppers, Tomatoes, Watercress, Citrus fruits
Flavonols	Quercetin, Kaempferol, Myricetin	Apples, Berries, Broccoli, Cabbages, Chives, Cranberries, Grapes, Kale, Onions, Peppers, Spinach, Swiss chard, Tomatoes, Watercress
Flavanones	Naringenin, Hesperetin	Oranges and Other Citrus fruits
Flavanonols	Taxifolin	Citrus fruits
Anthocyanidins	Cyanidin, Delphinidin, Malvidin, Pelargonidin, Peonidin, Petunidin	Blueberries, Blackberries, Cranberries, Egg plants, Pomegranates, Plums, Raspberries, Red onions, Red potatoes, Red grapes, Red radishes, Strawberries, Other Red-purple fruits and vegetables
Flavanols/Procyanidins	Catechin, Epicatechin, and Their Gallic Acid Esters, Monomers, Dimers (Procyanidin B1, B2), and Oligomers	Apples, Cherries, Berries, Grapes,
Chalcones	Xanthohumol, Phloretin	Hops, Apple
Isoflavonolids	Daidzein, Genistein	Soybean Sprouts

Flavanols: Flavan-3-ol is the most abundant type of flavanols. It has an –OH group connected to the 3 position of the elemental flavan skeleton. Catechin is the most prevalent flavan-3-ol which contained in green tea, cocoa powder, red wine and other herbs. Epicatechin is distinct from catechin in terms of spatial orientation of its –OH group (Crozier et al., 2010). Figure 2.7 exhibits fundamental chemical structure.

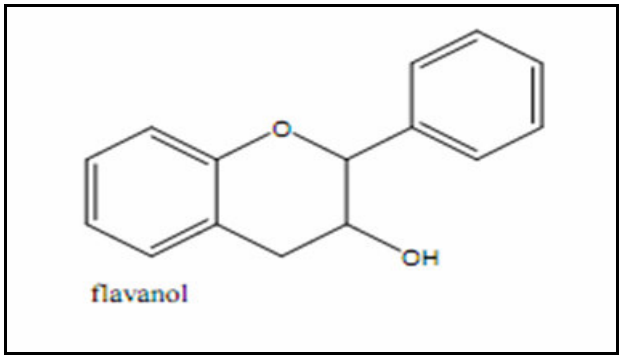

Figure 2.7. The basic chemical structure of Flavanols

Flavonols: The elementary flavonol skeleton has the –OH at position 3 and the =O at position 4. It is also different from the flavanols by containing a double bond between carbons 2 and 3 on the C ring. The most prominent flavonol, quercetin, found in many of herbs and foods such as onions (Dixon and Pasinetti, 2010). Figure 2.8 shows basic chemical structure.

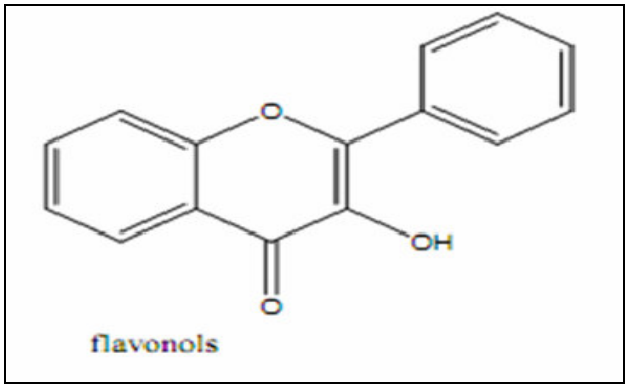

Figure 2.8. The basic chemical structure of Flavonols

Isoflavones: Isoflavones stands for the isomer of flavones. Isoflavones differs from flavones by having position of B ring attachment to C ring; the connection is at the 3 position of C ring instead of the usual 2 position on the flavones. High amount of isoflavones such as daidzein and genistein could be found in soy and other legumes (Dixon and Pasinetti, 2010).

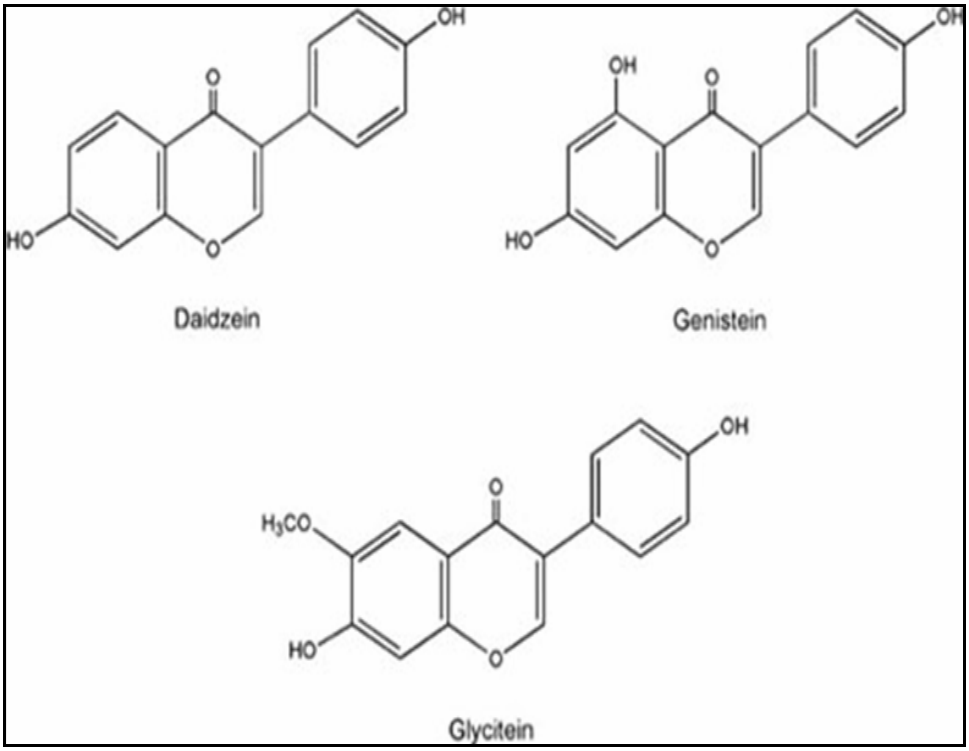

Figure 2.9. Some of the Isoflavones for example daidzein, genistein and glycitein

Anthocyanidins and anthocyanins: They are usually found in fruits and vegetables. They are the pigments that give dark red, blue and purple colours to the plants. Anthocyanins include a sugar molecule at position 3. Also other positions can be glycosylated. Figure 2.10 shows basic chemical structure of anthocyanidins and anthocyanins (Crozier et al., 2010).

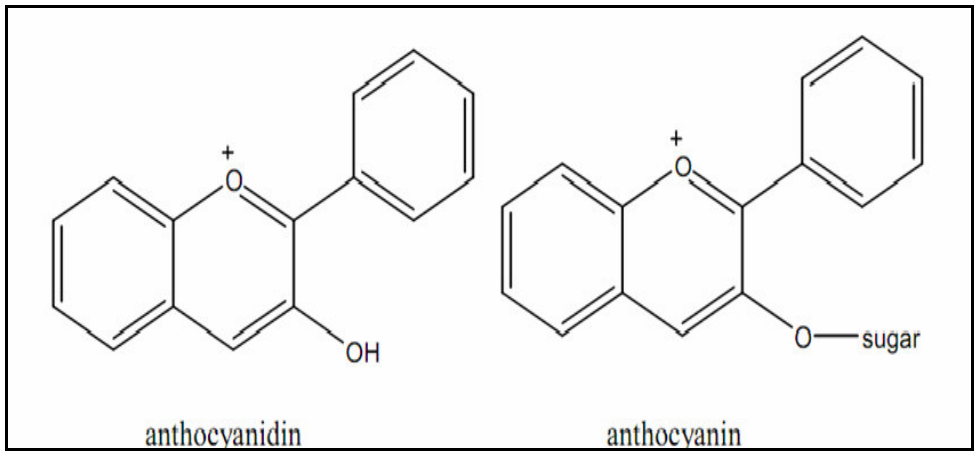

Figure 2.10. The basic chemical structure of anthocyanidins and anthocyanins

Proanthocyanidins or condensed tannins: These molecules also known as catechins. They consist of polymers made from multiple flavanols, which can have two to ten or more subunits. Proanthocyanidins will break into cyaniding, under acid hydrolysis. Oligomeric proanthocyanidins are water-soluble short chain polymers. Their main responsibility is astringency in many fruits (grape skins, blueberries) and other dark colored plant parts. Red wine also has high content of proanthocyanidins (Sharma et al., 2011). The basic chemical structure of proanthocyanidins is given in Figure 2.11.

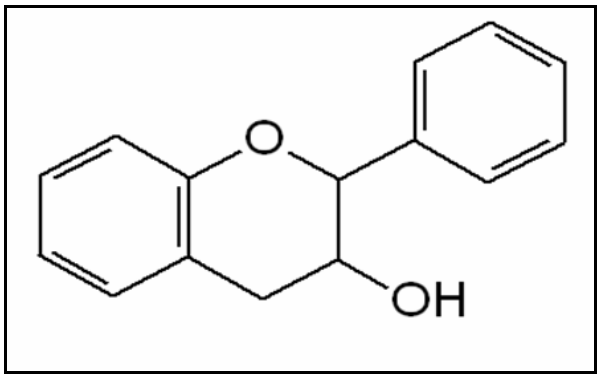

Figure 2.11. The basic chemical structure of proanthocyanidins

2.5. Olive Leaf and Its Characteristic Properties

Olive tree (*Olea europaea* L.) is one of the most important fruit trees in Mediterranean countries, covering ~8 million hectares in the world (Erbay and Icier, 2009). Olive tree (*Olea europaea*) is an evergreen tree that can reach 8-15 m in height. Archaeological evidence presents olive trees back to 6000 bc (Ryan and Robards, 1998). It has been known that olive is beneficial for health for centuries, especially in the Mediterranean region. Olives and olive leaves historically have been used as a folk remedy for many diseases and several study have shown that olive leaf has been used the capacity to lower blood pressure in animals and increase blood flow in the coronary arteries, relieving arrhythmia and preventing intestinal muscle spasms (Lee and Lee, 2010; El and Karakaya, 2009).

Several studies have shown the importance of olives and olive oil. However there have been few studies related to olive leaves. Olive leaf extract contain five major groups of compounds. These are oleuropeosides; flavones; flavonols; flavan-3-ols and substituted phenols. Table 2.3. demonstrates the phenolic groups of Olive Leaf Extract and chemical structures of the most abundant phenolics in olive leaf extract (Benavente-Garcia et al., 2000; El and Karakaya, 2009).

Table 2.3. The phenolic groups of Olive Leaf extract
(Source: Benavente- Garcia et al., 2000)

Group	Examples
Oleuropeosides	Oleuropein, Verbascoside
Flavones	Luteolin-7-glucoside, Apigenin-7-glucoside, Diosmetin-7- glucoside, Luteolin, Diosmetin
Flavonols	Rutin
Flavan-3-ols	Catechin
Substituted Phenols	Tyrosol, Hydroxytyrosol, Vanilin, Vanillic acid, Caffeic acid

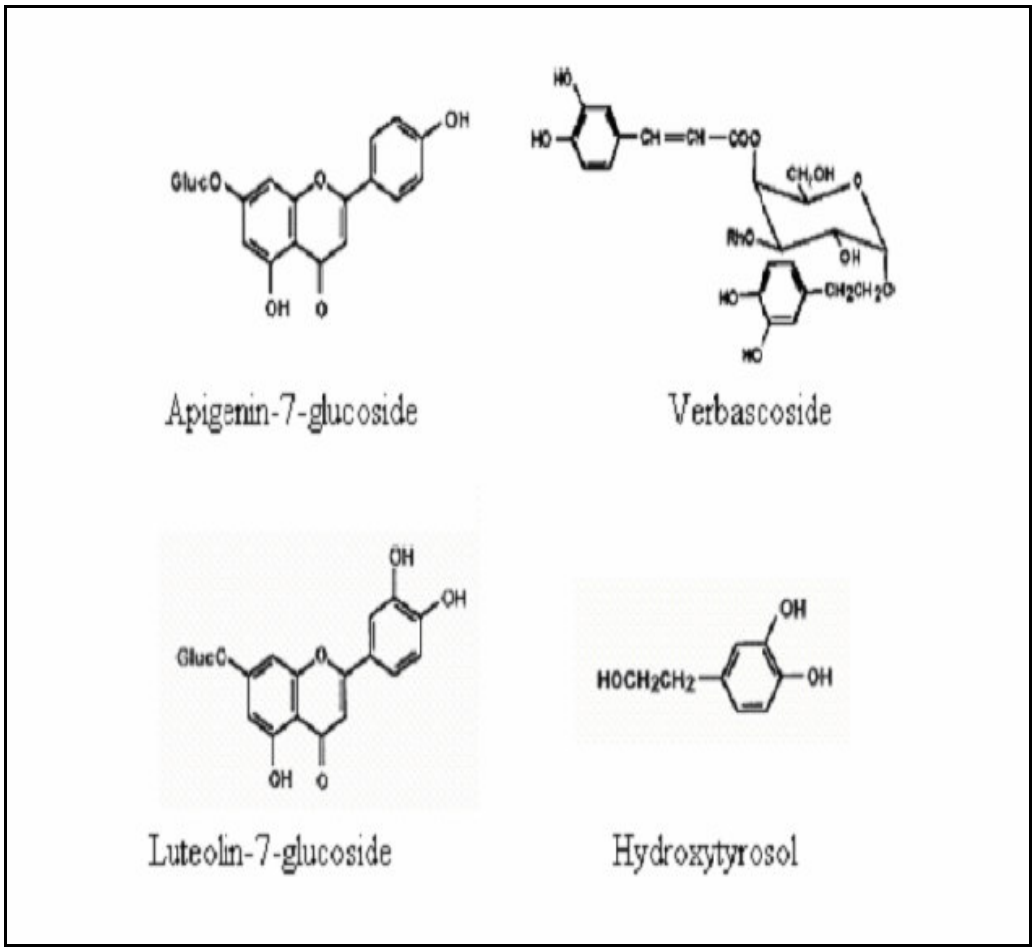

Figure 2.12. The chemical structures of the most abundant phenolics in olive leaf extract (Source: Benavente-Garcia et al., 2000).

Garcia et al. (2000) reported the sequence of the antioxidant capacity of the flavanoids in olive leaf extract as; rutin > catechin ≈ luteolin > OL ≈ hydroxytyrosol > diosmetin > caffeic acid > verbascoside > oleuropein > luteolin-7-glucoside ≈ vanillic acid ≈ diosmetin-7- glucoside > apigenin-7-glucoside > tyrosol > vanillin.

The high antioxidant capacity of rutin, catechin and luteolin exhibit the significance of the flavonoid B-ring catechol structure (rutin, catechin, luteolin); the 3- hydroxyl free or glycosylated group (catechin and rutin); and the 2,3-double bond conjugated with a 4-oxo function (rutin and luteolin). Its antioxidant activity is more or less the same to rutin and luteolin which confirms the importance of flavonoid B-ring structure of catechol and the existence of a free 3-hydroxyl group even though the 2,3- double bond conjugated with a 4-oxo function is absent in catechin. Antioxidant activity of oleuropein is mainly due to the hydroxytyrosol moiety in its structure. However, owing to the fact that its high molecular weight, its antioxidant

capacity is lower than the hydroxytyrosol (Benavente-Garcia et al., 2000).

Olive leaf extract has a remarkable antioxidant capacity (Kiritrakis et al., 2010; Leonardis et al., 2008; El-Gohary et al., 2009). Besides its has shown antimicrobial activities against several species of bacteria, dermatophytes and yeast. These microorganisms such as *E. coli, Pseudomonas aeruginosa, S. aureus, B. subtilis* and *K. pneumonia, Trichophyton mentagrophytes, Microsporum canis, T. rubrum* and *Candida albicans*. (Markin et al., 2003; Lee and Lee, 2010; Sudjanaa et al., 2009) , and antiviral activity against *viral haemorrhagic septicaemia rhabdovirus* (VHSV) (Micol et al., 2005; Yamada et al., 2009).

Finally, Figure 2.13. represents the HPLC chromatogram of olive leaf extract. Oleuropein is the most abundant polyphenolic component in olive leaf and rutin follows it. Oleuropein and rutin quantity in olive leaf is a lot higger compared to the other small components (Benavente-Garcia et al., 2000; Huang et al., 2003).

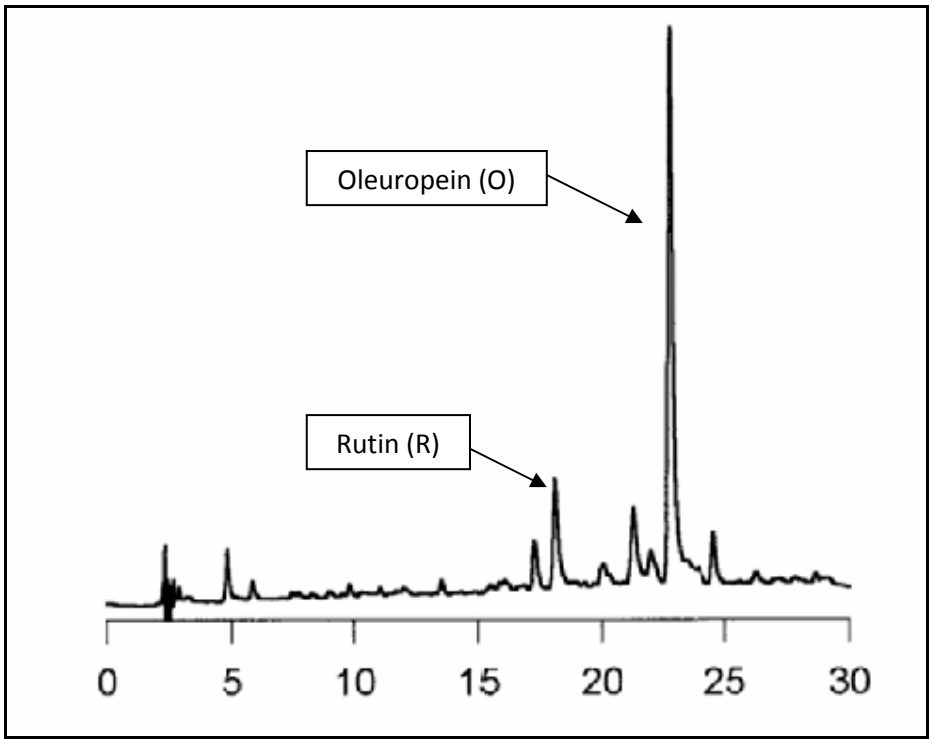

Figure 2.13. HPLC chromatogram of olive leaf extract, R: Rutin; O: Oleuropein (Source: Benavente-Garcia et al.,2000).

2.6. Oleuropein and Its Properties

Oleuropein is a phenolic compound found in naturally olive leaf from the olive tree and is responsible for the characteristic bitterness of olive fruit. It is the major phenolic compound in olive leaves. Oleuropein is an ester of 2-(3, 4-dihydroxyphenyl) ethanol (hydroxytyrosol) with elenolic acid glucoside (Nenadis et al., 2007; Omar, 2010; Soler-Rivas et al., 2000). The structure of oleuropein and its metabolites are shown in Figure 2.14.

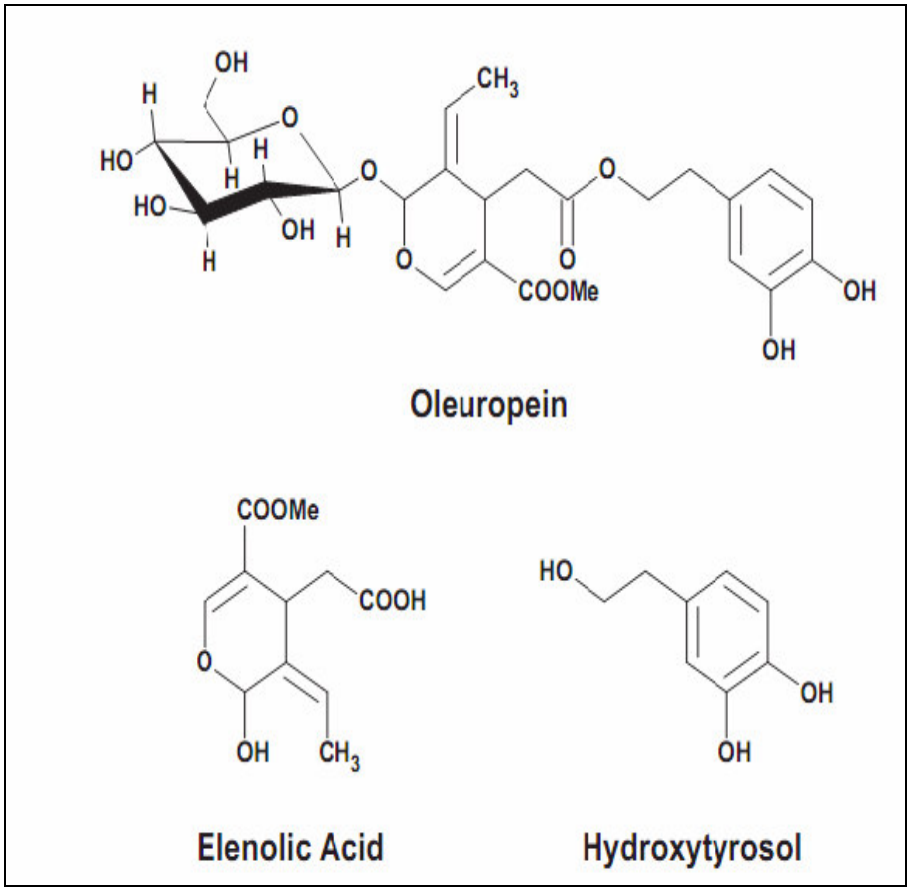

Figure 2.14. Structure of the oleuropein and its metabolites elenolic acids and hydroxytyrosol.

Several studies indicate that oleuropein has many benefits for health, including, antioxidant, antimicrobial (Lee and Lee, 2010), anti-inflammatory (Süntar et al., 2010; Kim et al., 2010; De la Puerta and Pasinetti, 1999), anti-atherogenic (Rigacci et al., 2010), anti-cancer (Bozoti et al., 2010; Han et al., 2009; Goulas et al., 2009),

cardiovascular diseases (Kremastinos et al., 2008) and antiviral (Zhao et al., 2009; Omar, 2010) properties. Moreover, oleuropein has been shown to exhibit anti-ischemic and hypolipidemic activities (Andreadou et al., 2006). Figure 2.15. shows the usage of the oleuropein.

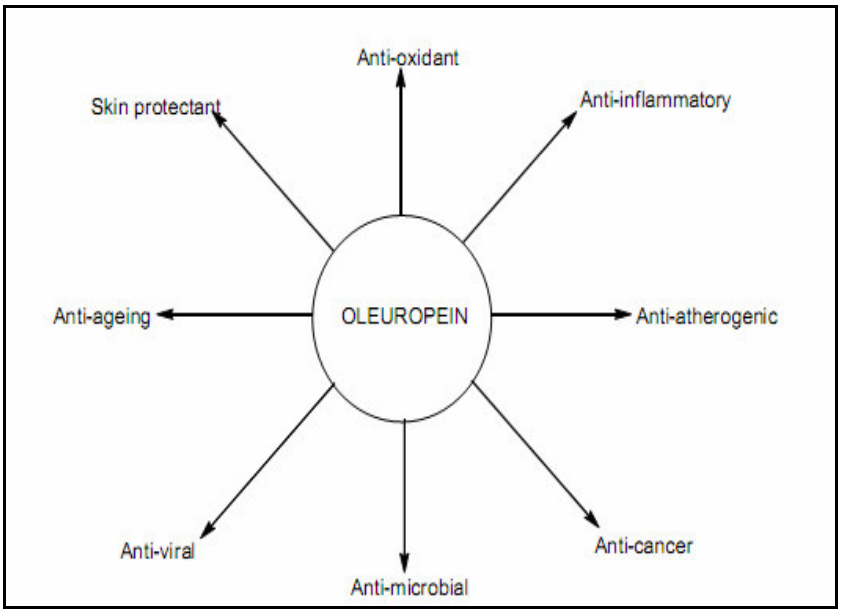

Figure 2.15. Usage of the oleuropein
(Source: Omar, 2010).

Oleuropein acts as an antioxidant at both prevention and intervention levels. Oleuropein prevents the free radicals formation via chelating metal ions, such as copper and iron, which catalyze the free radical generation (Omar, 2010).

Antioxidant activity: Oleuropein strongly and dose-dependently inhibits copper sulphate-induced oxidation of low-density lipoproteins (LDL) (Visioli et al., 2002). Oleuropein can both scavenge nitric oxide and cause an increase in the inducible nitric oxide synthase (iNOS) expression in the cell (Puerta et al., 2001). A scavenging effect of oleuropein was demonstrated with respect to hypochlorous acid (HOCl) (Visioli et al., 2002). HOCl is an oxidative substance produced in vivo by neutrophil myeloperoxidase at the site of inflammation and can cause damage to proteins including enzymes.

Antimicrobial effect: Oleuropein has strong antimicrobial activity against both Gram-negative and Gram-positive bacteria and mycoplasma (Omar, 2010). Phenolic structures similar to oleuropein seem to create its antibacterial effect by harming the bacterial membrane and/or disrupting cell peptidoglycans.

Oleuropein and hydrolysis products have ability to impede the creation and development of enterotoxin B by *Staphylococcus aureus*, the development of *Salmonella enteritidis* and the germination and consequent development of spores of *Bacillus cereus* (Furneri at al., 2002). Oleuropein and other phenolic compounds (p-hydroxybenzoic, vanillic and p-coumaric acids) completely inhibit the development of *Klebsiella pneumoniae*, *Escherichia coli* and *B. cereus* (Korukluoğlu et al., 2010)

Antiviral effect: HIV-1 gp41 (surface glycoprotein subunit), which is responsible for HIV entry into normal cells, is one of the suspected targets for olive leaf extract (mainly oleuropein) action. One of the suspected targets for olive leaf extract (mainly oleuropein) action is HIV-1 gp41, which is responsible for HIV entry into normal cells (Lee-Huang et al., 2007).

2.7. Adsorption

Adsorption is a process that occurs when a gas or liquid solute accumulates on the surface of a solid or a liquid (adsorbent), forming a molecular or atomic film (the adsorbate). It is different from absorption, in which a substance diffuses into a liquid or solid to form a solution. The term sorption encompasses both processes, while desorption is the reverse process.

Adsorption is operative in most natural physical, biological, and chemical systems. It is widely used in laboratory research, industrial applications. For example, activated carbon, the most common adsorbent, is used for the adsorption of organic substances and nonpolar adsorbates, and for waste gas and wastewater treatment. Silica gel is used for drying gases and adsorption of heavy (polar) hydrocarbons from natural gas (Malek and Farooq, 1997). Zeolites are useful for the drying of process air, carbon dioxide removal from natural gas, carbon monoxide removal from reforming gas, air separation, catalytic cracking, and catalytic synthesis and reforming. In addition, finely

divided platinum and palladium are good adsorbents of certain gases and serve as catalysts in chemical reactions (Kulprathipanja, 2002).

Solvent and solute components usually take place in the adsorption from liquid solution. The availability of the solvent makes the adsorption from liquid solution more complex than the gas phase. All the interactions between solute-surface, solvent-surface as well as solute-solvent are involved in the liquid-phase adsorption (Yang, 2003). Adsorbate and solvent molecules may compete to adsorb on the surface of the adsorbent. Due to this reason, suitable solvent should be utilized to accumulate the target adsorbate on the adsorbent.

2.7.1. The Mechanism of Adsorption

Attractive forces between the adsorbate and adsorbent enable adsorption from solution. The adsorbate is taken onto the surface to the lower energy state, where it has a lower free energy than in solution. Hence, it keeps with the second law of thermodynamics during equilibration (Montgomery, 1985).

Adsorption can be grouped as either physical adsorption (physisorption) or chemical adsorption (chemisorption) based on the nature of the bonding between adsorbate and adsorbent.

2.7.1.1. Physical Adsorption

Physical adsorption is non-specific, the bonds are weaker, and therefore the process is reversible. Bonds created in physical adsorption are held by electrostatic forces or hydrophobic bonding. The electrostatic forces create in the ionic atoms and polar groups on the surface. The physical interactions between molecules, based on electrostatic forces, contain dipole-dipole interactions, dispersion interactions and hydrogen bonding. Molecule to have a dipole moment, when there is a net separation of positive and negative charges within it. The attraction between two dipoles, when they are near, these molecules are called dipole-dipole interaction. In Hydrogen bonding, the hydrogen atom in a molecule has a partial positive charge and attracts an atom on another molecule, which has a partial negative charge. Hydrogen bonding is an example

of dipole-dipole interaction. A weak polarization is induced, when two neutral molecules, which have no permanent dipoles, approach each other due to quantum mechanical interactions between their distributions of charge. This is known as the dispersion interaction or the London-van der Waals force (Montgomery, 1985).

Nonpolar compounds are adsorbed more strongly to nonpolar adsorbents. This is called hydrophobic bonding. Hydrocarbon chain is more nonpolar, when it is longer. Therefore degree of this type of adsorption increases with increasing molecular length (Montgomery, 1985). Table 2.4. shows the characteristics of physical and chemical Adsorption (Tutornext, 2011).

Table 2.4. Characteristics of physical and chemical adsorption
(Source: Tutornext, 2011)

Physical Adsorption	**Chemical Adsorption**
Low adsorption temperature	High adsorption temperature
Non-specific	Highly specific
Definite in relatively lower temperature	Wide range of temperature
Fast and reversible	Slow and Irreversible
No electron transfer although adsorbate polarization occurs	Chemical bonds are occurred during electron transfer
Monolayer or multi-layer adsorption	Only mono-layer adsorption

2.7.1.2. Chemical Adsorption

Chemisorption has stronger attraction between adsorbent and adsorbate. Covalent or electrostatic chemical bonds with shorter bond length and higher bond energy formed between atoms. Chemisorption is two-dimensional chemical reaction and consists of electron transfer. The bond between adsorbate and surface varies with respect to particular sites or functional groups on the surface of the adsorbent (Montgomery, 1985; Yang, 2003).

2.7.2. Adsorption Equilibrium

In practice, capacity of adsorbent cannot be utilized due to the mass transfer effects involved in the adsorption systems. It is important to have information on adsorption equilibrium, to determine the adsorption capacity of adsorbent. Adsorption takes place, when an adsorbent and a particular composition of adsorbate are in contact. After an adequate time of operation the adsorbent and the adsorbate reach equilibrium. Adsorption isotherm is the relation between amount adsorbed q, and concentration of the adsorbate C, at constant temperature T (Suzuki, 1990).

The isotherms fall into two main types, in the case of adsorption from solution.

Type L: Isotherm is concave to the concentration axis, having a long well-defined plateau which is associated with monolayer adsorption of the solute and minimal competition from the solvent.

Type S: Isotherm is initially convex and then concave to the concentration axis. This isotherm is explained by the existence of a distinct balance between the adsorbate-adsorbent and adsorbate-adsorbate interactions (Rouquerol, 1999).

2.7.2.1. Langmuir Adsorption Isotherm

The Langmuir adsorption isotherm is simple and has ability to fit a broad range of experimental data; therefore it has broad range of applicability in adsorption from solution (Montgomery, 1985). Due to the Langmuir Isotherm;

- Energy of adsorption is free from degree of coverage.
- Bonding is reversible
- Monolayer adsorption occurs (Montgomery, 1985).

Langmuir isotherm as it is shown in Figure 2.16 has the curved shape. This is due to the competition between the adsorbate molecules for adsorption sites (Janson and Ryden, 1989). The equilibrium concentration in this figure is represented by C_e, the

adsorbate amount per unit weight of adsorbent is represented by q. Figure 2.16. shows the curved shape of Langmuir isotherm.

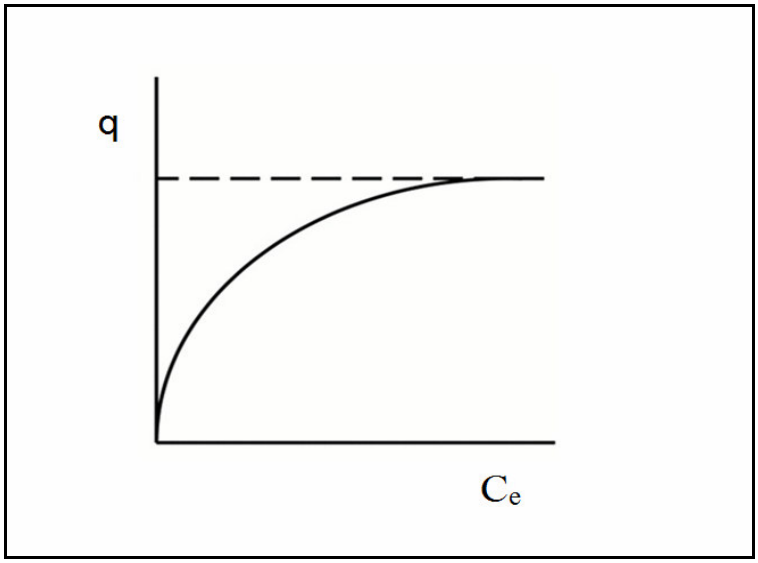

Figure 2.16. Langmuir isotherm

The concentration in the fluid phase by C. the equilibrium relation of the adsorption and desorption rates can be shown as follows (Scordino et al., 2004).

$$Q_c = \frac{Q_m K_L C_e}{1 + K_L C_e} \tag{2.11}$$

Where Qe: the equilibrium adsorption capacity (mg/g resin)

Q_m: maximum adsorption capacity (mg/g resin)

K_L : Langmuir constant (ml/mg)

C_e: equilibrium solute concentration (mg/ml)

2.7.2.2. Freundlich Adsorption Isotherm

The Freundlich Adsorption Isotherm is a term for the variety of the energy of adsorption on real surfaces. Because of the Freundlich isotherm;

- The frequency of sites related with a free energy of adsorption decays exponentially with increasing energy (Montgomery, 1985).
- Isotherm equation is empirical (Geankoplis, 1993).

The Freundlich Isotherm equation approximates data for many physical adsorption systems. It is also helpful for liquids. Figure 2.17 shows the general shape of the Freundlich isotherm. The equilibrium concentration in this figure is denoted by Ce, the adsorbate amount per unit weight of adsorbent is denoted by q (Scordino et al., 2004).

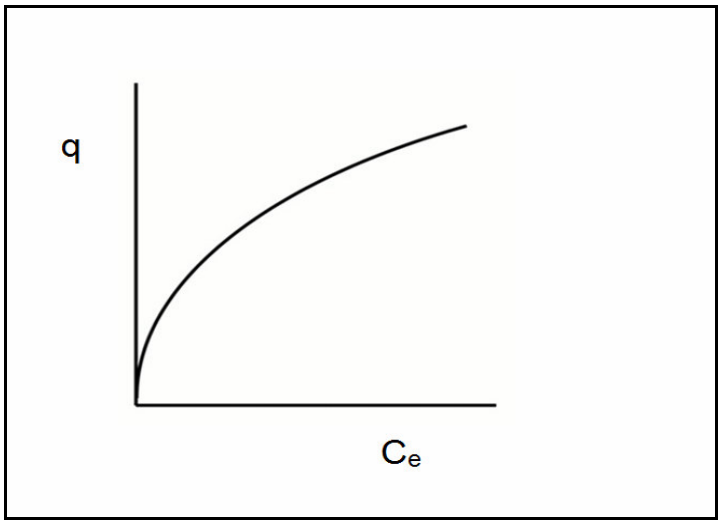

Figure 2.17. Freundlich isotherm.

Following equation is the Freundlich Isotherm equation;

$$Q_c = K_F C_e^{1/n} \tag{2.12}$$

where Q_e: the equilibrium adsorption capacity (mg/g resin)

C_e: equilibrium solute concentration (mg/ml)

K_F: Freundlich constant

1/n: the Freundlich parameter

2.7.3. Effect of Parameters on Adsorption Isotherms

Solid/liquid ratio, temperature and pH are the most important factors affecting the adsorption from solution. Beside them, many other parameters affect the adsorption and adsorption isotherms like nature of the solvent, nature of support, ionic strength, particle size, presence of extraneous ions.

pH effect: The pH of the medium has important effects the adsorption in aqueous solutions. It directly affects the surface charge of the adsorbent. The negatively and positively charged molecular species exists in equal concentration, at point of zero charge (PZC). Zero net charge in proteins is called isoelectric point (pI). Molecules behave variously at different pH values, because of to their isoelectric point or point of zero charge. If the medium of the pH is less than that of pI, surface of the adsorbent is positively charged and electrostatic interactions begin to occur between the adsorbent and adsorbate (Friedman and Jürgens, 2000; Agrawal et al., 2004).

Temperature: Temperature can affect the adsorption capacity of adsorbents in both ways. Process is called endothermic if the adsorbed amount increases with the higher temperature. Process is called exothermic, if the adsorption decreases with the higher temperature, in this case the heat of adsorption is negative.

Solid/Liquid Ratio: The adsorption efficiency can change both ways with increasing solid/liquid ratio. This is because of the availability of the surface area of the adsorbent during the adsorption (Bucic–Kojic et al., 2006; Scordino et al., 2004; Agrawal et al., 2004).

2.7.4. Adsorbents

Adsorbents have to posses particular engineering properties based on the application. Many adsorbents have been developed for a wide range of separations. Usually, the adsorbents are in the form of small pellets, beads, or granules varying from 0.1 mm to 12 mm in size. The performance of an adsorption process determined mostly by capacity of the adsorbent.

It is essential for all adsorbents to have large surface area. The amount they adsorb is approximately proportional to the surface area of the adsorbent, so that they must have porous structures.

Pore size and total pore volume of adsorbents are very important as well as the shape of the pores. IUPAC use the following classification of pores based on the width are given the Table 2.5. (Kaneko, 1994).

Table 2.5. Adsorbents classification of pores size based on the width
(Source: Kaneko, 1994)

Macropores	> 50 nm.
Mesopores	2-50 nm.
Micropores	<< 2 nm.

In addition to the above properties, the usefulness of an adsorbent is also determined by composition, hydrophilicity and hydrophobicity, ligand or other functional groups, mechanical and chemical stability. Besides, adsorbents used in bioprocesses should be biocompatible, sterilisable, and resistant to micro-organisms, of constant quality.

Adsorbents can be classified in three main groups based on the binding mechanisms. Table 2.6. shows the main groups (Montgomery, 1985).

Table 2.6. Adsorbents based on the binding mechanisms
(Source: Montgomery, 1985).

Inorganic	silica, carbon, calcium phosphate, zeolites,etc.
Synthetic polymers or resins	dextran, polysulfone, etc.
Composites	silica –dextran

Inorganic adsorbents such as activated carbon, silica and alumina are normally rigid, stable and available in many sizes and shapes. On the other hand, the selectivity is low and regeneration is difficult, therefore lifetime is limited.

Synthetic polymers are formed by polymerizing two major types of monomers. They exists in a gel type and a macroreticular sponge like structure. They are used in various applications such as in the recovery of antibiotics, and adsorbing organic and inorganic pigments etc. Their mechanical strength, especially that of gel type limits their applicability in large scale processes. They are mostly used in chromatography (Montgomery, 1985).

The composite adsorbents possess the advantages of the inorganic rigid carrier and the favourable adsorption behaviour of polymeric adsorbents. The inside of an inorganic carrier is covered with a very thin layer of an organic material. Composite adsorbents are used in the recovery of proteins.

In addition, the resins can be classified according to polarity and mainly divided into three types – non-polar resins, medium polar resins and polar resins. Non-polar resins, they usually show non-polar or hydrophobic behaviour and so adsorb non-polar organic molecules from polar solvent, for example, water. Polar resins, they usually show polar or hydrophilic behaviour and adsorb organic molecules with some degree of polarity from non-polar solvents, for example, hydrocarbons. Medium polar resins, they show both hydrophobic and hydrophilic behaviours (Wang et al., 2001; Tu et al., 2004).

2.8. Purification Techniques

2.8.1. Fluidised (Expanded) Bed Adsorption

Fluidised bed adsorption is an efficient recovery method. Also it is proven to have significant advantages compared to conventional procedural sequences, e.g. discrete feedstock clarification followed by fixed bed adsorption of the product. Liquid is pumped upwards through a bed of adsorbent beads in fluidized beds. Compared to packed bed, it is not constrained by an upper flow adapter. Therefore, the bed can enlarge and spaces between the adsorbent beads can widen. The increased voidage of the bed enables particulates, which are in the feed, to pass freely through the spaces without entrapment (see Figure 2.18.). Following the adsorption stage, the remaining feedstock and particulates are washed from the adsorbent bed. Then product is eluted either in fluidized or packed bed mode. As a result, initial fractionation is combined in one unit operation. Hence fluidized beds show significant potential for simplifying downstream processes with savings in capital and operating costs. Previously fluidized beds have been utilized for scale recovery of the antibiotics streptomycin (Barthels et al., 1958) and novobiocin (Belter et al., 1973). On the other hand, recently substantial attention is given for the use of fluidized beds for the direct extraction of proteins from whole fermentation broths (Chase, 1994; Gailliot et al., 1990) and purify flavonoids from *Ginkgo biloba* L (Li and Chase, 2009).

The adsorbent particles are fixed when the flow velocity below minimum fluidization velocity. The voidage, i.e. the inter-particle space, is minimal. Hence, feedstock clarification is obligatory to evade clogging of the bed. The adsorbent bed is enabled to expand by irrigation with feedstock in a fluidized / expanded bed. Increased bed voidage is enabling the passage of particulates in the feed. The diameters of the adsorbent beds are enhanced for illustrative purpose.

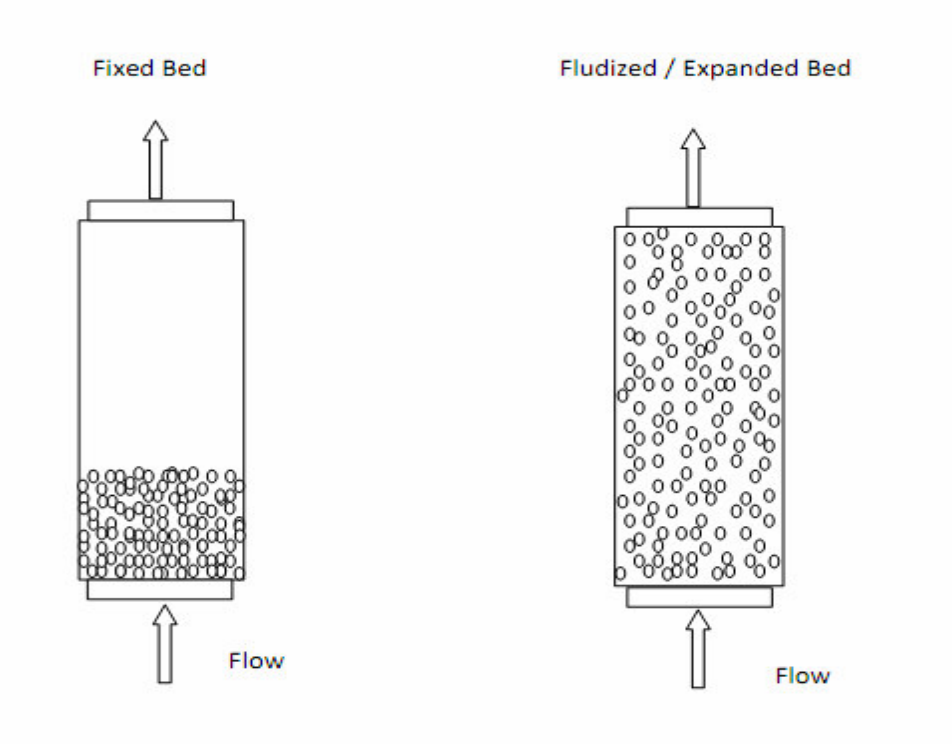

Figure 2.18. Fix Bed and Fluidized Bed Adsorption representation

2.8.2. Matrices for Fluidized (Expanded) Bed Adsorption

Particle fluidization is reached with pumping liquid up through a settled bed of adsorbent particles. Liquid percolates through the spaces between the adsorbent beads at low fluidization velocities. Settled beads start to move apart as a result of increasing the flow velocity. By increasing velocity more, the particles can become suspended in the liquid, which can be named as the minimum fluidization velocity U_{mf} (see Figure 2.19). If the fluidization velocity is increased further above U_{mf}, the bed enlarges as the adsorbent particles move apart, which result in a progressive bed expansion named as steady state fluidization (Kunii and Levenspiel, 1969). If velocity increased even more, critical velocity can be attained. At that point adsorbent particles begin to entrain from the bed and the bed destabilises. Maximum fluidization velocity or terminal velocity U_t is the flow velocity at this point, which can be approximately estimated by Stokes law (Equation 2.13). Stokes law explains single particle's settling velocity at infinite dilution.

$$U_t = \frac{g(\rho_p - \rho_l)d_p^2}{18\mu} \tag{2.13}$$

Due to adhesion forces, particles in a fluidized bed interact, especially when fluidized at higher viscosities. They can't be considered as individual particles.

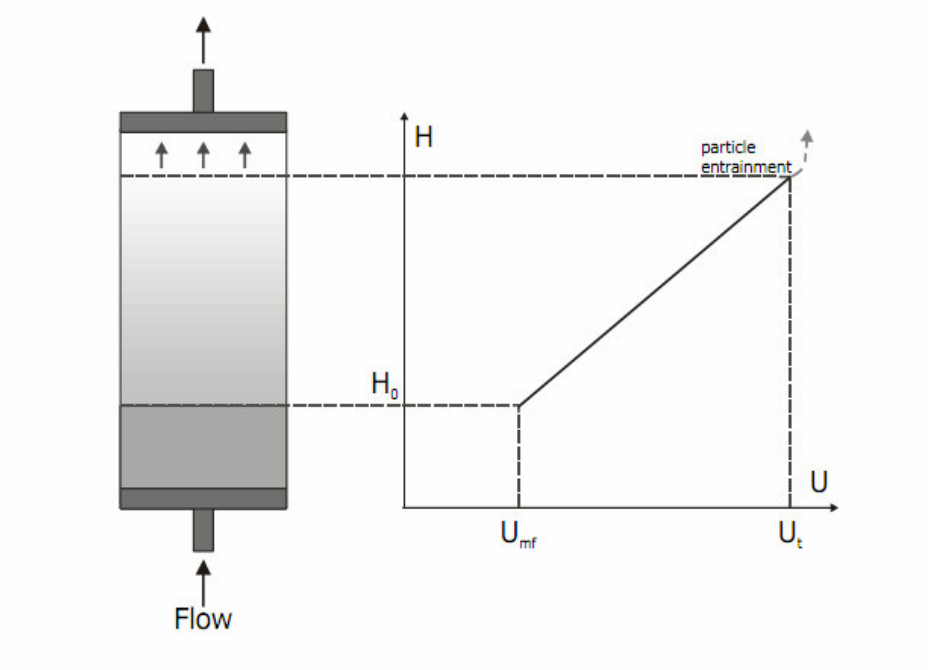

Figure 2.19. Simple representation of minimum fluidization velocity U_{mf} and terminal velocity U_t

The operational window of a fluidized bed process is determined by the minimum fluidization velocity U_{mf} when settled bed of adsorbent beads starts to fluidize and the terminal velocity (U_t) when the bed stabilises and adsorbent beads are entrained from the bed.

Equation 2.13 is an estimation of the terminal velocity and also it reflects the parameters that affect the terminal velocity of a particle. Hence equations 2.13 determine the operational window with regard to fluidization velocity. The terminal velocity is proportional to the density difference between the particle (ρ_p) and the fluidising liquid (ρ_l); square of the particle diameter (d_p). It is inversely proportional to the fluid viscosity (η).

2.9. Adsorption of Polyphenolic Compounds

The active ingredients of the plants are separated and purified from the crude plants and then made into various convenient forms. Solvent extraction is one of the conventional techniques for separating and purifying active ingredients from crude plants (Huie, 2002). However, this technique has several disadvantages. A large amount of solvent is consumed during the extraction. It also tends to adsorb most organic chemicals randomly and it difficult to recover solvent for reuse.

Adsorption resin technology, a modern method to separate and purify active ingredients from crude plants, can overcome these difficulties. This technique can reduce the cost of operation because of its less consumption of solvents and process operating time. Moreover, the resins are easily regenerated and the adsorbed active ingredients of crude plants. These adsorbates are recovered for use by organic solvents elution. Furthermore, their high loading capacity made it possible to separate compounds in large amounts. Therefore, this technique can be performed on a large scale (Kammerer et al., 2010).

There are many researches related with the adsorption of polyphenols from different plant by different adsorbents and experimental setup. These studies also give information the interactions between various adsorbent materials and polyphenols. As a result of this literature survey, very few of them were performed with fluidized (expanded) bed adsorption some of which are showed in Table 2.7.

Huang et al. studied the adsorption characteristics of tea polyphenols onto three polymeric adsorbents with amide group. PMVBA (poly (N-methyl-N-p-vinylbenzylacetamide)), PMVBU (poly (N-methyl-N-p-vinylbenzylurea)), and PMA (poly (N-methylacrylamide)) were used as adsorbent. Based on the results of adsorption isotherms and adsorption kinetics experiments, PMVBU was chosen as the best resin for adsorption capacity and adsorption enthalpy for tea polyphenols. Adsorption mechanism suggests that multiple hydrogen bonding and hydrophobic interaction are included adsorption of tea polyphenols onto the three adsorbents in aqueous solution (Huang et al., 2007).

Bayraktar and his research group chose silk fibroin to isolation of polyphenols from olive leaves. The adsorbed amounts of rutin and oleuropein were found 15 mg rutin/g silk fibroin and 96 mg oleuropein/g silk fibroin. Silk fibroin is an edible protein

polymer which has functional amino acids in its structure. Its hydrophobic character makes it a good choice to be used in adsorption studies (Altıok et al., 2008).

In a study, four resins including XAD-7, XAD-16, EXA-90 and EXA-118 were used to compare their performances in adsorbing and desorbing flavonoids in *Inga edulis* leaves. The experimental results showed that the XAD-7 resin gave the best adsorption capacity and XAD-16 the worst one (Silva et al., 2006).

Kranz et al. tried to find bitterness problem in citrus juices. Bitterness is an important for the quality of the fruit juices. Flavour adsorption was studied during debittering citrus juice using a downflow column packed with macroporous adsorption resin XAD-7HP (Kranz et al., 2011).

Ye et al. studied adsorption and desorption characteristics using Polyamide-6 (PA) as an adsorbent. Tea catechins were separated from the green tea extract. The adsorption capacity of total catechins for PA was 193.128 mg g^{-1} with an adsorption selectivity coefficient KA of total catechins over caffeine 21.717. The Langmuir model and the pseudo-second order model were primely fitted to describe its equilibrium data and adsorption kinetics (Ye et al., 2010).

Adsorption of anthocyanins from purple-fleshed potatoes on tree resins which are macro porous SDVB, acrylic and methacrylic were studied in order to see their adsorption capacities by Liu et al. (2007). Adsorption data were fitted to the Langmuir and Freundlich isotherms. Both models were found suitable to explain the adsorption isotherms of anthocyanins on the resins. Adsorption capacities for anthocyanins increased with the rise of temperature for SDVB resins but decreased for metharcylic resins. XAD-1600 resin gave the highest adsorption capacity for anthocyanins.

Table 2.7. Some of the adsorption studies of polyphenols and their attributes.

REFERENCE	ADSORPTION SYSTEMS	EXPERIMENTAL SETUP	ANALYTICAL TECHNIQUE	ATTRIBUTES
Huang et al., 2007	Tea Polyphenols , PMVBA, PMVBU, PMA	Static Adsorption	UV-visible spectrophometry	Freundlich Isotherms
Altıok et al., 2008	Olive Leaves ,Silk Fibrion	Fıxed Bed Column Adsorption	HPLC,ABTS antioxidant analysis	Hydrophobic interaction
Silva et al., 2006	Inga edulis leaves, XAD-7, XAD-16, EXA-90 and EXA-118	Static Adsorption	Folin-Ciocalteu colorimetric total phenol method	Langmuir and Freundlich Isotherms
Kranz et al., 2011	Citrus juices, XAD-7HP	Fıxed Bed Column Adsorption	HPLC, HS-GC	Lagergren adsorption model
Ye et al., 2010	tea catechins, Polyamide-(PA)	Fıxed Bed Column Adsorption	HPLC	The Langmuir model and the pseudo-second order model
Liu et al., 2007	Anthocyanins from Purple-fleshed Potato , SDVB ,XAD-1600	Static Adsorption	HPLC	the Langmuir and Freundlich isotherms
Li and Chase, 2009	flavonoids from Ginkgo biloba L.,XAD7HP	Expanded Bed Adsorption	HPLC	Hydrophobic interaction

In this study Li and Chase, three techniques (liquid–liquid extraction, packed bed adsorption and expanded bed adsorption) have been compared for the purification of flavonoids from the leaves of *Ginkgo biloba* L. Amberlite XAD7HP was selected as the adsorbent and clarified extract was used as the feedstock. The dynamic adsorption breakthrough curves and elution profiles were measured.

Generally, commercial adsorbents were used on the removal of flavonoids from liquid phase compared to the natural ones. There is an increasing trend to clarify many other polyphenols from plants, which have antioxidative, antimicrobial and antiviral properties. One of these plants is olive leaf, which have antimicrobial, antioxidative and anti-inflammatory effects. Oleuropein and rutin are the two essential components of the olive leaf indicating these properties.

2.10. Comparison of the Separation Strategies

A comparison of the purification steps needed to isolate flavonoids using either packed bed adsorption chromatography or fluidized (expanded) bed adsorption chromatography is shown in Figure 2.20. In the packed bed adsorption process, the clarification step caused the loss of nearly half of the flavonoids (Li and Chase, 2009) but was necessary so as to produce a suitable feedstock for packed bed operation.

However, the EBA process eliminated the need for the centrifugation and filtration steps, and consisted of direct loading and purification step, which significantly clarified the separation process. Li and Chase were found the following results in this study. Although the recovery ratio of the flavonoids present in the feed-stock obtained in the fluidized (expanded) bed unit was lower than that obtained in the packed bed, the use of EBA has several benefits.

- the overall recovery ratio from Ginkgo leaves using the EBA process will not be lower than that of packed bed process since the clarification steps usually lead to a 40% loss in flavonoids
- EBA permits the elimination of a number of steps and thus can save much process time.

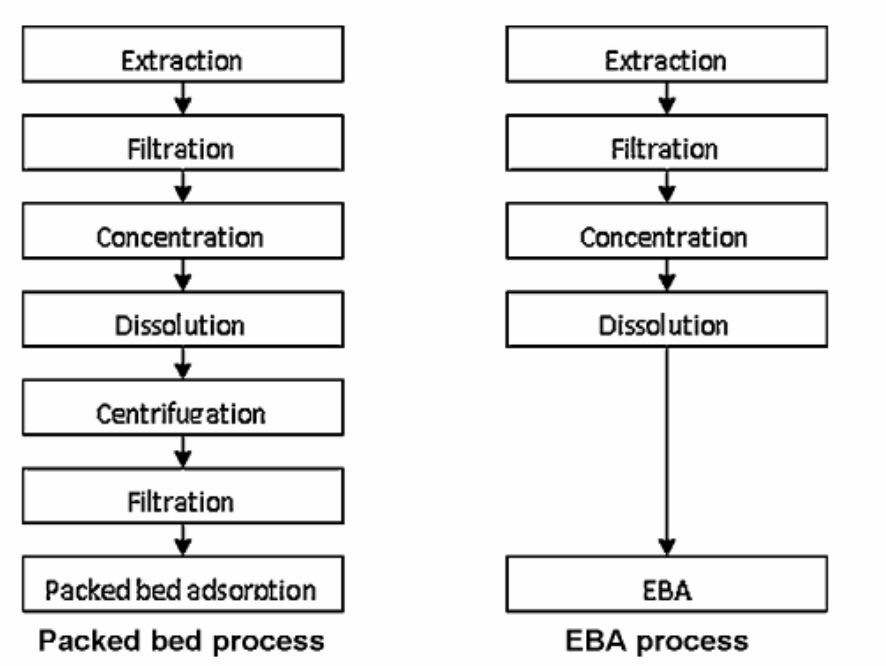

Figure 2.20. The comparison of schematic diagram for the purification of flavonoids from Olive leaves using packed bed process and fluidized (expanded) bed adsorption.

.

Consequently, the question of whether or not it would be useful to include fluidized (expanded) bed adsorption. In this study, it has not been feasible to make simply comparisons of the performance of the packed bed and fluidized (expanded) bed adsorption processes by setting all the operational parameters to the same values for both processes. The reason for this, although there are technical similarities between packed bed and fluidized (expanded) bed adsorption, many factors, such as the consumption of feed materials, working conditions and operational parameters are different when the techniques are used in practice.

CHAPTER 3

OBJECTIVES

The primary aim of this study was to achieve the adsorption and desorption of olive leaf antioxidants, especially oleuropein and rutin on XAD7HP macro porous resin. In accordance with this aim, the effectiveness of the packed (fixed) bed adsorption and the fluidized (expanded) bed adsorption were compared. Besides, the expansion and hydrodynamic properties of expanded beds were investigated and analyzed.

The goals of this study can be summarized as follows:

- To qualify and quantify oleuropein and rutin in olive leaves,
- To investigate the adsorption of oleuropein and rutin on XAD7HP macroporous resin,
- To study the adsorption kinetics and adsorption isotherms
- To understand XAD7HP macroporous resin-polyphenols interactions by changing the alcohol content of adsorption medium,
- To investigate fluidized bed adsorption and desorb fractionation of olive leave extract,
- To study the effects of the flow velocity on fluidized bed adsorption ,
- Determination of the total phenol content analysis and antioxidant capacities in the desorb fractions.

CHAPTER 4

EXPERIMENTAL STUDY

4.1. Materials

4.1.1. Plant Materials and Chemicals

Olive leaves were gathered from the olive trees in the campus of Izmir Institute of Technology in Izmir in Turkey. Oleuropein from Extrasynthese (Genay, France); rutin (98.5 + %) from Merck Co. (Darmstadt, Germany); high performance liquid chromatography (HPLC) grade ethanol (for extraction) from Riedel-de Haën (Seelze, Germany), HPLC grade acetonitrile (mobile phase for HPLC) from Sigma-Aldrich Chemie (Steinheim, Germany) and HPLC grade acetic acid (mobile phase for HPLC) from Merck Co. (Dermstadt, Germany) were used in this study. In extraction experiments analytical grade ethanol (C2H5OH) was used from Merck (Germany). Folin-ciocalteu was used in order to determine total phenol content obtained from Sigma (USA). Sodium carbonate anhydrous (99.5%) was used from Fluka (Switzerland). Trolox (6-hydroxy-2,5,7,8,-tetramethylchroman-2-carboxylic acid), ABTS (2,2'-azinobis (3-ethylbenzothiazoline-6-sulphonic acid)) reagents and potassium persulfate (K2O8H8) from Fluka (Germany) were used for antioxidant analysis.

4.1.2. Instruments and Equipments

Olive leaves were dried in Memmert UFP 800TS oven. After grinding, extractions were performed in Thermo MaxQ-4000 orbital shaker. Evaporation was achieved with Heidolph Laborata 4001 rotary evaporator and aqueous solution was frozen. Telstar Cryodos-50 freeze drier was used in order to obtain dry crude extracts. Hettich ROTINA 38R was used for centrifugation operations. Watson-Marlow 323E peristaltic pump was used for column studies Phenolic compounds of olive leaf crude extract was analysed with HPLC Agilent Technologies 1100 Series. Multiscan UV

spectrophotometer from Thermo was used in order to find total phenol contents and antioxidant capacity of extract. Sartorius – Arium 611VF water sanitizer was used in all experiments to obtain ultra pure water.

4.2. Methods

This study consisted of extraction, adsorption and analysis of the feed and downstream solutions. At the extraction stage, pre-treatment and extraction of olive leaf polyphenols experiments were performed.

Second part is the adsorption of olive leaf antioxidants on XAD7HP. This part can be divided into two subgroups. First, olive leaf extract solution prepared with EtOH and without EtOH was examined for the adsorption capacity of resin. Fixed bed and fluidized bed experiments were performed with the same initial bed height and concentration with various feed rates. So, the dynamic adsorption capacities of the bed were examined for the velocities of interest.

The final part is to investigate the total phenol content and antioxidant capacities of samples which were obtained from the column studies. The experimental procedure is schematically represented in Figure 4.1. and 4.2.

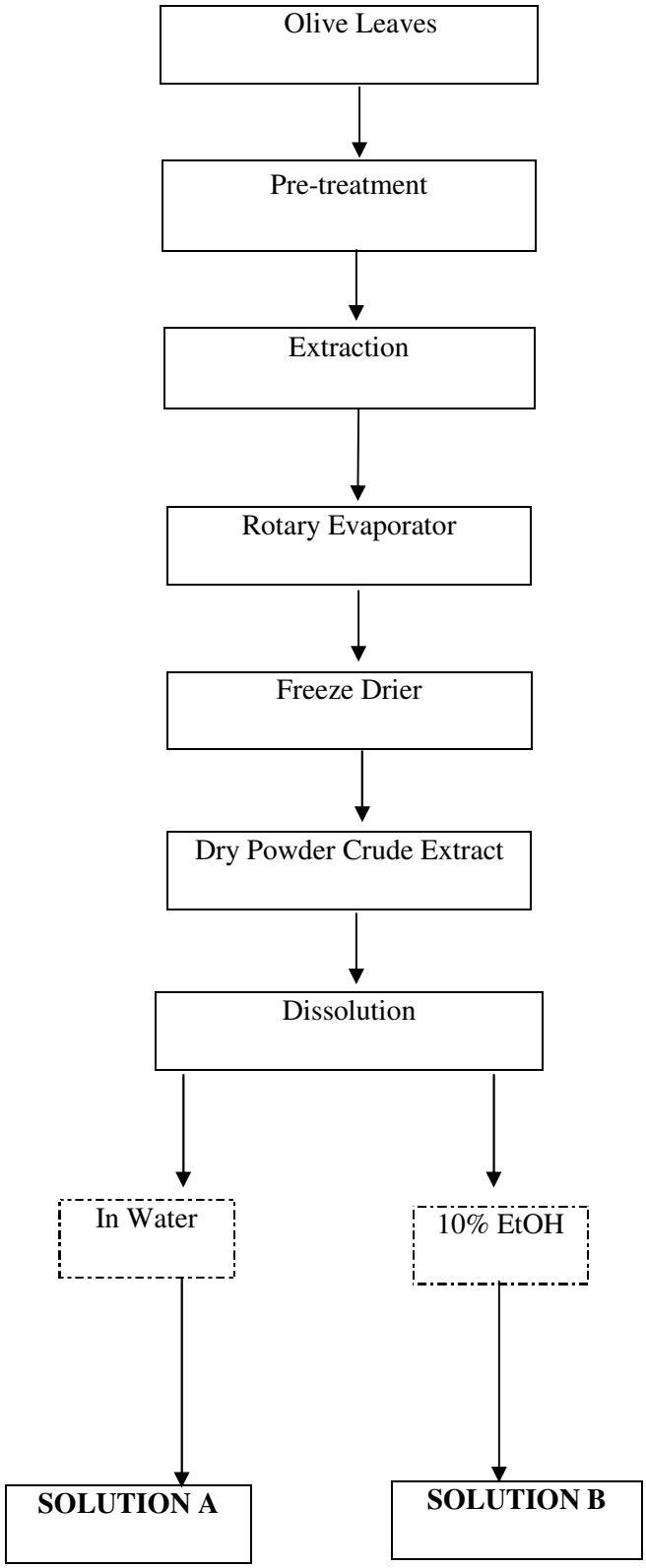

Figure 4.1.Schematic representation of experimental procedure.

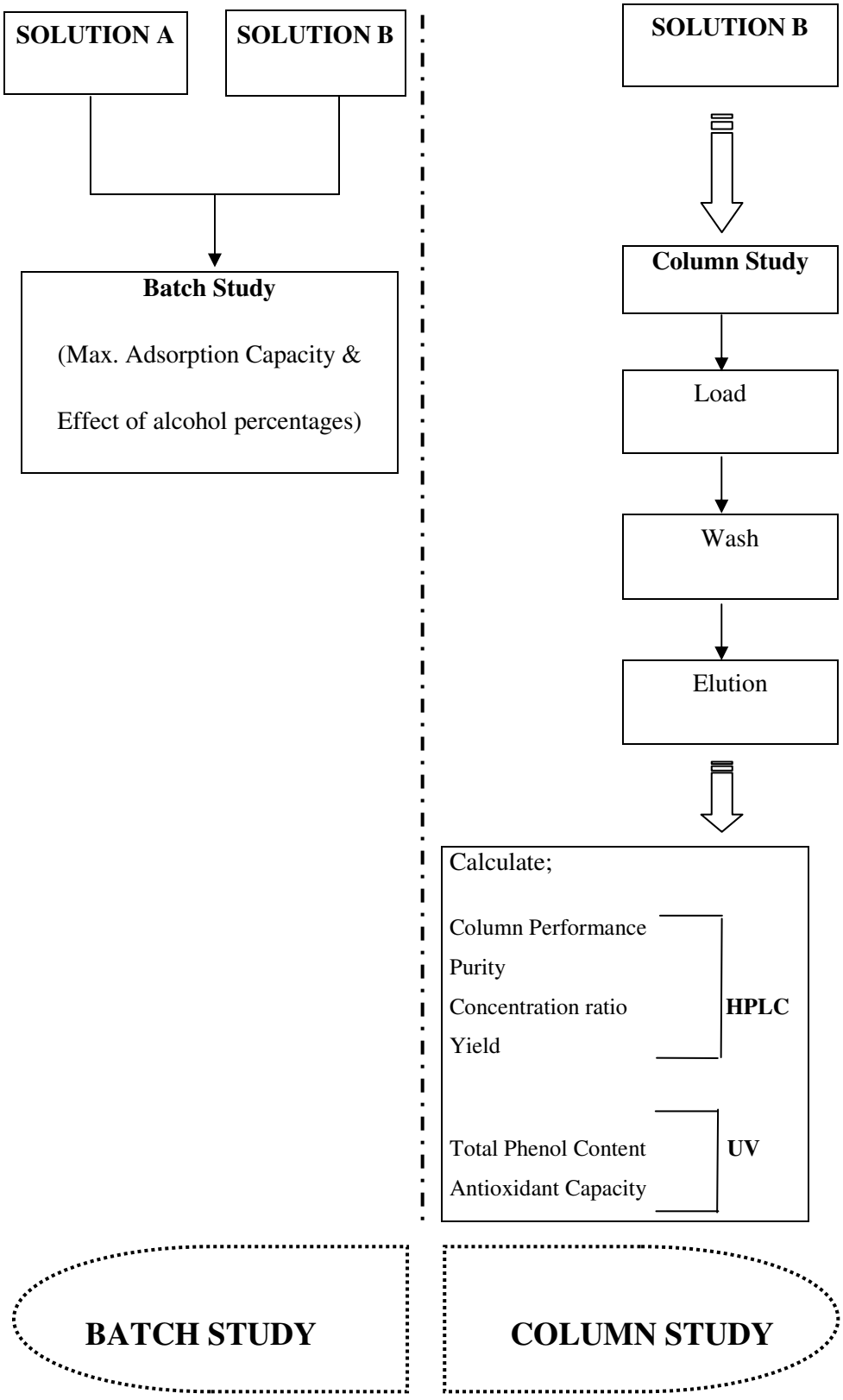

Figure 4.2.Schematic representation of experimental procedure.

4.2.1. Pre-treatment of Olive Leaves

Olive leaves were washed with deionized water, and then they were dried in the oven at 37 ºC for 3 days. 37 ºC is a critical temperature for drying because of the fact that there is a degradation risk of antioxidants over 40 ºC. After 3 days, grinding was employed and the grinder was used till the leaves became fine powder to particle sizes about 90-150 micron. The grinding was achieved in 5 minutes intervals to preclude frictional heating of the sample.

4.2.2. Extraction of Olive Leaves

As extracting solvent, aqueous ethanol solution was used because of its low cost and non-toxic nature. In the study of Hızal (2006), it was observed that the highest oleuropein and rutin yields were obtained by 70 % aqueous ethanol solution. Hence 70 % aqueous ethanol solution was used in the extraction of olive leaves. After the suitable ethanol-water ratio was decided, olive leaf powder was treated with this solvent in 1/20 solid/liquid ratio. Extraction was done in Termo Thermo shaker for 2 hours at 180 rpm and 25 ºC in order to ensure a complete homogenization of the solution. Centrifugation was the following step that enables to remove insoluble particles from the extraction medium. For this aim, the solution was centrifuged in Hettich Rotina 38R centrifuge at 5,000 rpm for 15 minutes. Then the liquid phase, separated in the centrifugation process, was transferred to the Heidolph rotary evaporator. Rotary evaporator was operated at 40 ºC and 120 rpm rotation under vacuum. In the rotary evaporator, ethanol and partial water evaporation is reached with a vacuum technique by decreasing the interior pressure. The final step of the extraction was the lyophilization. Solvent free olive leaf extract was put in Telstar Cryodos freeze drier to remove the water content of the extract. Olive leaf extract was dried in a freeze drier system at -52 ºC and below 0.2 mbar. After all these procedures, olive leaf crude extract was obtained to be used in the next studies.

4.2.3. HPLC Analysis and Identification of Phenolic Compounds

High performance liquid chromatography (HPLC) analysis was conducted for the analytical qualification and quantification of the phenolics in olive leaf extract. The operating conditions and properties of HPLC are given in Table 4.1.

Table 4.1. Operation conditions and properties of the High Performance Liquid Chromatography system

Property	**Value or Attribute**
Column	Column C18 LiChrospher 100 analytical column
Column Length	250 mm
Column Diameter	4 mm
Particle Size	5 μm
Mobile Phase	Mobile Phase A: 2.5 % acetic acid in deionied water
	Mobile Phase B: 100 % acetonitrile
Flow Rate	1 ml/min
Temperature	30 ºC
Detector	Diode Array Detector
Absorbance	280 nm

Table 4.2. HPLC elution program

Time (min)	**Mobile phase A 2.5 % Acetic Acid in Deionized Water**	**Mobile phase B 100 % acetonitrile**
0	95 %	5 %
20	75 %	25 %
40	50 %	50 %
50	20 %	80 %
60	5 %	95 %

Phenolics in olive leaf extract identified by comparing their retention times with the corresponding standards. In this study, identification of the two major phenolics of olive leaf extract, oleuropein and rutin, was considered. For this reason oleuropein and rutin in the olive leaf extract was initially qualified by comparing its retention time with its standard. Then quantification was done by using the calibration curve. Calibration curves of oleuropein and rutin were given in Appendix A.

4.2.4. Selection of Amberlite Resins

Adsorption efficiency was used to evaluate the adsorption performance of the resin. Three resins namely XAD4, XAD 16 and XAD7HP were used in this study. The experiments were conducted at 298.0 ± 0.5 K using 60 ml adsorbate solution and a fixed adsorbent dosage of 3.00 g. The adsorption efficiencies of three resins for oleuropein and rutin were compared. Their physical properties are listed in Table 4.3. (Dow, 2011).

Table.4.3. Physical properties of Amberlite XAD4, XAD16 and XAD7HP adsorbents (Source: Dow, 2011)

	XAD4	**XAD16**	**XAD7HP**
Polarity	Non-polar	Non-polar	Moderate polar
Mesh size	20-60	20-60	20-60
Dry/wet density (g/ml)	1.08-1.02	1.08-1.02	1.24/1.05
Pore volume (ml/g)	0.98	0.82	1.14
Surface area (m^2/g)	750	800	380
Average pore diameter (nm)	5	10	9
Porosity (ml/ml)	≥0.50	≥0.50	≥0.50
Particle size (mm)	0.3-1.2	0.3-1.2	0.3-1.2

4.2.5. Static Experiments

Static experiments are carried out in a rotary shaker in order to select the appropriate resin; determine the adsorption isotherm, investigate the factor affecting adsorption capacity of macroporous adsorption resin such as alcohol content.

In each static experiment, 60 ml of liquid extract were added to 3.00 g resin in a 150 ml erlen flask at 298 K. Solid liquid ratio was chosen as 1/20. The flasks were shaken in a shaker under 250 rpm. The static adsorptions were performed for 4 hours. Then, the equilibrium concentrations of oleuropein and rutin adsorption capacities were determined. The set-up for static adsorption is showed in Figure 4.3.

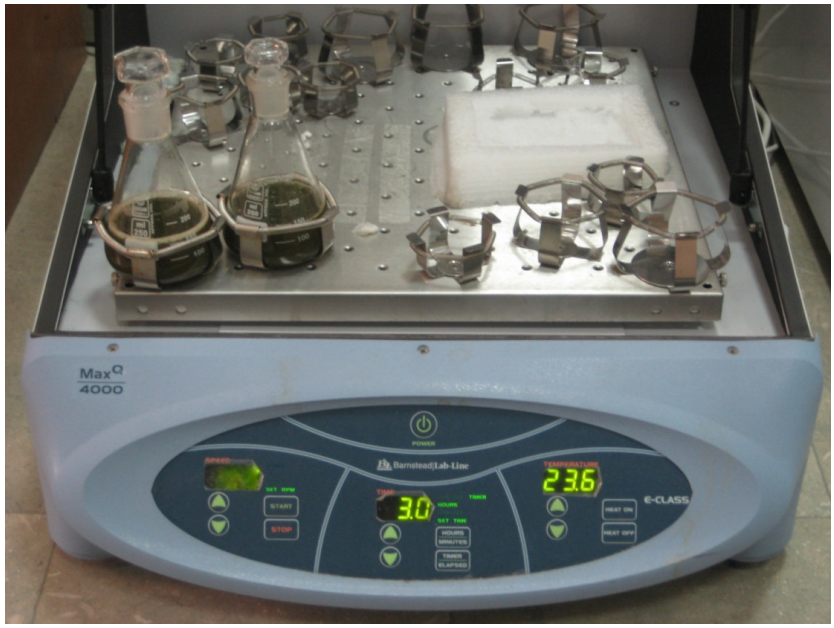

Figure 4.3. The experimental set-up for static adsorption

The adsorption capacity was calculated as follows:

$$Q_c = (C_i - C_e)\frac{V}{W} \tag{4.1}$$

Where Qe is the adsorption capacity at adsorption equilibrium (mg/g resin); Co and Ce are the initial and equilibrium concentrations of adsorbate in the solutions respectively (mg/ml); V is the volume of the initial sample solution (ml) and W is the weight of the macroporous adsorption resins (g).

4.2.6. Dynamic Experiments

Dynamic experiments can be divided into two main parts which are expansion characteristics and dynamic adsorption study

4.2.6.1. Expansion characteristics

The expansion properties of expanded beds were investigated and analyzed. The Richardson–Zaki correlation equation (Li et al., 2009) describes expansion properties of the expanded bed as a function of fluid velocity. Using the results of the bed expansion studies The Richardson–Zaki parameters can be estimated. Following equation can be utilized.

$$u = u_t \varepsilon^n \tag{4.2}$$

Theoretical predictions of the correlation parameters u_t and n were improved by modifying equations in the literature, where u stands the superficial liquid velocity and u_t stands for the terminal velocity of a single adsorbent particle in a volume of stagnant liquid. ε is the voidage of expanded bed and n is the Richardson–Zaki parameter. In this study the voidage of a settled bed was assumed to be 0.4 and can be used to calculate the ε as below:

$$\varepsilon = 1 - (1 - 0.4)(\frac{H_0}{H_{exp}}) \tag{4.3}$$

H_{exp} and H_0 denote the height of expanded bed and the height of initial settled bed respectively. u (superficial flow velocity) and ε (expanded bed voidage) are known for each experiment, and a regression of ln u against ln ε can be investigated to specify values of ut and n. In the literature (Li et al., 2009), there are studies suggesting that ut and n can also be derived theoretically from knowledge of the physical properties of the adsorbent beads and the liquid phase in the bed. In certain situations, u_t can be estimated from Stokes' law:

$$U_{t-Stokes} = \frac{g(\rho_p - \rho_l)d_p^2}{18\mu} \tag{4.4}$$

where d_p and ρ_p are the mean diameter and density of the adsorbent beads respectively, ρ_l and μ are the density and viscosity of the liquid phase respectively.

There is another procedure of explaining the fluidization behaviour of particles with using two dimensionless numbers, the Galileo number (Ga) and the terminal Reynolds number (Ret) (Li et al., 2009).

$$Ga = \frac{\rho_p g(\rho_p - \rho_l)d_p^3}{\mu^2} \tag{4.5}$$

$$Re_t = \left[\frac{23}{Ga} + \frac{0.6}{Ga^{0.5}}\right]^{-1} \frac{1}{1 + 2.35(d_p/d_c)} \tag{4.6}$$

$$Re_t = \frac{u_t \rho_p d_p}{\mu} \tag{4.7}$$

$$\frac{5.1-n}{n-2.4} = 0.016Ga^{0.67} \tag{4.8}$$

Where dc is the diameter of column. These equations can be utilized to calculate values of ut and n.

4.2.6.2. Dynamic Adsorption Study

Dynamic experiments are carried out 90 cm height and 2.5 cm diameter glass column. In initial studies, it had been decided that 10 % ethanolic aqueous extract solution was the appropriate feed composition for the dynamic adsorption process. A column packed with XAD7HP resin having a bed height of 55 cm was prepared. Extract solutions were fed to the column at various flow velocities in order to investigate the effect of feed rate on dynamic adsorption performance. Feed stream consisting of 10 % ethanolic aqueous extract solution had a constant initial concentration, and the column was packed with the same quantity of resin for all experiments. Investigated feed flow velocities were 122 cm/h, 367 cm/h and 611 cm/h. Experiments were used by feeding unclarified extract solution having initial oleuropein concentration of 2 mg/ml and rutin concentration 0.44 mg/ml. For each experiment, the effluent fractions of the adsorption stage were collected. The efflux was analyzed by HPLC for compositional analysis.

The adsorption and desorption process included four main stages. These steps are conditioning, adsorption, washing and elution respectively. At the first stage, the column was conditioned with pure ethanol and deionized water. Second stage is adsorption; the sample solution was fed at constant flow velocity into the column until equilibrium is attained. Then, column was washed with deionized water in order to remove residuals and impurities. Eventually, loaded column was eluted with a certain volume of aqueous solutions with 40% and 90% ethanol content.

4.2.6.3. Desorption Study

The desorption experiments were performed after adsorption stage. Firstly, saturated column was eluted with 2,000 ml of de-ionized water. Later on, a certain volume of aqueous ethanol solution having 40 % and 90 % ethanol concentration passed through the column in two elution steps. The same flow velocities used in adsorption were also used during desorption. De-ionized water, 2,000 ml; 40 % aqueous ethanol solution, 4,000ml and 90 % aqueous ethanol solution, 3,000 ml were chosen as elution solution. All elution solutions were passed through the column twice. Elution stages and used volumes are given in Table 4.4.

Table 4.4. Elution stages and used elution volumes

Flow Velocities (cm/h)			**122**	**367**	**611**
Elution 1	De-ionized water	(ml)	2,000	2,000	2,000
Elution 2	40% EtOH	(ml)	4,000	4,000	4,000
Elution 3	90% EtOH	(ml)	3,000	3,000	3,000

Afterwards, in desorption experiments for three different flow velocities, 1 ml samples were taken from downstream within 3 minutes intervals. Therefore concentration of effluent stream was monitored through HPLC analysis.Shematic representation was shown in Figure 4.4.

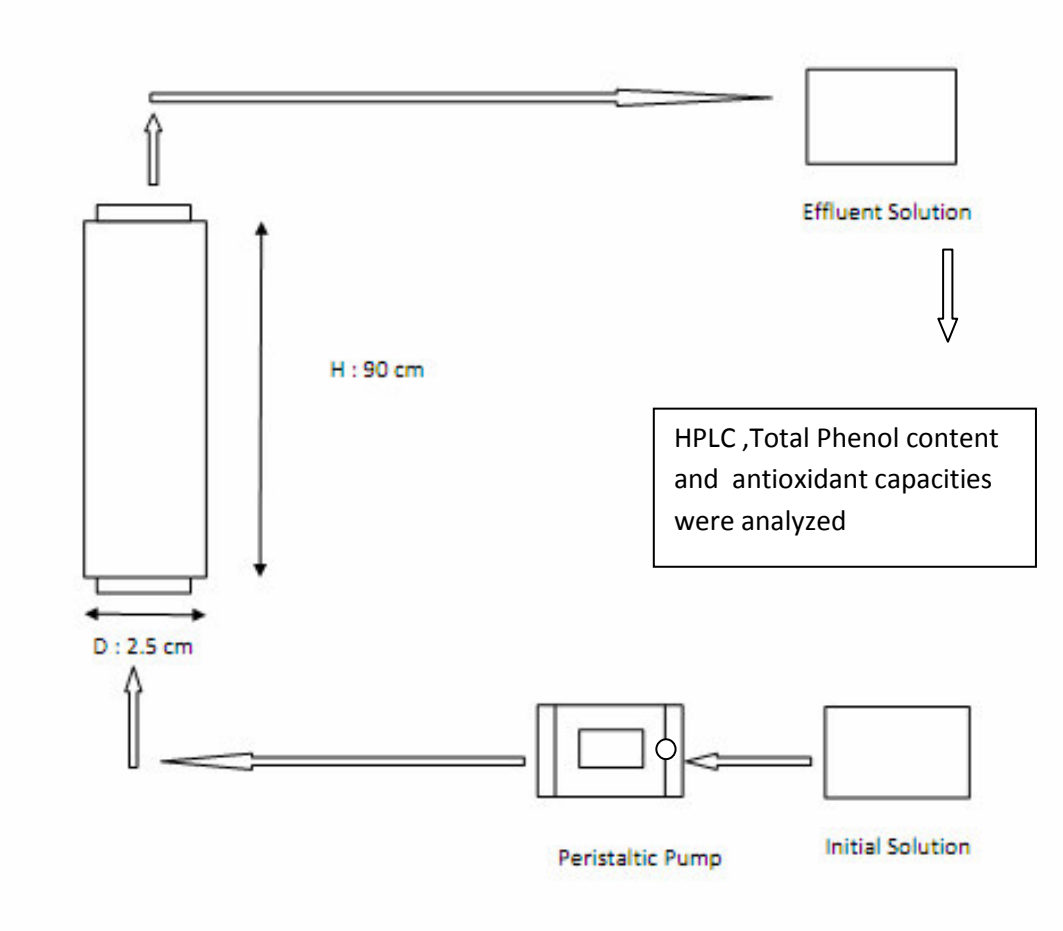

Figure 4.4.General schematic representation of adsorption and desorption procedure.

The adsorption process included four main stages. These steps were conditioning the solid phase (resin), loading solution into the column (adsorption), washing and elution respectively. At the first stage, the column was conditioned with pure ethanol and then deionized water. Second stage was adsorption; the sample solution was fed at constant flowrate into the column until equilibrium was reached. Then, column was washed with deionized water in order to remove residuals and impurities. Eventually, loaded column was eluted with a certain volume of aqueous solutions with 40% and 90% ethanol content.

Dynamic experiments were carried out to investigate the effect of feed flow velocity on the breakthrough point of the breakthrough curve and the effects of eluent composition and flow velocity on the desorption performance of the column.

4.2.7. Total Phenol Analysis

Total phenol analysis of the olive leaf extract fractions were done by Folin-ciocalteu method using gallic acid as a standard. For the total phenol analysis, calibration curve was constructed for gallic acid standard 250 mg gallic acid was firstly dissolved in 10 ml ethanol and then it was diluted to 500 ml by distilled water for the construction of calibration curve. The prepared 0.5 mg/ml stock gallic acid standard was kept at +4 ºC. Next, working standards of 0.02, 0.03, 0.04, 0.05 and 0.06 mg/ml were prepared for calibration. Finally, absorbance values at 725 nm versus gallic acid concentrations were plotted and the calibration curve of gallic acid was constructed with an R^2 value of 0.9981 (Appendix B). Olive leaf extract fractions were dissolved in DMSO in a ratio of 1 g extract in 20 ml solvent. Appropriate dilutions were prepared for the samples. Next, 500 µl of the diluted sample solution were blended with 2.5 ml Folin-ciocalteu reagent that was previously diluted in 1:10 ratio. The blend was left at room temperature for 2.5 minutes to allow folin-ciocalteu reagent to react fully with the oxidizable substances or phenolates. Then 2 ml of Na_2CO_3 (7.5 %) was added to destroy the residual reagent. Then, the blend was incubated for 1 hour at room temperature in a dark place. Incubated samples can be seen in Figure 4.5.

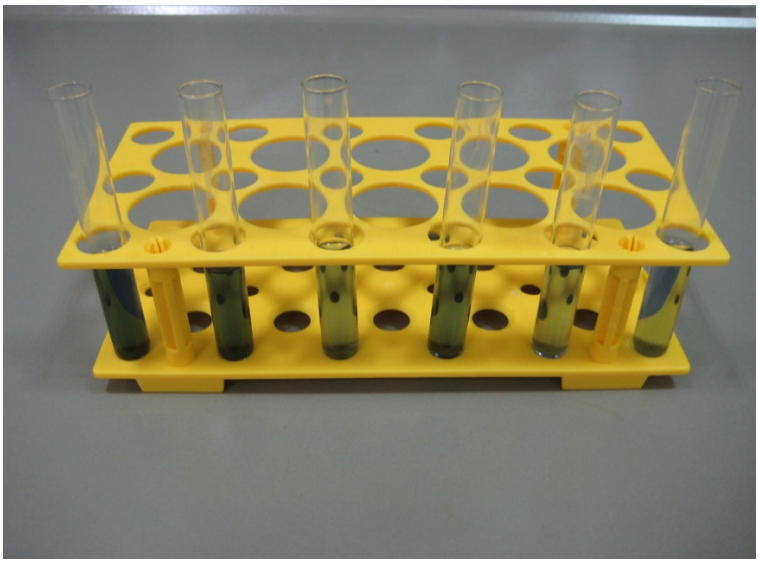

Figure 4.5. Samples after incubating 1 hour in a dark place

Afterwards, absorbance values were measured at 725 nm by UV-Visible Spectrophotometer. All samples were analyzed at least three times.

4.2.8. Antioxidant Analysis

Many tests have been used for the measurement of the total antioxidant activity of body fluids, food extracts, and pure compounds (Re et al., 1999). The method used in this study based on the ability of olive leaf antioxidants to scavenge the ABTS+ (ABTS radical cation) compared with a standard antioxidant (Trolox) in a dose-response curve. 7 mM aqueous ABTS solution mixed with 2.45 mM potassium persulfate solution to form ABTS+. Then mixture stayed in the dark at ambient temperature for 12-16 hours to complete the reaction. The ABTS+ solution diluted with ethanol to an absorbance of 0.7 (±0.02) at 734 nm and equilibrated at 30 °C. Stock solutions of phenolics in ethanol were prepared as they produced inhibition between 20 % - 80 %. 20 µl of phenolic compounds was added to 2 ml of diluted ABTS+ solution. Absorbance was taken at each 1 minute during 6 minutes at Thermo Multiscan UV spectrophotometer (Appendix C).

CHAPTER 5

RESULTS AND DISCUSSION

5.1. Extraction Yield of Olive Leaf

As a result of the standardized extraction protocol, extraction yield was obtained for olive leaf. Extraction yield was found as 21.9 %. This result was calculated from the initial weight and expressed in terms of percentage. For olive leaf, 10 gram fine powder was used and after extraction procedure, 2.19 gram dry crude extract was obtained. This extract was weighted and the value was converted into percentages.

5.2. HPLC Analysis and Identification of Phenolic Compounds

Oleuropein and Rutin are the two major polyphenols, contributing to total antioxidant capacity of olive leaf. So, identification of this compound is essential in olive leaf related studies. Qualitative and quantitative specification of oleuropein and rutin can be achieved by HPLC analysis. Oleuropein and rutin were qualified by analyzing their retention times with the corresponding standards and then they were quantified calibration methods. These calibration methods and the calibration curves for oleuropein and rutin are given in Appendix A.

HPLC chromatogram of olive leaf crude extract and abundance of the two main phenolic compounds with the retention times are given in Figure 5.1.

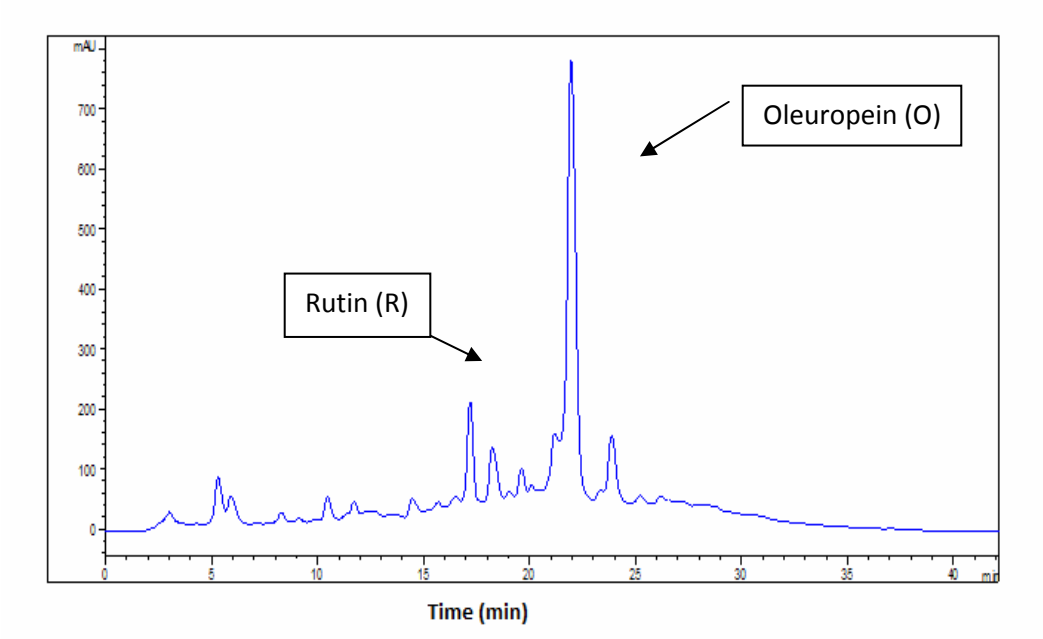

Figure 5.1. HPLC chromatogram of olive leaf. R: Rutin; O: Oleuropein

Oleuropein, the main phenolic compound of olive leaf extract, was first qualitatively specified by comparing its retention time with its standard and then it was quantitatively determined by using calibration methods. These methods are stated in detail. The calibration curves for oleuropein and rutin presented in Appendix A. Retention time of oleuropein in olive leaf extract was 21.96 and rutin in olive leaf extract was 17.20 minutes due to their different polarities gives and an idea about its polarity. Reversed phase HPLC is a combination of non-polar column with high polar mobile phase. High polarity solutes elute first in reversed phase HPLC, which means rutin is more polar than oleuropein.

5.3. Selection of Macroporous Amberlite Resins

Resins that is used in my experiment can be separated into two groups . XAD4 and XAD16 are non-polar and XAD7HP is moderate-polar. Table 4.3. shows physical properties of Amberlite XAD4, XAD16 and XAD7HP adsorbents. According to results, adsorption of oleuropein and rutin occurred on all non-polar and moderate polar resins but at different levels. The extent of adsorption depends on the interactions between the adsorbates and each adsorbent. Weak physical forces between hydrophobic parts of the

organic molecule and the resin is one of the interactions responsible for adsorption. Also, the chemical structure such as types of functional groups and physical properties e.g. porosity and surface area of resin identify its adsorption capacity.

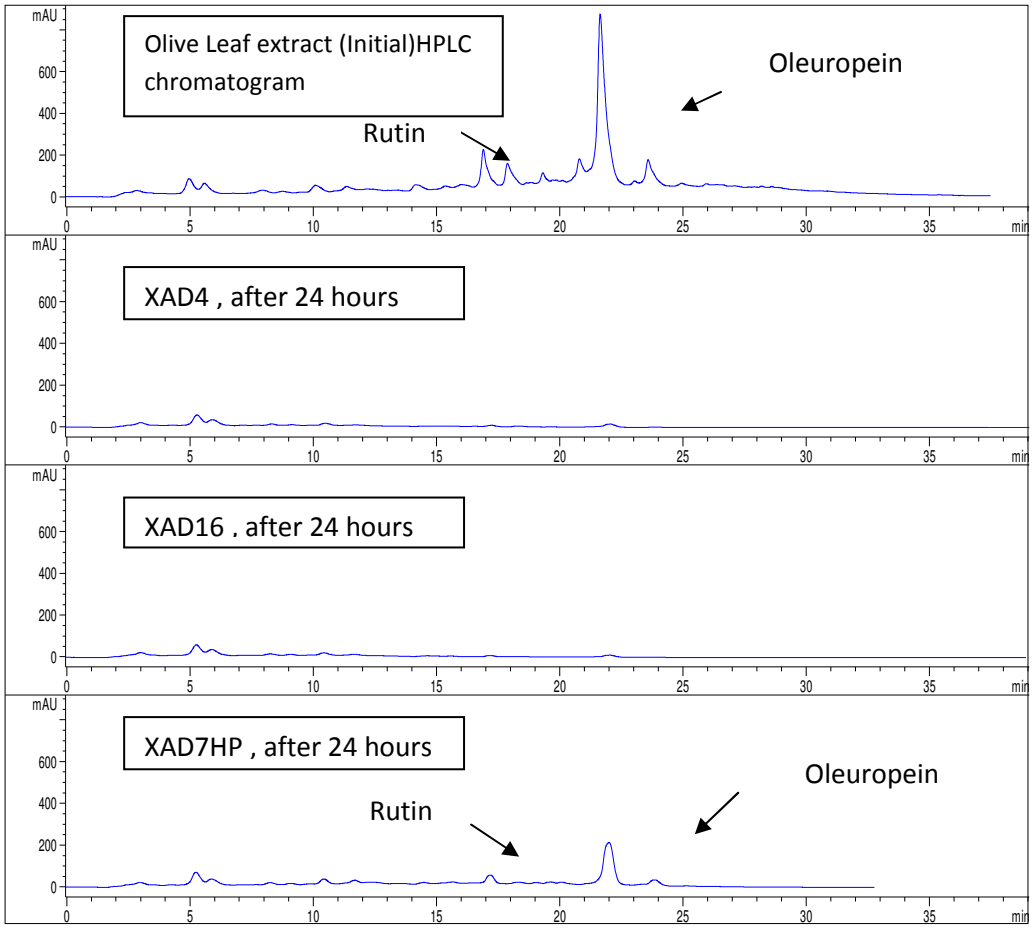

Figure 5.2. Adsorption efficiencies of Amberlite resins.

Figure 5.2. Shows that the adsorption efficiencies of oleuropein and rutin on non-polar resins were higher than their efficiencies on moderate polar resins. This shows that non-polar resins adsorbed oleuropein and rutin more effectively than moderate polar. Surface area is a factor affecting adsorption efficiency of a resin. The surface area of non-polar resins XAD4 (750 m^2/g) and XAD16 (800 m^2/g) are much larger than XAD7HP (380 m^2/g). The surface area of XAD4 (750 m^2/g) was approximately 40% larger than that of XAD7HP (380 m^2/g). The surface area of XAD16 (800 m^2/g) was approximately 43.75 % larger than that of XAD7HP (380 m^2/g).

Pore size of resin is another factor which can affect the adsorption capacity and the adsorption efficiency. The average pore diameters of all the resins are nearly the same. All have around 5-10 nm pore diameter which is much larger than the estimated molecular size of oleuropein and rutin. Estimated molecular size of oleuropein and rutin were 1.08 nm (Alexander et al., 2007). Therefore, oleuropein and rutin can be distributed through the pores easily to the internal surface. This demonstrates the difference in adsorption efficiency was not related to average pore diameters. However, the non polar resins XAD4 and XAD16 adsorbed almost all compounds in the olive leaf liquid extract. This situation may cause some desorption problems. For this reason and according to many literature studies, XAD7HP was chosen as an efficient adsorbent for further experiments.

5.4. Static Experiments

5.4.1. Adsorption Equilibrium

When adsorbate confronts adsorbent, the phenomena called as adsorption occurs and within an adequate time interval, adsorbent saturates and the adsorption seizes. The adsorption of oleuropein and rutin on specified resin was monitored for 240 minutes in order to determine kinetic adsorption behaviour of the system. Figure 5.3. shows the adsorbed amount of oleuropein and rutin versus time.

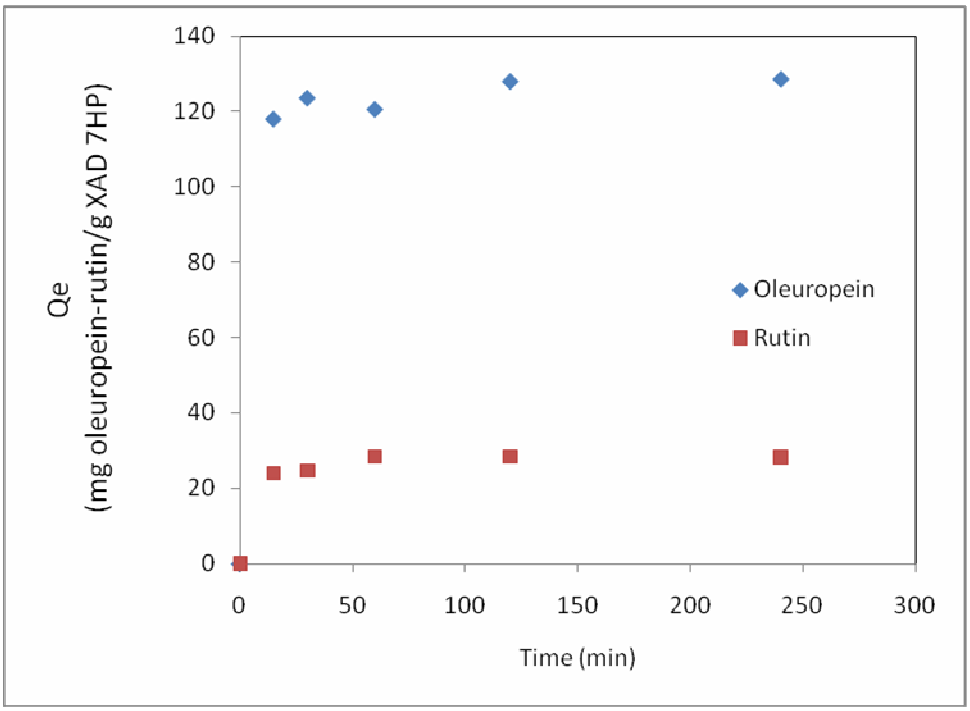

Figure 5.3. Adsorption behavior of XAD7HP during 4 hours.

Adsorption considerably occurred in the first fifteen minutes and then increased in total adsorbed amount gradually for 30 minutes. After 30 minutes, the adsorption reached an equilibrium. Therefore, 30 minutes was satisfactory for the removal of olive leaf antioxidants and after 30-minute contact time, the equilibrium assumption was valid for this system. In this study, adsorption was performed for 4 hours. On the other hand, the studies in the literature indicated that approximately 2 or 3 hour adsorption time was typically enough to obtain polyphenols (Silva et al., 2006; Karammer et al., 2009;Li et al 2004). The equilibrium time has great importance to find out the maximum adsorption capacity of the system and to form adsorption isotherms.

5.4.2. Adsorption Isotherms

The adsorption isotherms represent the relations between equilibrium concentrations of the adsorbates in the liquid phase (C) and the solid phase (Q) at a constant temperature. Solid phase concentration of adsorbates is described as mass adsorbed per unit mass of original adsorbent. Olive leaf extracts with five different initial concentrations and two different alcohol contents were used in this study to

understand the effect of initial oleuropein and rutin concentration on adsorption.

Ethanol contents were determined considering limitations of industrial extraction process. In conventional extraction, ground feedstock is simply mixed with solvent which is grain alcohol for most cases, and the extract is distilled to remove ethanol. This process ends with a certain amount of residual ethanol because of difficulties in the separation process for ethanol and water creates an azeotropic binary system. The adsoption process proposed for selective adsorption of oleuropein and rutin from such extracts have been assumed to have boundary conditions as 10 % ethanol content that represents the actual case, and 0% ethanol which is the ideal case. While Figure 5.4. demonstrates the increase in adsorption when initial olive leaf extract concentration varies from 10 mg/ml to 50 mg/ml at constant temperature. Figures 5.4.-5.7. displays the adsorption isotherms of oleuropein and rutin on XAD7HP resins at the two different alcohol percentages, 0 % and 10 %. The Langmuir model and Freundlich model (Warren, 2005) were used to explain the adsorption isotherms obtained experimentally. One sample calculation is given in Appendix D.

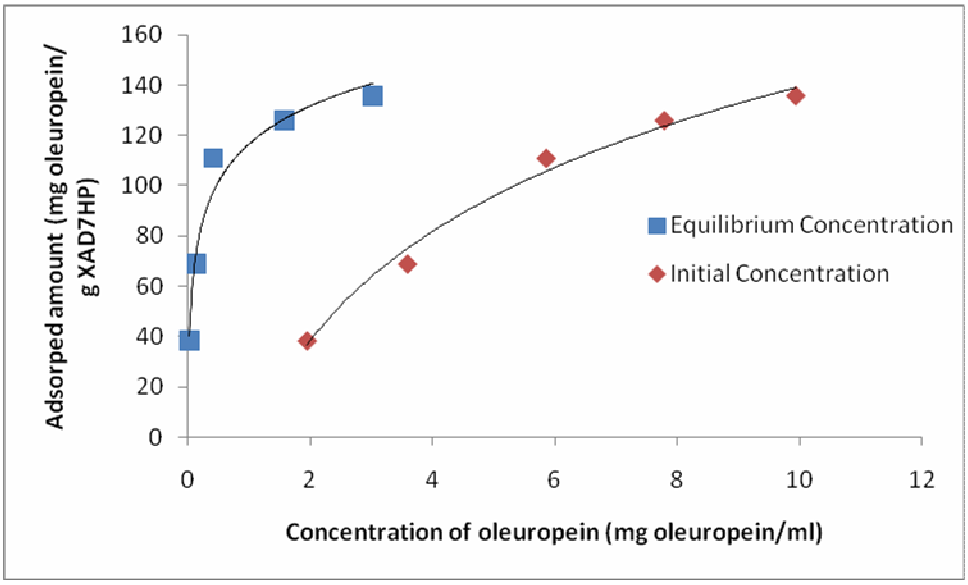

Figure 5.4. The adsorption isotherms of oleuropein on XAD7HP resinat 0 % alcohol content.

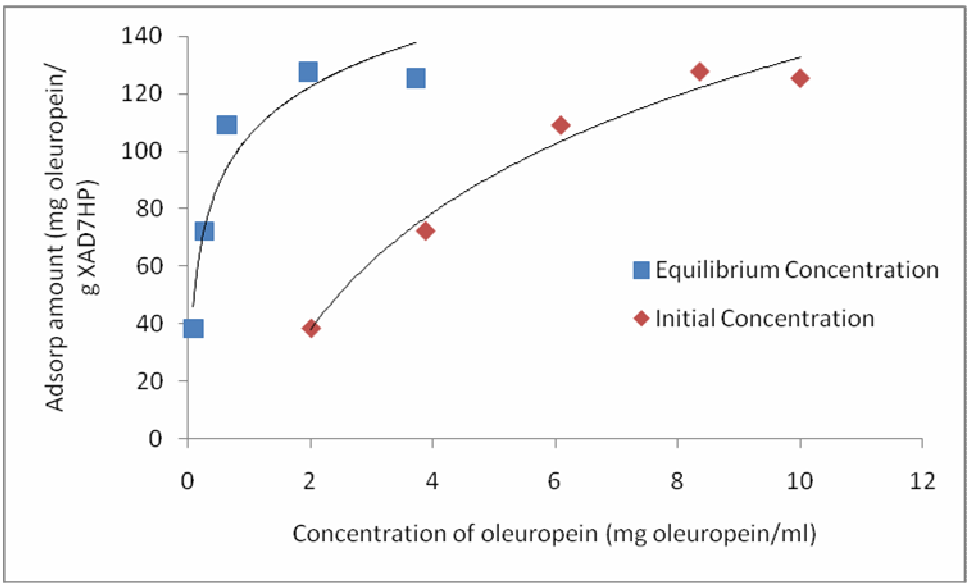

Figure 5.5. The adsorption isotherms of oleuropein on XAD7HP resin at 10 % alcohol content.

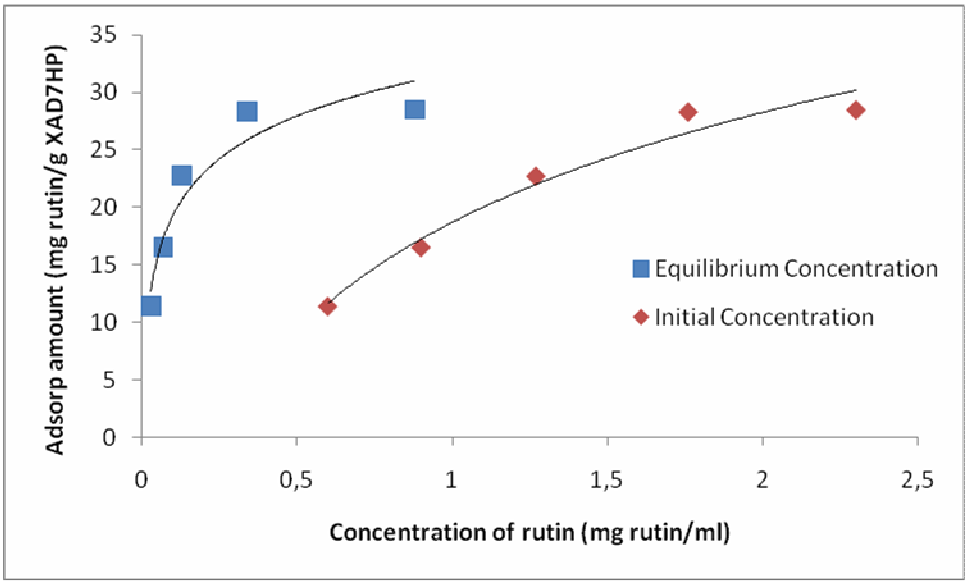

Figure 5.6. The adsorption isotherms of rutin on XAD7HP resin at 0 % alcohol content

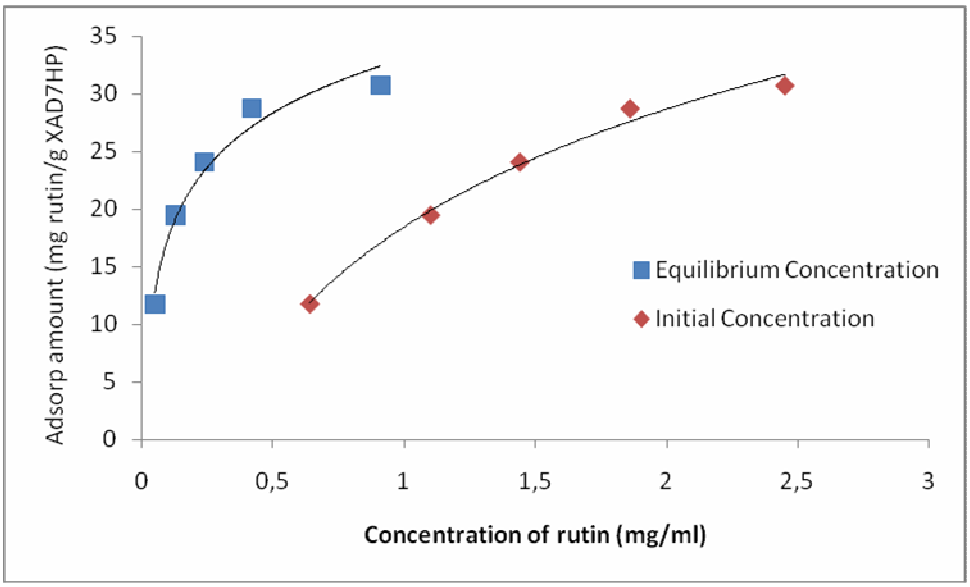

Figure 5.7. The adsorption isotherms of rutin on XAD7HP resin at 10 % alcohol content.

Increasing the olive leaf extract concentration, which also increased the concentration of oleuropein and rutin in the solution. The initial concentration of oleuropein was changed from 1.95 mg/ml to 9.94 mg/ml for 0% alcohol and changed from 2.01 mg/ml to 10 mg/ml for 10% alcohol. Besides the inital oleuropein concentartion, the initial concentration of rutin was changed from 0.6 mg/ml to 2.3 mg/ml for 0 % alcohol and changed from 0.64 mg/ml to 2.45 mg/ml for 10 % alcohol a significant increase in the adsorption of oleuropein and rutin were observed until initial olive leaf extract concentration was set to 40 mg/ml and concentrations over 40 mg/ml did not affect the adsorption of oleuropein and rutin.

The Langmuir isotherm can be described as, (Scordino et al., 2004)

$$Q_e = \frac{Q_m K_L C_e}{1 + K_L C_e} \tag{5.1}$$

The model is built on monolayer adsorption onto a surface with a finite number of identical sites with the same heat of adsorption for all sites.

The Freundlich isotherm model can be described as, (Scordino et al., 2004)

$$Q_e = K_F (C_e)^{1/n} \tag{5.2}$$

The model is built on multilayer adsorption of adsorbates on the heterogeneous surface.

Langmuir adsorption equilibrium constant is denoted as K_L. Freundlich adsorption equilibrium constant is denoted as K_F. Q_m stands for maximum adsorption capacity and 1/n demonstrates energy or intensity of the adsorption.

The linearized Langmuir model and Freundlich model equations can be presented as (Scordino et al., 2004)

$$\frac{1}{Q_e} = \frac{1}{Q_m} + \frac{1}{K_L Q_m C_e} \tag{5.3}$$

$$\ln Q_e = \ln K_F + \frac{1}{n} \ln C_e \tag{5.4}$$

The adsorption data was used to estimate linear form of the Langmuir model equation. The Langmuir isotherms can be derived by plotting $1/Q_e$ against $1/C_e$ as presented in Figures 5.8-5.11. This gives the Langmuir isotherms for oleuropein with 0 %, 10 % and rutin with 0 %, 10 % alcohol content respectively. The intercept of regression lines at $1/Q_e$ axis is $1/Q_m$ and the slope of lines is $1/K_L Q_m$. Table 5.1 shows the Q_m, K_L and r^2 (correlation coefficient) values.

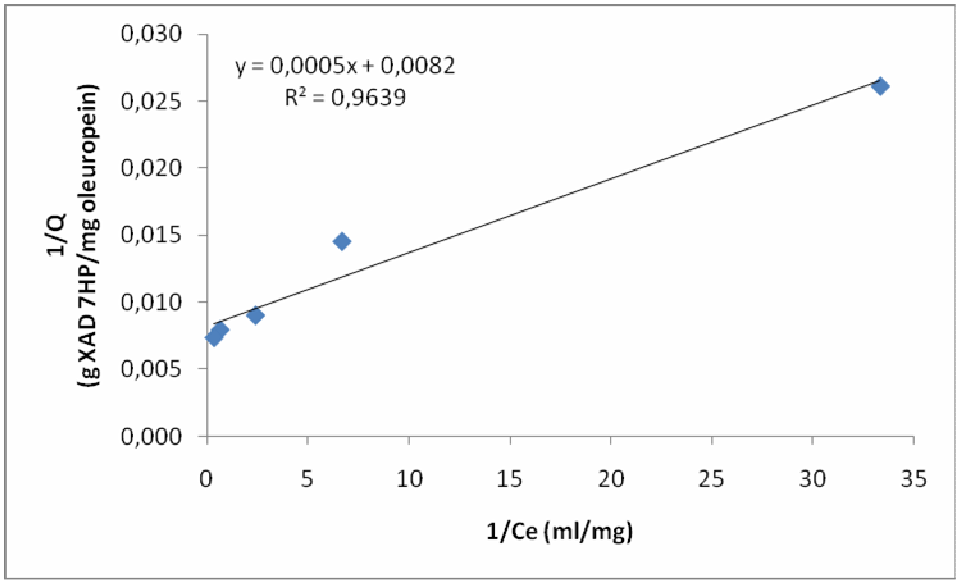

Figure 5.8. Langmuir isotherm for oleuropein with 0 % alcohol content (The plot of $1/Q_e$ against $1/C_e$).

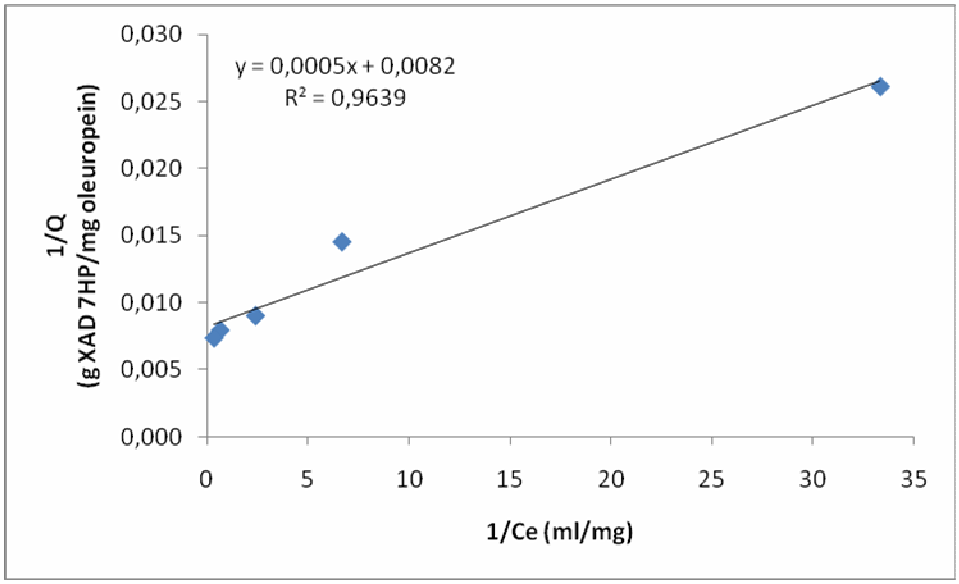

Figure 5.9. Langmuir isotherm for oleuropein with 10 % alcohol content (The plot of $1/Q_e$ against $1/C_e$).

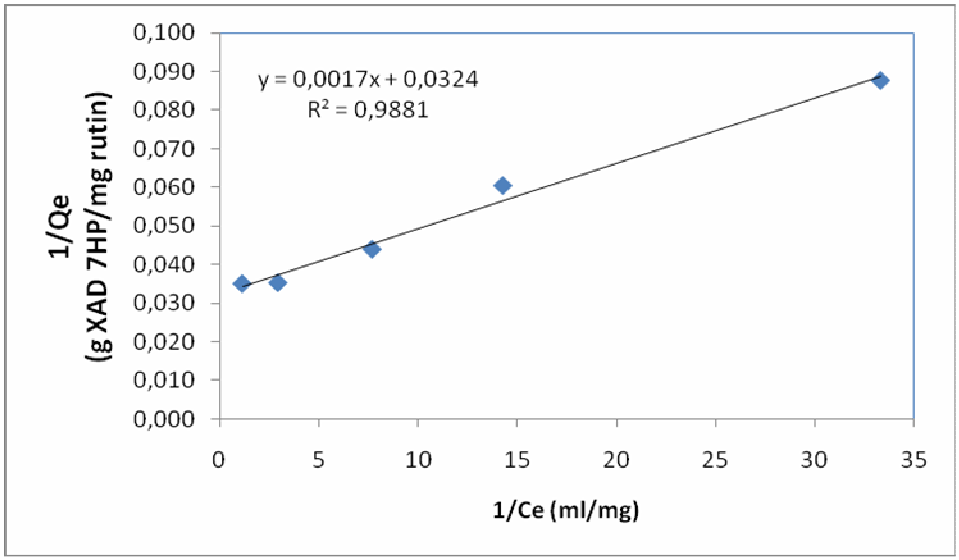

Figure 5.10. Langmuir isotherm for rutin with 0 % alcohol content (The plot of $1/Q_e$ against $1/C_e$).

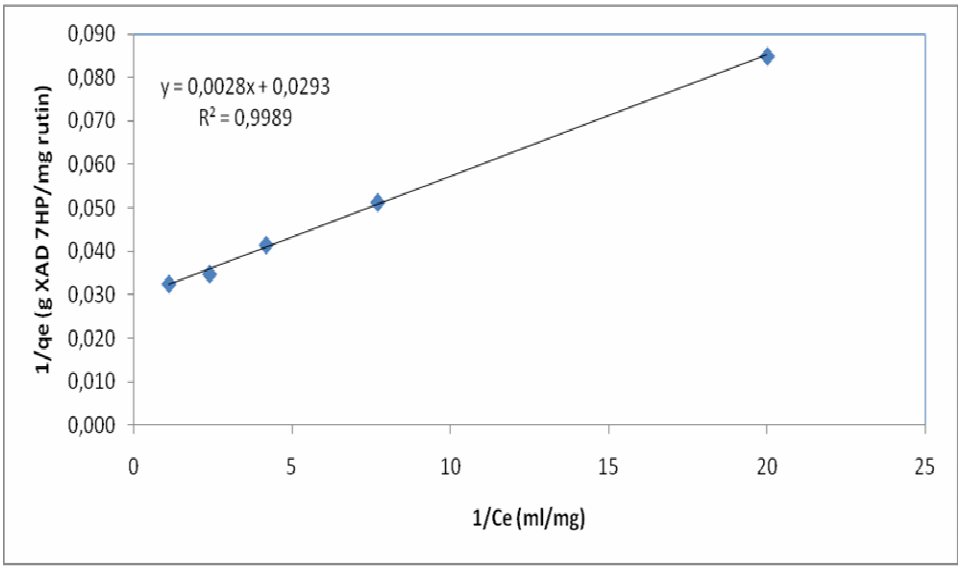

Figure 5.11. Langmuir isotherm for rutin with 10 % alcohol content (The plot of $1/Q_e$ against $1/C_e$).

Table 5.1. Langmuir Constants at different alcohol percent.

	Temperature (K)	Q_m (mg/g resin)	K_L	r^2
Oleuropein , 0 % alcohol content	298	121.95	16.4	0.9639
Oleuropein , 10 % alcohol content	298	140.84	14.2	0.997
Rutin, 0 % alcohol content	298	30.86	19.05	0.9881
Rutin, 10 % alcohol content	298	34.13	10.46	0,9989

The increase in maximum adsorption capacity Q_m were shows that adsorption was higher at a higher alcohol content. Experimental results were consistent with the rise in Q_m with higher alcohol content. In the next step of the study, extract solution with 10% alcohol content is used since usage of 10 % alcohol has positive effects on maximum adsorption capacity.

Q_m for 10 % alcohol content, the maximum adsorption capacity of XAD7HP for oleuropein was evaluated as 140.84 mg oleuropein/g XAD7HP and evaluated as 34.13 mg rutin/g XAD7HP by using the Langmuir equation. From the plateau of the adsorption isotherm given in Figure 5.5 and 5.7, the maximum adsorption capacity was determined as 127.71 mg oleuropein/g XAD7HP and determined as 30.74 rutin/g XAD7HP. The closeness of these values with experimental data and the model proved the validity of the monolayer coverage.

Freundlich isotherms can be derived by plotting $\ln Q_e$ against $\ln C_e$. The K_F is equal to the intercept and 1/n is equal to the slope of the regression lines. On the other hand, the adsorption data was not estimated on the linear form of the Freundlich model equation since there is a limit in the adsorption capacity of XAD7HP.

5.5. Characterization of Adsorbent for Possible Use in the Fluidized (Expanded) Bed Adsorption

5.5.1. Expansion Characteristics of XAD7HP

Expansion experiments were conducted with the Amberlite XAD7HP adsorbent with initial sedimented bed heights of 55 cm. The flow velocity is limited by column height, since a column with 90 cm height was used in the experiments. Deionized water was pumped upward into the column at a particular flowrate. The bed height was recorded every 1 min. The bed height was measured three times for each flowrate after the expansion reached an equilibrium and the mean value of bed height was used to estimate the expansion factor and bed voidage. Figure 5.12 shows the bed expansion ratio as a function of time for various flow velocities with the Amberlite XAD7H adsorbent. The same approach was conducted for each flow velocity employed in experiments.

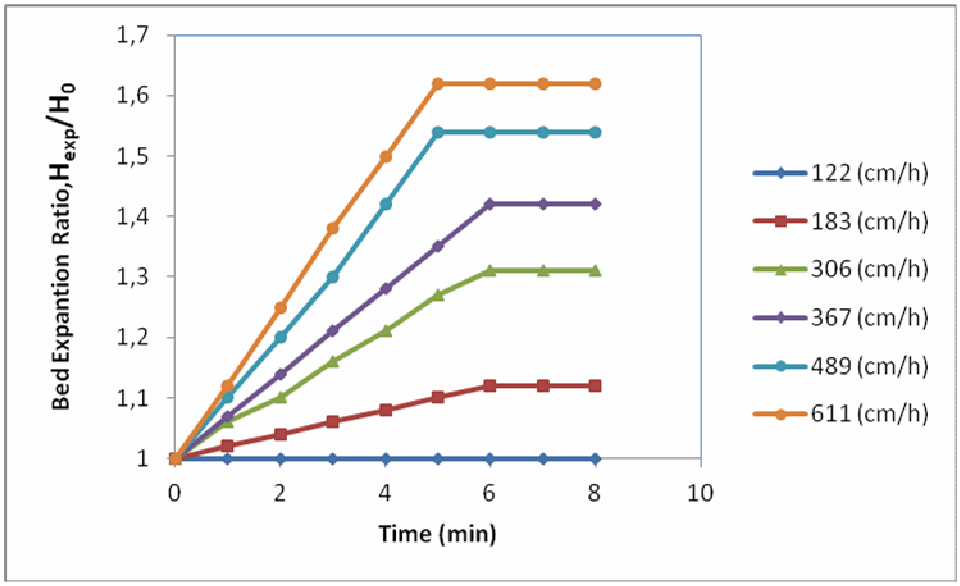

Figure 5.12. Bed expansion ratio as a function of time for various flow velocities with the Amberlite XAD7H adsorbent (H_0 = 55 cm).

5.5.2. Correlation of Bed Expansion Ratio and Liquid Fow Velocity

The results of the bed expansion studies were used to calculate the values of experimental Richardson–Zaki parameters. The gradient of the R–Z plot yields values of the R–Z parameter, n is 3.43.

Figure 5.13 exhibits the R–Z plot of ln u against ln ε. The data shows linear relationship and fit the R–Z correlation well. The R^2 value for the R–Z plot of 55-cm bed is 0.9823. The gradient of the R–Z plot reveals values of the R–Z parameter, n is 3.43. The intercept of the y-axis gives the value of ln u_t hence enabling u_t to be calculated using the linearized version of equation.

Table 5.2. Experimental Richardson–Zaki parameters for the Amberlite XAD7HP.

	Amberlite XAD7HP
	55 cm Fixed Initial Bed Height
n	3.43
u_t (ml/min)	2640.7

Stokes' law Eq. (4.4), or Martin's Eqs. (4.5)– (4.7) can be used to calculate theoretical values of u_t and n can be estimated using Eq. (4.8). Table 5.3. presents theoretical and experimental values of n and u_t for comparison. There are differences between the experimental and theoretical predictions of the value of u_t and n, since Stokes' equation is appropriate only in the ideal condition in which the particle suspension is infinitely dilute. Richardson–Zaki equation tries to explain the behavior during hindered settings. Figure 5.13 shows the relationship between flow velocity and bed expansion ratio at initial bed height of 55 cm.

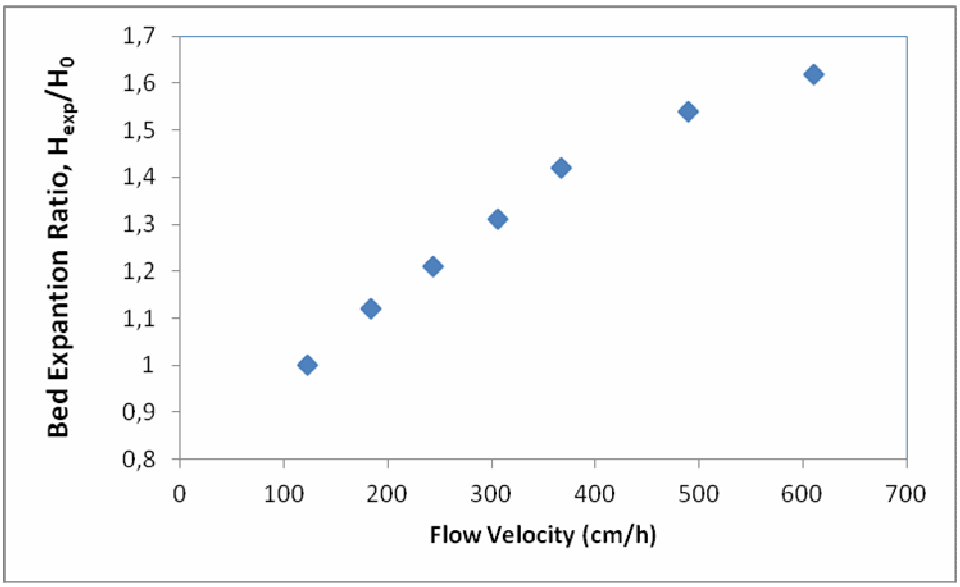

Figure 5.13. Relationship between flow velocity and bed expansion ratio at initial bed height of 55 cm.

Table 5.3. Comparison of experimental and theoretical Richardson-Zaki parameters for the Amberlite XAD7HP.

	u_t (cm/h)			n	
	Experimental	Stoke' Law	Eqs.(4.5)-(4.7)	Experimental	Eqs.(4.5)–(4.7)
XAD7HP	2640,7	2463.04	1552.9	3.4	4.6

5.6. Dynamic Study

5.6.1. Column Adsorption Study

In the previous section 5.4., it was explained which alcohol content of crude extract solution affected the maximum adsorption capacity. The results showed that adsorption capacity of an alcoholic aqueous extract solution with 10 % ethanol was better than aqueous extract solution which contained no ethanol. Therefore it was decided to carry out further studies with 10% alcoholic aqueous extracts for investigating dynamic adsorption behaviour.

The dynamic adsorption experiments were performed to compare the

performances of fixed bed and fluidized bed column. The concentration and bed depth parameters were kept constant. Only feed flow velocity was changed. Experiments were performed by feeding unclarified extract solution having initial oleuropein concentration of 2.04 mg/ml and rutin concentration 0.44 mg/ml. The column was fed at a flow velocity of 122 cm/h, corresponding to 10 ml/min flow rate operated as a fixed bed while operation was in an expanded bed mode at flow velocity of 367 cm/h, 611 cm/h, corresponding to 30 ml/min and 50 ml/min flow rates, respectively. The same column and the experimental setup were used in all experiment in this study. Fluidized bed properties at different flow velocity were given in Figure 5.14.

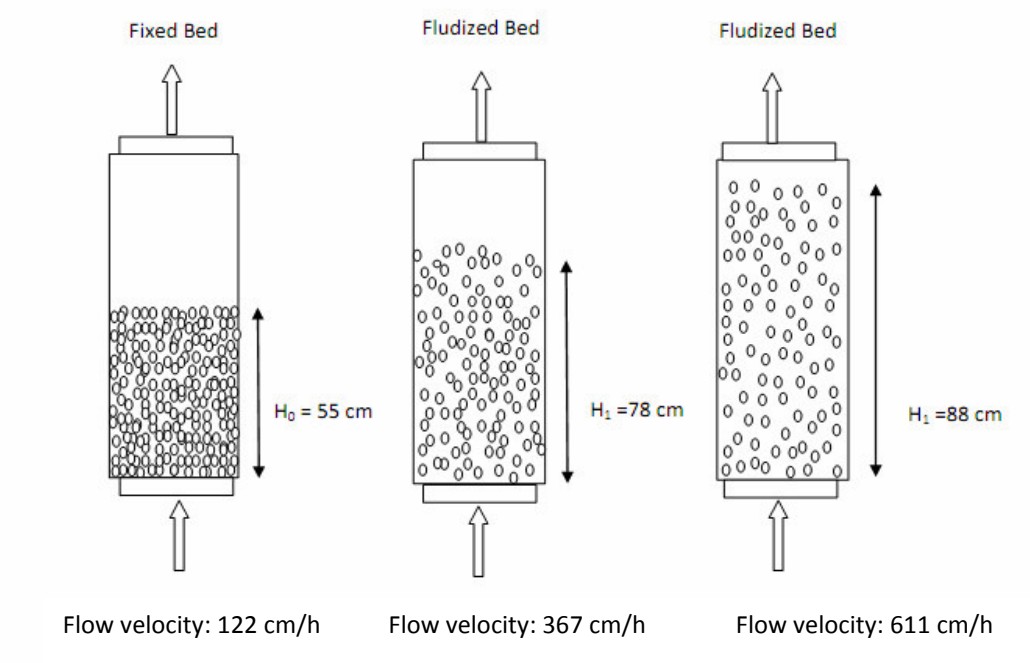

Figure 5.14. Schematic representation of fluidized bed at different flow velocity.

Fixed bed was operated at a chosen flow velocity value below minimum fludization velocity. The experimental conditions for all cases were as listed in Table 5.4.

Table 5.4. The experimental conditions for column

	Fixed Bed	Fluidized Bed	Fluidized Bed
Feed Flow velocity (cm/h)	122	367	611
Initial Oleuropein Concentration (mg/ml)	2.04	2.04	2.04
Initial Rutin Concentration (mg/ml)	0.44	0.44	0.44
Settled Bed Height (cm)	55	55	55
Expansion Ratio	1	1.42	1.62
Expanded Bed Height (cm)	55	78	88

5.6.1.1. Effect of Feed Flow Velocity

The operating parameters comprising only the feed flow velocities were examined by the effect of flow velocity on the breakthrough point of the breakthrough curve.

Dynamic binding capacities can be predicted from the breakthrough curves of oleuropein and rutin. The corresponding total amount of flavonoids bound per unit volume of the adsorbent in the column at 5 % of the breakthrough point was managed for fixed bed adsorption and 50 % for fluidized bed adsorption. The dynamic binding capacities in the current study were computed by the graphic integration method.

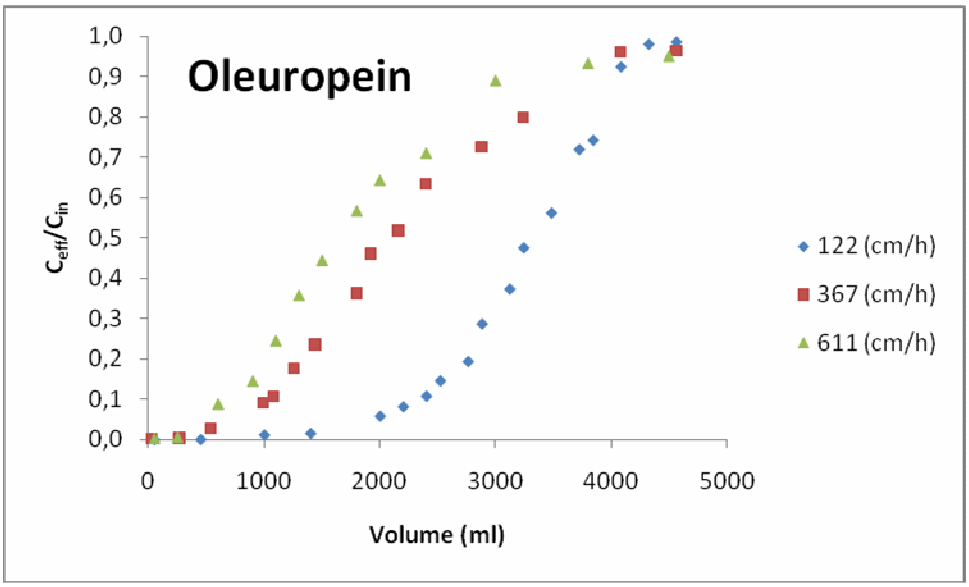

Figure 5.15. The breakthrough curves of oleuropein adsorption in three feed flow velocities. C/C0 = 0.5 for 122 (cm/h), C/C0 = 0.05 for 367 (cm/h) and 611 (cm/h)

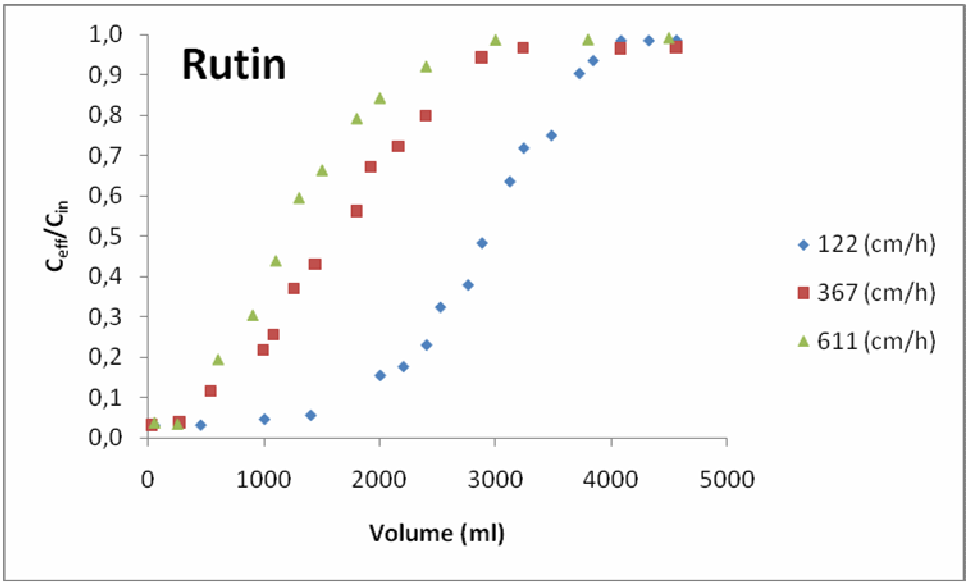

Figure 5.16. The breakthrough curves of rutin adsorption in three feed flow velocities. C/C0 = 0.5 for 122 (cm/h), C/C0 = 0.05 for 367 (cm/h) and 611 (cm/h)

Table 5.5. The Initial concentration of oleuropein (C_i), the breakthrough volume (BV), breakthrough time (BT) at the breakthrough points and the dynamic binding capacity (DBC) in three feed flow velocities.

	Feed flow velocities (cm/h)	**C_i (mg/ml)**	**BV (ml)**	**BT (min)**	**DBC (mg/g adsorbent)**
Fixed Bed-10	122	2.04	1892.85	189.3	33.94
Fluidized Bed-30	367	2.04	2118.10	70.6	24.13
Fluidized Bed-50	611	2.04	1659.06	33.18	19,78

Table 5.6. The Initial concentration of rutin (C_i), the breakthrough volume (BV), breakthrough time (BT) at the breakthrough points and the dynamic binding capacity (DBC) in three feed flow velocities.

	Feed flow velocity (cm/h)	**C_i (mg/ml)**	**BV (ml)**	**BT (min)**	**DBC (mg/g adsorbent)**
Fixed Bed-10	122	0.44	1382.46	138.24	6.97
Fluidized Bed-30	367	0.44	1638.40	54.61	4.84
Fluidized Bed-50	611	0.44	1148.2	22.96	3.89

The experimental results for three feed flow velocities were listed in Table 5.5., 5.6. Figure 5.15., 5.16. shows that breakthrough point of Fluidized Bed-50 case was reached in shorter intervals due to higher feed flow velocity. The earlier breakthrough at high flow velocity may be attributed to the effect of feed flow velocity on the inter particle diffusion of oleuropein molecules into the interior surface of the resin for adsorption. Oleuropein molecules didn't have enough time for diffusion in the course of

pores into the interior active sites for adsorption, so that the leakage comprised earlier. The residence time for oleuropein molecules in the resin was not sufficient for an optimum operation, since the feed flow velocity was too high to obtain maximum yield. Eventually, the adsorbed amount decreased when the feed flow velocity increased.

5.6.2. Column Desorption Study

The desorption experiments were carried out after loading the sample extract solution with a suitable loading volume. The loaded column was first eluted with 2,000 ml of de-ionized water followed by a certain volume of aqueous ethanol solution with in two steps 40 % and 90 % ethanol content. The same flow velocities were used in adsorption and desorption experiments. 40 % aqueous ethanol solution, 4,000ml and 90% aqueous ethanol solution, 3,000 ml were chosen. 2,000 ml de-ionized water was passed through the column twice. Afterwards, 4,000 ml 40 % aqueous ethanol solution was passed through the column twice. In the same way, 3000 ml 90 % aqueous ethanol solution was passed through the column twice. The effluent fractions of the elution steps were collected into tightly closed storage containers and were kept in a dark place at room temperature in order to investigate elution performances of each operation. This investigation was important since desorption is a critical stage for applicability of column work in a continuous operation. So desorption performance exhibits polar interactions between adsorbate and adsorbent, which makes a feasible process impossible when it is too strong.

In this study, the hydrophobic XAD7HP resin adsorbs hydrophobic oleuropein and rutin molecules from aqueous solution since they obey ‘like attracts like’ principle. Success of the desorption shows that the attraction between them is weak physical forces rather than polar attractions.

The adsorbate could be eluted from the resin if the attraction between the adsorbate and the eluent is greater than that of the adsorbate and the resin. Thus an appropriate solvent is chosen to disrupt weak physical forces that retain the adsorbate. The aqueous ethanol was chosen as the only elution solvent in the study because oleuropein and rutin have high solubility in ethanol. Thus, adsorbed oleuropein and rutin could partly be desorbed from the resin. In addition, ethanol is non-toxic and environmental friendly. The concentrated and purified oleuropein and rutin molecules

desorbed from the XAD7HP resin was recovered for use in medical and food applications. Hence, the non-toxic feature of the solvent is very considerable. In this study, gradient elution was used rather than isocratic elution as the former could improve the separation efficiency. Water and ethanol solvents systems differ in polarity. While performing the desorption experiments, elution solvents were deionized water, 40 % and 90 % aqueous ethanol solutions with different that varied polarity. If the relatively more polar impurities match with the polarity of solvent, they will be eluted out with deionized water at first. Then, the relatively non-polar oleuropein and rutin molecules will be mostly eluted out with 40% water-ethanol solution afterwards which constitutes the selective recovery of oleuropein and rutin.

Consequently, the oleuropein and rutin molecules can be completely separated from other compounds which were also adsorbed by the resin with 90% water-ethanol solution and an efficient separation can be achieved. In Table 5.7. recovery ratios and oleuropein purities are given for the process where oleuropein desorbed with 40 % aqueous ethanol was recovered at the greatest extent. Further desorption was achieved in 90 % aqueous ethanol, and then water that is called as wash stream to achieve the ultimate desorption. When the results given in Table 5.7. were examined, it was observed that the highest yield of separation was achieved at the lowest flow velocity.

Table 5.7. Comparison of some operation parameters and recovery of oleuropein between packed bed adsorption and expanded bed adsorption.

Initial Feed Stream	**Operation Flow Velocity**	**(cm/h)**	**122**	**367**	**611**
	Volume	**(ml)**	4560	4560	4500
	Oleuropein	**(mg/ml)**	2.04	2.04	2.04
	Oleuropein	**(mg)**	9302.4	9302.4	9180
	Impurities	**(mg/ml)**	17.86	17.86	17.86
	Impurities	**(mg)**	81441.6	81441.6	80370
	Total Con.	**(mg/ml)**	19.9	19.9	19.9
	Total	**(mg)**	90744	90744	89550
	Prutiy of Oleuropein	**%**	11.42	11.42	11.42
Effluent Stream	**Volume**	**(ml)**	4560	4560	4500
	Oleuropein Con.	**(mg/ml)**	1.42	1.586	1.65
	Oleuropein	**(mg)**	6475.2	7232.16	7425
	Impurities Con.	**(mg/ml)**	14.9	15.2	15.5
	Impurities	**(mg)**	67944	69312	69750
	Total Con.	**(mg/ml)**	16.32	16.79	17.15
	Total	**(mg)**	74419.2	76544.16	77175
	Prutiy of Oleuropein	**%**	9.53	10.43	10.64
Adsorption	**Oleuropein**	**(mg)**	2827.2	2070.24	1755
	Impurities	**(mg)**	13497.6	12129.6	10620
	Total	**(mg)**	16324	14199.84	12375
	Process Time	**(hr)**	7.6	2.53	1.52
Water	**Total Volume**	**(ml)**	2000	2000	2000
	Total Con.	**(mg/ml)**	0.907	0.49	0.503
	Total	**(mg)**	1814.8	979.84	1005
	Oleuropein Con.	**(mg/ml)**	0.235	0.129	0.093
	Eluted Oleuropein	**(mg)**	470.94	258.88	185.52
	Bound Oleuropein	**%**	16.66	12.5	10.57
	Eluted Imp. Con.	**(mg/ml)**	0.67	0.36	0.4
	Eluted Impurities	**(mg)**	1343.85	720.96	819.47
	Bound Impurities	**%**	9.96	5.94	7.72
	Prutiy of Oleuropein	**%**	25.95	26.42	18.46
	Recovery Oleuropein Ratio	**%**	16.65	12.5	10.57
	Process Time	**(hr)**	3.3	1.11	1

(Cont. on next page)

Table 5.7. (cont.)

40% Alcohol	**Operation Flow Velocity**	**(cm/h)**	122	367	611
	Total Volume	**(ml)**	4000	4000	4000
	Total Con.	**(mg/ml)**	1.7	1.49	1.32
	Total	**(mg)**	6820	5980	5300
	Oleuropein Con.	**(mg/ml)**	0.4	0.29	0.3
	Eluted Oleuropein	**(mg)**	1518.56	1151.15	1070.8
	Bound Oleuropein	**%**	56.59	55.6	69.13
	Eluted Imp. Con.	**(mg/ml)**	1.305	1.207	1.02
	Eluted Impurities	**(mg)**	5220.03	4828.85	4086.83
	Bound Impurities	**%**	38.67	39.81	38.48
	Prutiy of Oleuropein	**%**	23.46	19.25	22.89
	Recovery Oleuropein Ratio	**%**	56.59	55.6	69.13
	Process Time	**(hr)**	6.66	2.2	1.33
90 % Alcohol	**Total Volume**	**(ml)**	3000	3000	3000
	Total Con.	**(mg/ml)**	7690	2.413	2.023
	Total	**(mg)**	2.563	7240	6070
	Oleuropein Con.	**(mg/ml)**	0.28	0.19	0.16
	Eluted Oleuropein	**(mg)**	836.67	583.54	491.67
	Bound Oleuropein	**%**	50.77	28.19	28.02
	Eluted Imp. Con.	**(mg/ml)**	2.28	2.218	1.859
	Eluted Impurities	**(mg)**	6853.33	6656.46	5578.33
	Bound Impurities	**%**	50.774	54878	52.527
	Prutiy of Oleuropein	**%**	10.88	8.06	8.1
	Recovery Oleuropein Ratio	**%**	26.76	28.18	28.01
	Process Time	**(hr)**	5	1.66	1
Total	**Operation Flow Velocity**	**(cm/h)**	122	367	611
	Impurities	**(mg)**	13417.46	12206.2	10484.63
	Oleuropein	**(mg)**	2826.17	1993.57	1747.99
	Total	**(mg)**	16243.63	14199.77	12232.62
	Overall Recovery Ratio of Oleuropein	**%**	99.96	96.29	99.6
	Process Time	**(hr)**	22.56	7.5	4.85

In Table 5.7. recovery ratios and oleuropein purities are given for the process where oleuropein was desorbed with water that is named as wash, 40% ethanol and then 90% ethanol solutions. Oleuropein was recovered at the greatest extent at the wash step with 40% ethanol solution where 56.6% of the recovery took place. At the lowest flow

velocity (122 ml/min), purity of oleuropein was improved to 23% with 40% ethanol portion. Further washes were achieved with 90% ethanol solution to regenerate resin. Sample recovery ratio and purity calculation is given appendix E.

Table 5.8. Comparison of some operation parameters and recovery of rutin between packed bed adsorption and expanded bed adsorption.

Initial Feed Stream	**Operation Flow Velocity**	**(cm/h)**	**122**	**367**	**611**
	Volume	**(ml)**	4560	4560	4500
	Rutin Con.	**(mg/ml)**	0.443	0.443	0.443
	Rutin	**(mg)**	2020.08	2020.08	1993.5
	Impurities	**(mg/ml)**	19.46	19.46	19.72
	Impurities	**(mg)**	88723.92	88723.92	88750.5
	Total Con.	**(mg/ml)**	19.9	19.9	20.165
	Total	**(mg)**	90744	90744	89550
	Prutiy of Rutin	**%**	2.28	2.28	2.28
Effluent Stream	**Volume**	**(ml)**	4560	4560	4500
	Rutin Con.	**(mg/ml)**	0.33	0.37	0.38
	Rutin	**(mg)**	1513.92	1682.64	1719
	Impurities	**(mg/ml)**	14.9	16.42	15.5
	Impurities	**(mg)**	72905.28	74861.52	75456
	Total Con.	**(mg/ml)**	16.32	16.79	17.15
	Total	**(mg)**	74419.2	76544.16	77175
	Prutiy of Rutin	**%**	2.22	2.2	2.46
Adsorption	**Rutin**	**(mg)**	506.16	337.44	274.5
	Impurities	**(mg)**	15818.64	13862.4	12100.5
	Total	**(mg)**	16324.8	14199.84	12375
	Process Time	**(hr)**	7.6	2.53	2.53

(Cont. on next page)

Table 5.8. (cont.)

Water	**Operation Flow Velocity**	**(cm/h)**	122	367	611
	Total Volume	**(ml)**	2000	2000	2000
	Total Con.	**(mg/ml)**	0.9	0.49	0.5
	Total	**(mg)**	1814.8	979.84	1005
	Rutin Con.	**(mg/ml)**	0.05	0.02	0.02
	Eluted Rutin	**(mg)**	101.27	44.39	41.1
	Bound Rutin	**%**	20.007	13.15	14.97
	Eluted Imp. Con.	**(mg/ml)**	0.86	0.47	0.48
	Eluted Impurities	**(mg)**	1713.53	935.45	963.9
	Bound Impurities	**%**	10.83	6.75	7.97
	Prutiy of Rutin	**%**	5.58	4.53	4.09
	Recovery Rutin Ratio	**%**	20	13.15	14.97
	Process Time	**(hr)**	3.3	1.11	1
40% Alcohol	**Operation Flow Velocity**	**(cm/h)**	122	367	611
	Total Volume	**(ml)**	4000	4000	4000
	Total Con.	**(mg/ml)**	1.7	1.5	1.32
	Total	**(mg)**	6820	5980	5300
	Rutin Con.	**(mg/ml)**	0.05	0.04	0.03
	Eluted Rutin	**(mg)**	208.69	149.5	128.26
	Bound Rutin	**%**	41.23	44.3	46.72
	Eluted Imp. Con.	**(mg/ml)**	1.65	1.457	1.292
	Eluted Impurities	**(mg)**	6611.3	5830.5	5171.74
	Bound Impurities	**%**	41.79	42.06	42.74
	Prutiy of Rutin	**%**	3.06	2.5	2.42
	Recovery Rutin Ratio	**%**	41.24	44.3	46.72
	Process Time	**(hr)**	6.66	2.2	1.33
90% Alcohol	**Operation Flow Velocity**	**(cm/h)**	122	367	611
	Total Volume	**(ml)**	3000	3000	3000
	Total Con.	**(mg/ml)**	2.563	2.413	2.023
	Total	**(mg)**	7690	7240	6070
	Rutin Con.	**(mg/ml)**	0.053	0.032	0.032
	Eluted Rutin	**(mg)**	157.64	96.29	91.66
	Bound Rutin	**%**	31.15	28.54	33.39
	Eluted Imp. Con.	**(mg/ml)**	2.51	2.381	1.99
	Eluted Impurities	**(mg)**	7532.35	7143.71	5978.38
	Bound Impurities	**%**	47.617	51.53	49.41
	Prutiy of Rutin	**%**	2.05	1.33	1.51
	Recovery Rutin Ratio	**%**	31.14	28.53	33.39
	Process Time	**(hr)**	5	1.66	1

(Cont. on next page)

Table 5.8. (cont.)

TOTAL	**Operation Flow Velocity**	**(cm/h)**	122	367	611
	Impurities	**(mg)**	15857.12	13909.66	12113.98
	Rutin	**(mg)**	467.603	290.18	261.02
	Total	**(mg)**	16324.8	14199.84	12375
	Overall Recovery Ratio of Rutin	**%**	92.38	85.99	95.09
	Process Time	**(hr)**	22.56	7.5	4.85

Besides oleuropein parameters, rutin has also same characteristic properties but also showed some differences. In Table 5.8. recovery ratios of rutin given for the process where rutin desorbed with 40 % aqueous ethanol was recovered at the greatest extent. Further desorption was achieved in 90 % aqueous ethanol, and then water that is called as wash stream to achieve the ultimate desorption. The results given in Table 5.8. have shown us that, the highest yield of separation was achieved at the lowest flow velocity.

5.6.3. Adsorption and Separation of Olive Leaf Crude Extract Polyphenols on XAD7HP

Adsorption of olive leaf extract polyphenols by XAD7HP filled fixed and fluidized bed column were performed to separate the bioactive compounds. The selective accumulation of oleuropein and rutin on the hydrophobic XAD7HP resin displayed the presence of interaction between XAD7HP and polyphenols during the adsorption process. The other polyphenols in olive leaf extract such as verbascoside, apigenin-7-glucoside, luteolin-7-glucoside which have closer retention times to retention time of rutin and oleuropein, were also adsorbed on XAD7HP macro porous resin.

The crude olive leaf extract solution was loaded to the column at three different flow velocities. Feed flow velocities were 122 cm/h, 367 cm/h and 611 cm/h. The XAD7HP macro porous resin was progressively saturated with oleuropein and rutin and also other polyphenols, so the amounts of polyphenols started to stabilize until the saturation of XAD7HP was obtained. Figure 5.17.-5.19. show the HPLC chromatograms of olive leaf extract solutions before and after adsorption study.

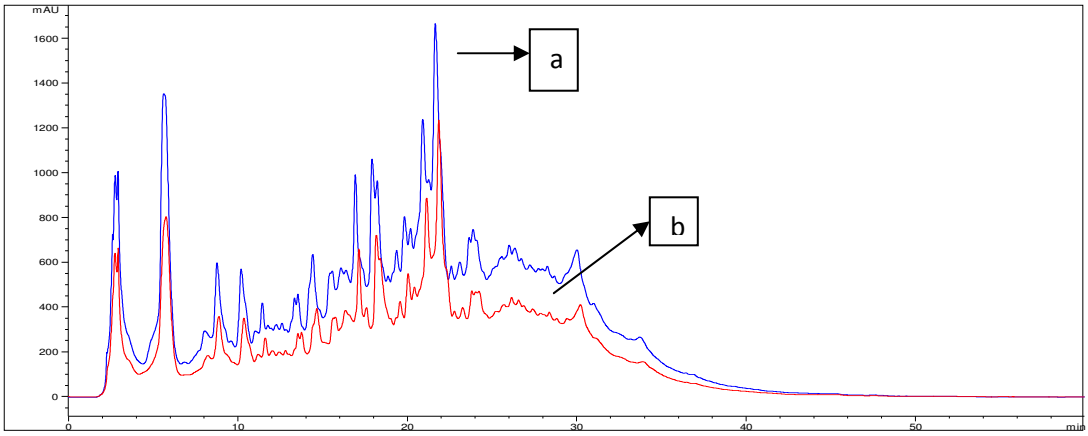

Figure 5.17. HPLC chromatograms of the crude olive leaf extract solution before (a) and after (b) adsorption study for flow velocity 122 cm/h

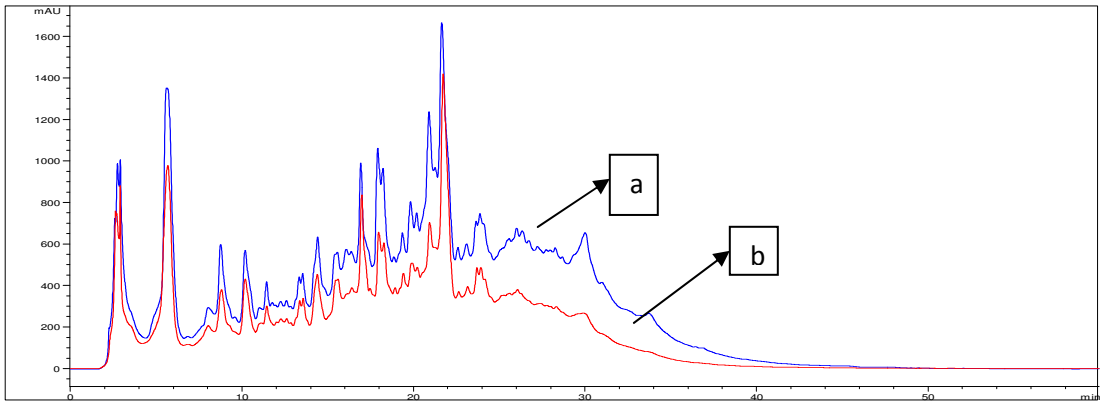

Figure 5.18. HPLC chromatograms of the crude olive leaf extract solution before (a) and after (b) adsorption study for flow velocity 367 cm/h

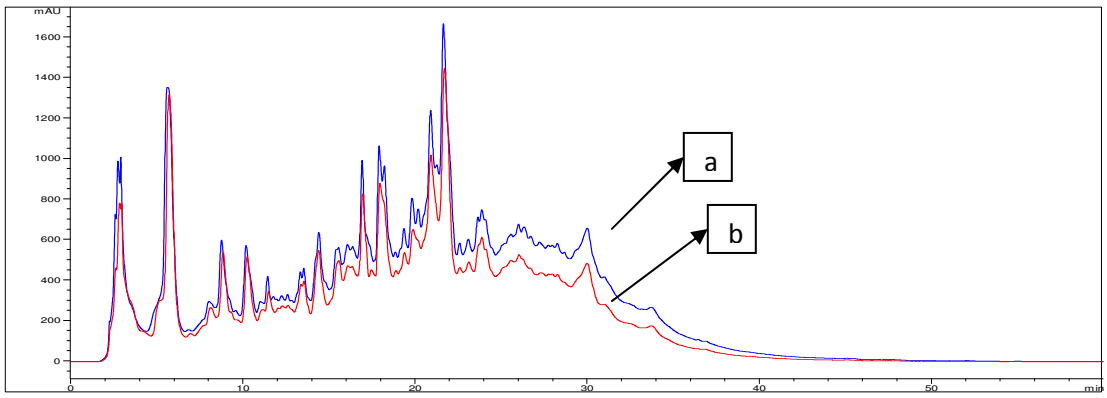

Figure 5.19. HPLC chromatograms of the crude olive leaf extract solution before (a) and after (b) adsorption study for flow velocity 611 cm/h

Initial oleuropein and rutin concentrations of the extract solution were not changed but only the flow velocity increased. The amount of adsorbed oleuropein on the XAD7HP macro porous resin increased with the lower flow velocity. This situation was attributed to the presence of a dynamic equilibrium in the column system

After reaching to the saturation of column, elutions of different fractions were performed first with deionized water and then 40 % and 90 % aqueous ethanol solutions.

2,000 millilitres of water was used to elute nearly all polar compounds from the column. 4,000 millilitres of 40 % aqueous ethanol solution was utilized to separate moderate polar compounds from the XAD7HP filled column. 3,000 millilitres of 90 % aqueous ethanol solution was used to separate non-polar compounds. The HPLC chromatograms of initial olive leaf extract solution, water fraction, 40 % aqueous ethanol fraction and 90 % aqueous ethanol fraction obtained at flow velocities of 122 cm/h, 367 cm/h and 611 cm/h are represented between Figures 5.20-5.22.

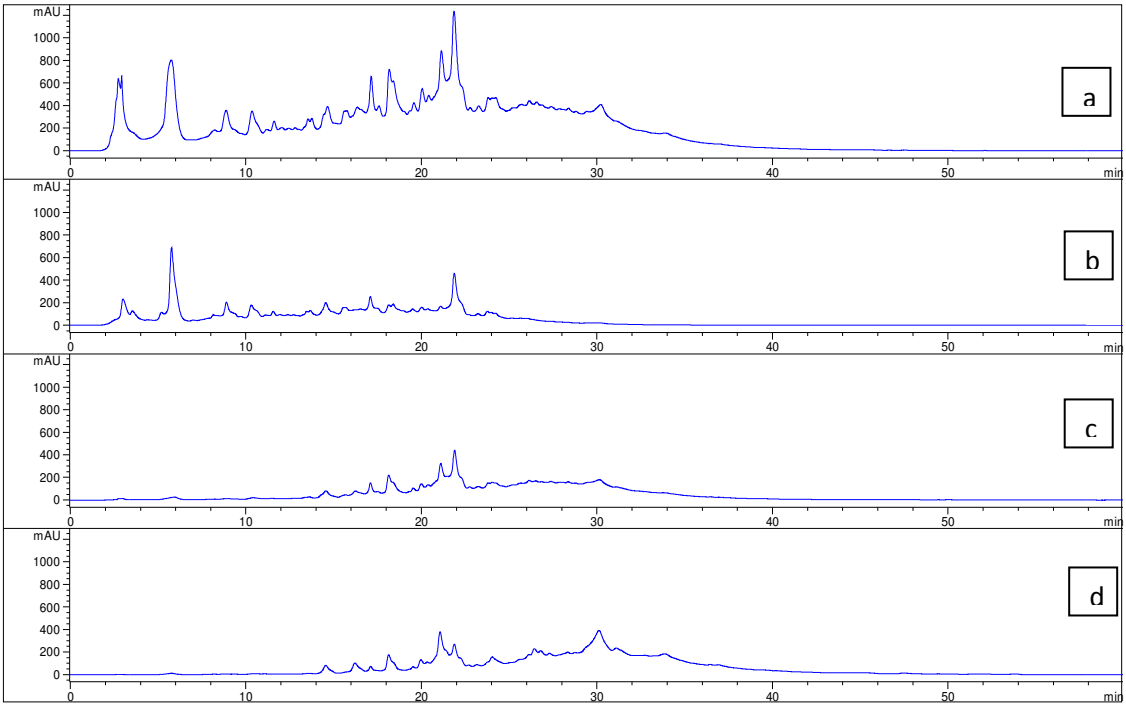

Figure 5.20. HPLC chromatograms of the crude olive leaf extract initial solution (a), water fraction (b), 40% aqueous ethanol fraction (c) and 90% aqueous ethanol fraction (d) for flow velocity 122 cm/h.

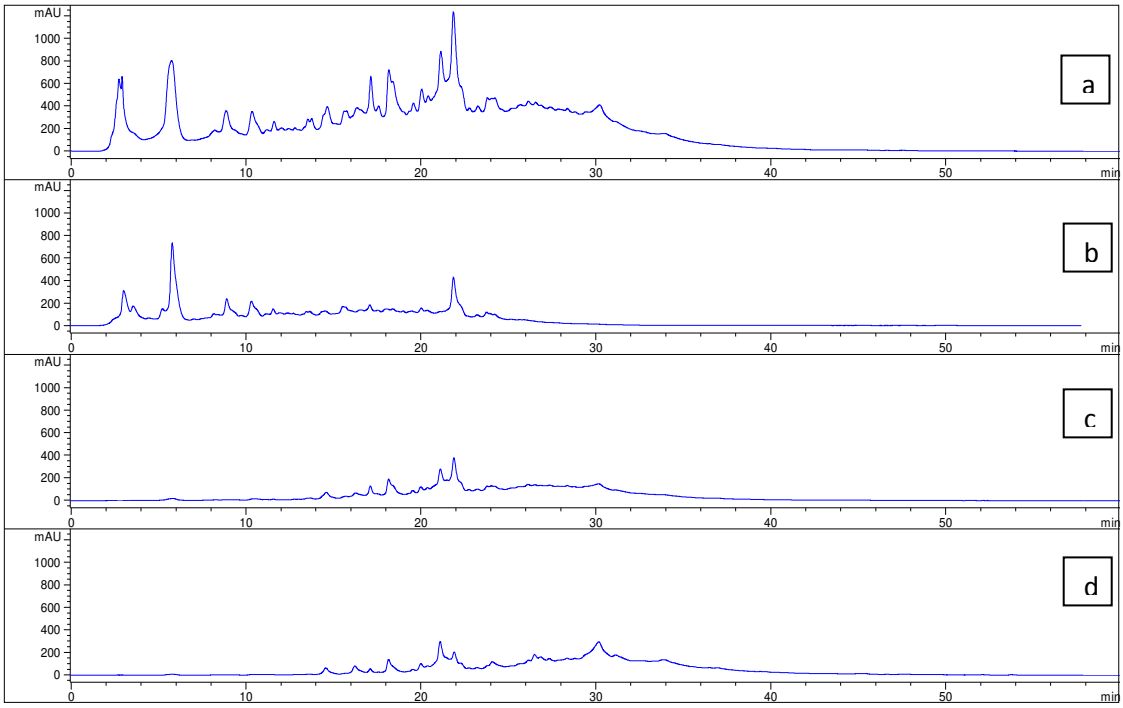

Figure 5.21. HPLC chromatograms of the crude olive leaf extract initial solution (a), water fraction (b) ,40% aqueous ethanol fraction (c) and 90% aqueous ethanol fraction (d) for flow velocity 367 cm/h.

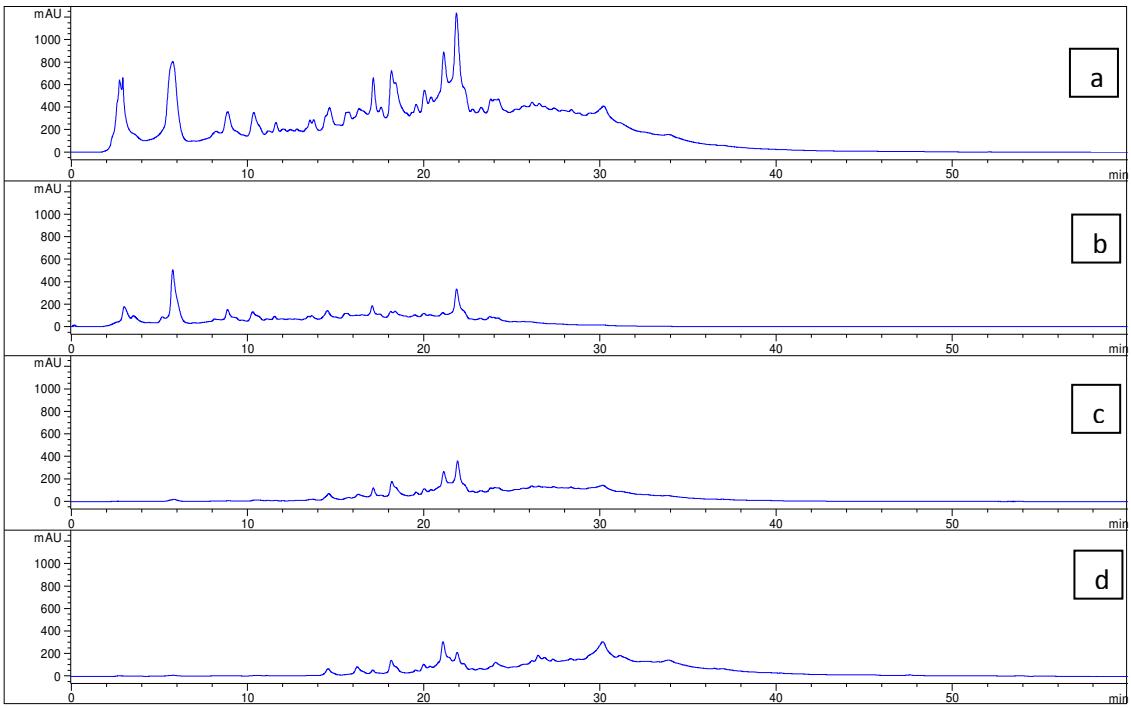

Figure 5.22. HPLC chromatograms of the crude olive leaf extract initial solution (a), water fraction (b), 40% aqueous ethanol fraction (c) and 90% aqueous ethanol fraction (d) for flow velocity 611 cm/h.

5.7. Total Phenol Analysis

In this study, antioxidant characteristics of phenolic compounds were determined, with the Folin-Ciocalteu method. When the flow velocity was increased, the experimental results showed that the total phenol contents of effluent fractions were decreased. The reason is that the residence time for oleuropein and rutin molecules in the XAD7HP was decreased, because the feed flow velocity was too fast. Oleuropein and rutin molecules didn't have sufficient time for diffusion in the pores into the active sites for adsorption. At last, the adsorbed amount decreased when the feed flow velocity increased. The total phenol content of initial feed stream and effluent stream were determined in terms of GAEq (mg/ml) and they are represented in Figure 5.23. The plot between the concentrations (mg/ml) versus absorbance were given in Appendix B.

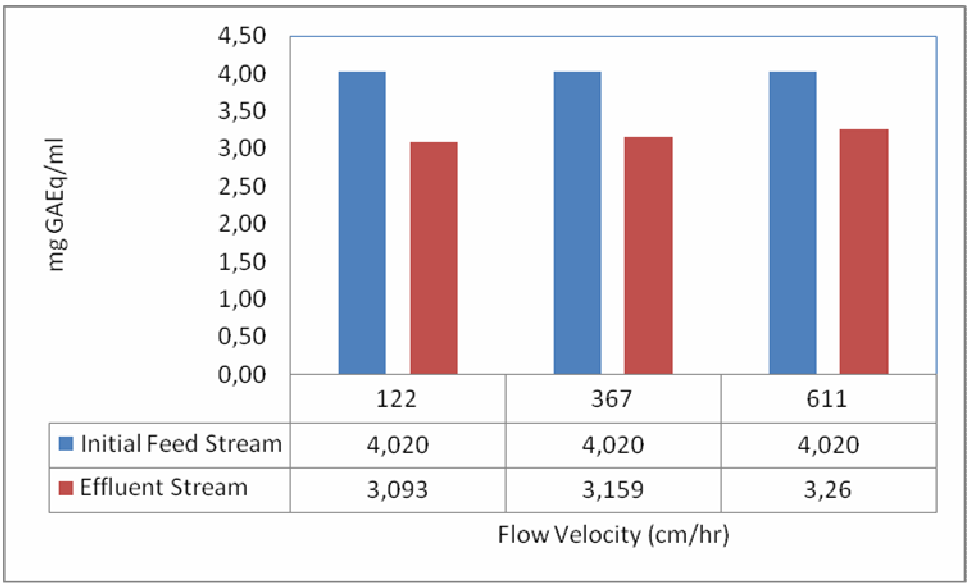

Figure 5.23. The total phenol content of initial feed stream and effluent streams.

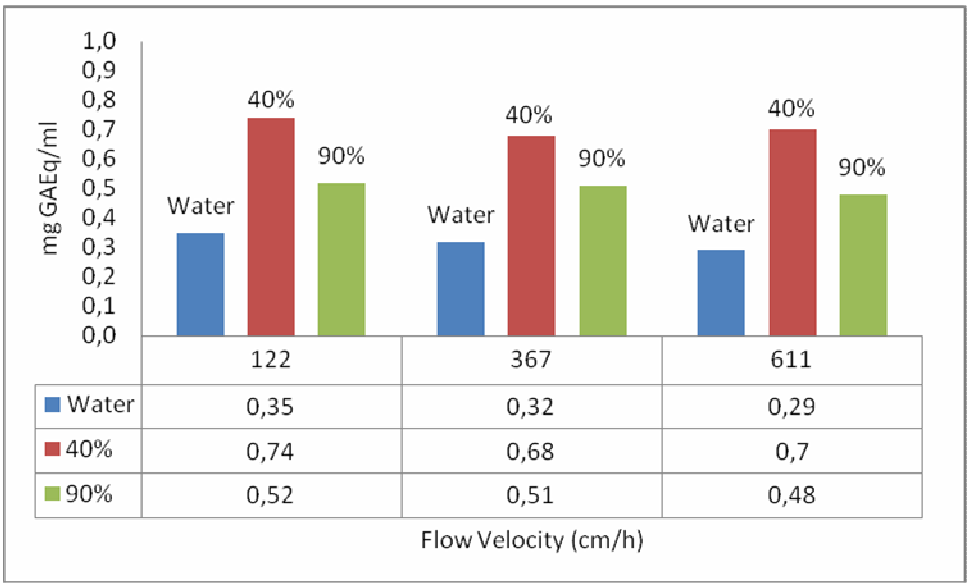

	122	367	611
Water	0,35	0,32	0,29
40%	0,74	0,68	0,7
90%	0,52	0,51	0,48

Figure 5.24. The total phenol content of water, 40% and 90% ethanol fractions.

The amount of desorbed total phenolic compounds varied in different flow velocities and eluents. The values ranged from 0.35 to 0.74 mgGAEq/ml for 122 cm/h, 0.32 to 0.68 mgGAEq/ml for 367 cm/h and 0.29 to 0.70 mgGAEq/ml for 611 cm/h. The highest total phenol capacity is measured at 40% aqueous ethanol solution, 90% aqueous ethanol solution and water, respectively. Figure 5.24. represents the adsorption efficiency at different flow velocities. It's clearly seen that if the eluent solutions were changed, different values of total phenolic compounds were obtained. It can be concluded that content of total phenolic compounds in water fraction is the smallest among other fractions.

5.8. Antioxidant Analysis

Antioxidant capacities of olive leaf crude extract and effluent fractions were analyzed in order to find the differences between these samples, shown in Figure 5.22. Afterwards water, 40 % and 90 % fractions were analyzed. The measured values were calculated in terms of TEAC (mg Trolox/ml). ABTS method was used to find the antioxidant capacity of olive leaf extract and isolated fractions. The plots between the concentration (mg/ml) versus % inhibition and time versus absorbance were given in Appendix C. All fractions exhibited antioxidant activity as they were to scavenge the

ABTS radical cation. Figure 5.25. gives the initial feed stream and effluent stream antioxidant capacities and Figure 5.26. gives the antioxidant capacities of the desorbed fractions.

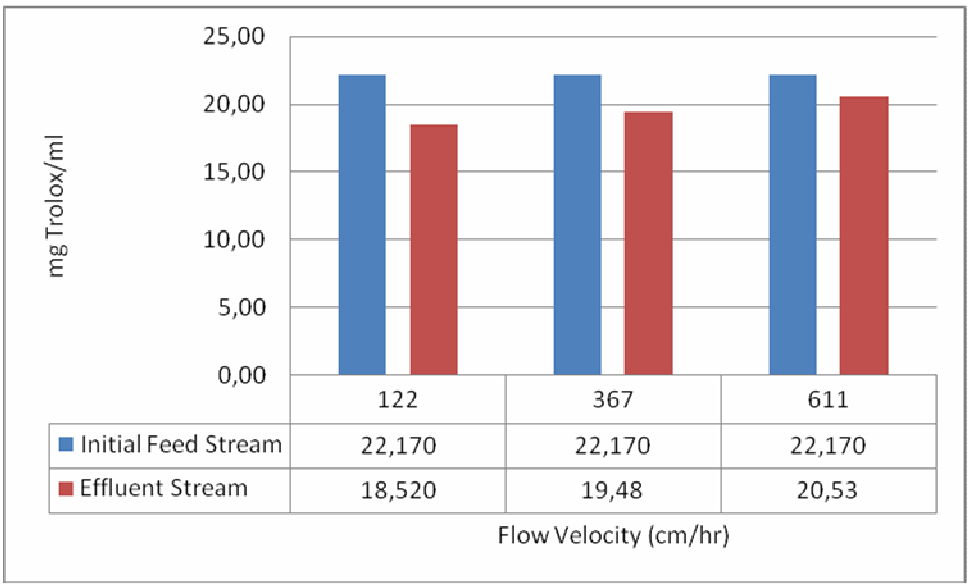

Figure 5.25. Antioxidant capacities of the initial feed stream and effluent streams.

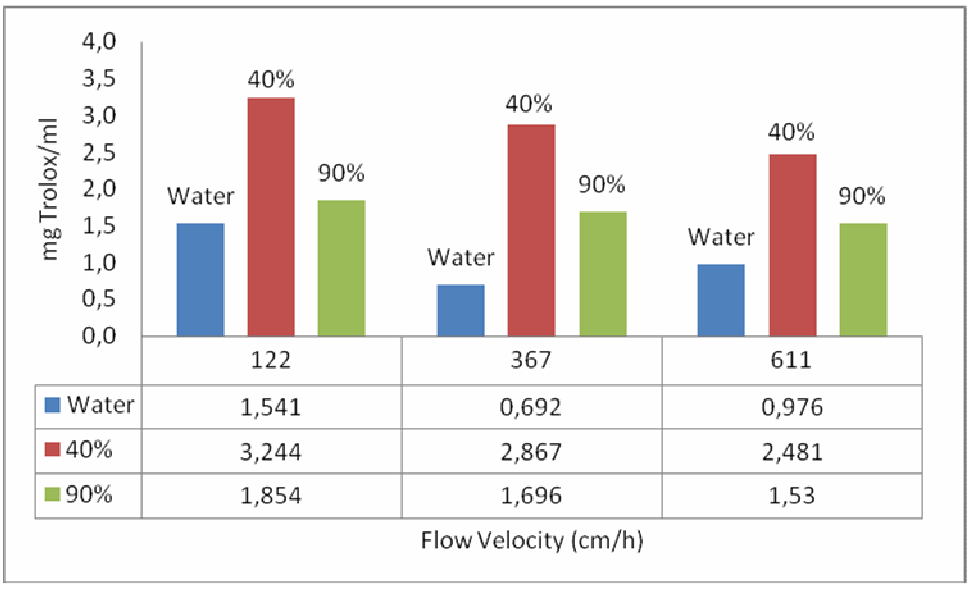

Figure 5.26. Antioxidant capacities of the desorb fractions.

Isolated fractions showed considerable antioxidant activity. Among them, 40 % aqueous ethanol fraction (rich in oleuropein and rutin) exhibited much higher antioxidant activity, compared to other fractions. On the other hand, water fraction and 90 % aqueous ethanol fraction were contrasted, it is clearly seen that 90% eluent showed higher antioxidant activity than that of water fraction.

CHAPTER 6

CONCLUSION

Amberlite XAD7HP macro porous resin was chosen as the adsorbent for use in this study as it has already found wide application in batch and column bed separations of flavonoids. Oleuropein and rutin were selectively adsorbed on XAD7HP resin, unlike other macro porous resins such as XAD4 and XAD16.

In the static study, whole adsorption completed within three hours. Moreover, the results indicated that adsorption capacity of an alcoholic solution with 10 % ethanol content was better than aqueous solution which contained no ethanol. Q_m for oleuropein, the maximum adsorption capacity of XAD7HP for 10 % alcohol was evaluated as 140.84 mg oleuropein/g XAD7HP and evaluated as 127.71 mg oleuropein/g XAD7HP for 0% alcohol. Q_m for rutin, the maximum adsorption capacity of XAD7HP for 10 % alcohol was determined as 34.13 mg rutin/g XAD7HP and determined as 30.74 rutin/g XAD7HP. The proximity of experimental data and the model supports the validity of the monolayer coverage.. The adsorption data of oleuropein and rutin on the XAD7HP resin fitted well to the Langmuir model while those on the XAD7HP resins were not fitted to the Freundlich model.

In the dynamic studies, the adsorption and desorption experiments were carried out on a glass column packed with XAD7HP resin. The column operating parameters including only feed flow velocity were explored for their effects on the adsorption performance of the column. Flow velocity of 122 cm/h, corresponding to 10 ml/min operated as a fixed bed while operation was in an expanded bed mode at 367 ml/min and 611 cm/h flow velocities, corresponding to 30 ml/min and 50 ml/min flow rates, respectively. The effectiveness of the packed (fixed) bed adsorption and the fluidized (expanded) bed adsorption was compared. The results revealed that the breakthrough occurred earlier when the feed flow velocities was increased.

In the elution step, elution program with 2,000 ml 0 %, 4,000 ml 40 % and 3,000 ml 90 % aqueous ethanol was used to achieve an efficient separation. For oleuropein, maximum recovery oleuropein ratio was obtained with 40% aqueous ethanol elution as a 69 %, even though maximum purity of oleuropein was achieved with water fraction as

a 26.42 %. For rutin, maximum recovery rutin ratio was obtained with 40% aqueous ethanol elution as a 46.72 %, even though maximum purity of rutin was achieved with water fraction as 5.58%.

Total phenol content and Antioxidant capacity of olive leaf crude extract and effluent fractions are analyzed. When the flow velocity was increased, the experimental results indicated that the total phenol contents of effluent fractions were decreased. The highest total phenol capacity was measured for 40 % aqueous ethanol solution (flow velocity of 122 cm/h), 0.74 GAEq (mg/ml solution), 90% aqueous ethanol solution (flow velocity of 122 cm/h), 0.52 GAEq (mg/ml solution) and water fraction (flow velocity of 122 cm/h), 0.35 GAEq (mg/ml solution), respectively. The highest antioxidant capacity was measured for 40% aqueous ethanol solution (flow velocity of 122 cm/h), 3.244 TEAC (mg Trolox/ml solution), 90% aqueous ethanol solution (flow velocity of 122 cm/h), 1.854 TEAC (mg Trolox/ml solution) and water fraction (flow velocity of 122 cm/h), 1.541 TEAC (mg Trolox/ml solution), respectively.

In this study, the primary objective was to develop the most economic strategy to purify flavonoids, rather than necessarily obtaining them at the highest recovery rate or purity. Considering its higher recovery ratio and purification time, fluidized bed adsorption is believed to represent a very considerable improvement for the scale-up of the extraction and purification of effective natural products from crude plant extracts. According to Table 5.7., in order to obtain a final product, the average process time for purification was 22.56 hour for the Fixed Bed-10, 7.5 hour for the Fluidized Bed-30 and 4.85 hour for the Fluidized Bed-50. Moreover, using the Fluidized Bed-30 process took about only 78.5% the amount of time that was used by the conventional fixed bed process. However, very few researches on the purification of natural products by fluidized bed adsorption technology from herbal and plant sources have been reported.

In this work, direct isolation of flavonoids from unclarified olive leaf extract solution using fluidized bed adsorption on Amberlite XAD7HP was evaluated. However, many factors, such as cost, operation time, waste treatment and process complexity need to be considered when calculating the overall performance. Depending on all these limitations, it can be regarded to be outstanding compared with fixed bed process. Fluidized bed adsorption process eliminated the need for the centrifugation and filtration steps, and consisted of direct loading and purification step, which significantly clarified the separation process.

This study proved that, when used to process crude olive leaf extracts, expanded bed adsorption, is a unique method that combines clarification, concentration and separation in a single step. It allows the processing of crude, particulate-containing feed stocks reduces the numbers of unit operations required and leads to lower operational cost and processing time than conventional fixed (packed) bed process but achieves approximately the same quality of final product.

Consequently, all these results suggest that fluidized (expanded) bed adsorption method is a promising for the recovery of natural products directly from crude plant materials.

REFERENCES

Ahmed A., Hasnain A., Akhtar S., Hussain A., Abaid-ullah, Yasin G.,Wahid A. and Mahmood S., 'Antioxidant enzymes as bio-markers for copper tolerance in safflower (Carthamus tinctorius L.)', *African Journal of Biotechnology,* **2010**, 9(33), 5441-5444.

Agarwal S., Wendorff J.H., Greiner A., 'Use of Electrospinning Technique for Biomedical Applications', *Polymer*, **2008**, 49, 5603-5621.

Agrawal A., Sahu K. K., Pandey B. D., 'A Comparative Adsorption Study of Copper on Various Industrial Solid Wastes', *American Institute of Chemical Engineers*, **2004**, 50, 2430-2438.

Alexander V. Pastukhov., Lidiya A. Levchenkoa and Anatoli P. Sadkova.'Spectroscopic study on binding of rutin to human serum albumin', *Journal of Molecular Structure*, **2007**, 842, 60-66.

Altıok E., Baycın D., Bayraktar O., Ulkü S., 'Isolation of Polyphenols From the Extracts of Olive Leaves (Olea europaea L.) by adsorption on silk fibroin', *Separation and Purification Technology*, **2008**, 62, 342–348.

Antolovich M., Prenzler P.D., 'Patsalides E., McDonald S. and Robards K., 'Methods for testing antioxidant activity', *The Analyst* , **2002** , 127, 183–198.

Andreadou I., Iliodromitis E. K., Mikros E., Constantinou M., Agalias A., Magiatis P., Skaltsounis A.L., Kamber E., Tsantili-Kakoulidou A. and Kremastinos D.T., 'The Olive Constituent Oleuropein Exhibits Anti-Ischemic, Antioxidative, and Hypolipidemic Effects in Anesthetized Rabbits', *The Journal of Nutrition*, **2006**, 136, 2213–2219.

Antioxidants-Health-Guide, Reactions initiated by free radicals in living organisms, http://www.antioxidants-health-guide.com/free-radicals.html, **2011**.

Barthels C. R., Kleinmann G., Korzon N.J. and Irish D.B., 'A Novel Ion-exchange Method for the Isolation of Streptomycin', *Chemical Engineering Progress*, **1958**, 54, 49-52.

Baycin D., Altıok E., Ülkü S., Bayraktar O., 'Adsorption of Olive Leaf (*Olea europaea L.*) Antioxidants on Silk Fibroin', *Journal of Agriculture and Food Chemistry*, **2007**, 55, 1227-1236.

Bazoti F.N., Gikas E.and Tsarbopoulosa A., 'Simultaneous quantii cation of oleuropein and its metabolites in rat plasma by liquid chromatography electrospray ionization tandem mass spectrometry', *Biomedical Chromatography*, **2010**, 24, 506-515.

Bucic–Kojic A., Planinic M., Tomas S., Bilic M., Velic D., 'Study of Solid–Liquid Extraction Kinetics of Total Polyphenols from Grape Seeds' *Journal of Food Engineering*, **2007**, 81, 236–242.

Benavente-Garcõa O., Castillo J., Lorente J., Ortuno A., Del Rio J.A., 'Antioxidant activity of phenolics extracted from Olea europaea L. Leaves', *Food Chemistry*, **2000**, 68, 457-462.

Belter P.A., Cunningham F.L. and Chen J.W., 'Development of a Recovery Process for Novobiocin', *Biotechnology and Bioengineering*, **1973**, 15, 533-549.

Chandrasekara A., Shahıdı F., 'Inhibitory Activities of Soluble and Bound Millet Seed Phenolics on Free Radicals and Reactive Oxygen Species', *Journal of Agricultural and Food Chemistry*, **2011**, 59, 428–436.

Chase H.A.,' Purification of proteins by adsorption chromatography in expanded beds', *Trends in Biotechnology*, **1994**, 12, 296-303.

Crozier A., Del Rio D., Clifford M.N., 'Bioavailability of Dietary Favonoids And Phenolic Compounds', *Molecular Aspects of Medicine*, **2010**, 31, 446-467.

De la Puerta R., Guttierrez V.R., Hoult J.S., 'Inhibition of Leukocyte 5-lipoxygenase by Phenolics from Virgin Olive Oil', Biochemical Pharmacology, **1999**, 57, 445-449.

Dixon R.A. and Pasinetti G.M., 'Flavonoids and Isoflavonoids: From Plant Biology to Agriculture and Neuroscience',*Plant Physiology*, **2010**, 154, 453-457.

Dow, Physical properties of Amberlite XAD4, XAD16 and XAD7HP adsorbents, http://www.dow.com/products/product_line_detail.page?productline, **2011**.

El-Gohary F.A., Badawy M.I., El-Khateeb M.A., El-Kalliny A.S., 'Integrated treatment of olive mill wastewater (OMW) by the combination of Fenton's reaction and anaerobic treatment' *Journal of Hazardous Materials*, **2009**, 162, 1536-1541.

El S.N. and Karakaya S., 'Olive Tree (Olea Europaea) Leaves: Potential Beneficial Efects on Human Health' Nutrition Reviews, **2009**, 67(11), 632-638.

Erbay Z., Icier F., 'Optimization of hot air drying of olive leaves using response surface methodology', *Journal of Food Engineering*, **2009**, 91, 533-541.

Ferrazzano G.F., Amato I., Ingenito A., De Natale A., Pollio A., 'Anti-cariogenic Effects of Polyphenols from Plant Stimulant Beverages (cocoa, coffee, tea)', *Fitoterapia*, **2009**,255–262.

Friedman M. and Jürgens H.S., 'Effect of pH on the Stability of Plant Phenolic Compounds', *Journal of Agricultural and Food Chemistry*, **2000**, 48, 2101-2110.

Furneri P.M., Marino A., Saija A., Uccella N., Giuseppe Bisignano G., 'In vitro antimycoplasmal activity of oleuropein', *International Journal of Antimicrobial Agents*, **2002**, 20, 293-296.

Gailliot F.P., Gleason C., Wilson J.J. and J. Zwarick J., 'Fluidised Bed Adsorption for Whole Broth Extraction', *Biotechnology Progress*, **1990**, 6, 370-375.

Geankoplis C.J., 'Transport Processes and Unit Operations', *PTR Prentice Hall*, **1993**.

Goulas V., Exarchou V., Troganis A.N., Psomiadou E., Fotsis T., Briasoulis E., Gerothanassis I.P., 'Phytochemicals in Olive-leaf Extracts And Their Antiproliferative Activity Against Cancer And Endothelial Cells', *Molecular Nutrition & Food Research*, **2009**, 53, 600-608.

Halliwell B., 'The wanderings of a free radical', *Free Radical Biology & Medicine*, **2009**, 46, 531–542.

Halliwell B., 'Free Radicals and Antioxidants – Quo Vadis?', *Trends in Pharmacological Sciences*, **2011**, 32(3), 125-130.

Han J., Talorete T.P., Yamada P., Isoda H., ' Anti-proliferative and apoptotic effects of oleuropein and hydroxytyrosol on human breast cancer MCF-7 cells', *Cytotechnology*, **2009**, 59, 45-53.

Healthfruit, Formation of free radicals, http://www.healthfruit.com/m/science/freeradicals, **2011**.

Ho C., Noryati I., Sulaiman S., Rosma A., 'In Vitro Antibacterial and Antioxidant Activities of Orthosiphon Stamineus Benth.Extracts Against Food-borne Bacteria', *Food Chemistry*, **2010**, 122, 1168–1172.

Hodgson J.M., Croft K.D., 'Tea Favonoids and Cardiovascular Health', Molecular Aspects of Medicine, **2010**, 31, 495-502.

Hsieh T., Wu J.M., 'Resveratrol: Biological and pharmaceutical properties as anticancer molecule', *BioFactors*, **2010**, 36(5), 360-369.

Huang J., Huang K., Liu S., Luo Q., Xu M., 'Adsorption Properties of Tea Polyphenols Onto Three Polymeric Adsorbents with Amide Group',*Journal of Colloid and Interface Science*, **2007**, 315, 407–414.

Huie C.W., 'A Review of Modern Sample-preparation Techniques for The Extraction and Analysis of Medicinal Plants', Analytical and Bioanalytical Chemistry, **2002**, 373, 23-30.

Janson J., Ryden L., 'Protein Purification: Principles, High-resolution Methods, and Applications, *John Wiley & Sons*, **1989**.

Kammerer D.R., Carle R., Stanley R.A. and Saleh Z.S., ' Pilot-scale Resin Adsorption As a Means to Recover and Fractionate Apple Polyphenols', *Journal of Agricultural and Food Chemistry*, **2010**, 58 (11), 6787-6796.

Kaneko K., 'Determination of pore size and pore size distribution 1. Adsorbents and catalysts', *Journal of Membrane Science,***1994**, 96, 59-89.

Kim Y., Choi Y., Park T., 'Hepatoprotective Effect of Oleuropein in Mice: Mechanisms Uncovered by Gene Expression Profiling', *Biotechnology Journal*, **2010**, 5(9), 950-960.

Kiritsakis K., Kontominas M.G., Kontogiorgis C., Hadjipavlou-Litina D., Moustakas A., A. Kiritsakis A., 'Composition and Antioxidant Activity of Olive Leaf Extracts from Greek Olive Cultivars', *Journal of the American Oil Chemists' Society*, **2010**, 87, 369-376.

Korukluglu M., Sahan Y., Yigit A., Ozer E.T. and Gücer S., 'Antibacterial Activity and Chemical Constitutions of Olea Europaea L. Leaf Extracts', *Journal of Food Processing and Preservation*, **2010**, 34, 383-396.

Kranz P., Adler P., Kunz B., 'Sorption of Citrus Flavour Compounds on XAD-7HP Resin During The Debittering of Grapefruit Juice' *International Journal of Food Science and Technology*, **2011**, 46, 30–36.

Kremastinos D.T., 'Olive and Oleuropein', *Hellenic Journal of Cardiology*, **2008**, 49, 295-296.

Kunii D. and Levenspiel O., 'Fluidization Engineering', *John Wiley & Sons, New York*, **1969**.

Kulprathipanja S., 'Reactive separation processes',*Taylor and Francis*, **2002**.

Lazarus S.A., Hammerstone J.F., Adamson G.E. and Schmitz H.H., ' High-performance liquid chromatography/mass spectrometry analysis of proanthocyanidins in food and beverages' *Methods in Enzymology*, **2001**, 335, 46-57.

Lee O., Lee B., 'Antioxidant and antimicrobial activities of individual and combined phenolics in Olea europaea leaf extract', *Bioresource Technology*, **2010**, 101, 3751-3754.

Lee-Huang S., Huang P.L., Zhang D., Lee J.W., Sun J.B.Y., Chang Y., Zhang J., Huang P.L., 'Discovery of Small-Molecule HIV-1 Fusion and Integrase Inhibitors Oleuropein and Hydroxytyrosol: Part I. Integrase Inhibition',*Biochemical and Biophysical Research Communications*, **2007**, 354, 872-878.

Lee-Huang S., Li Zhang., Huang P.L., Chang Y., and Huangd P.L., 'Anti-HIV Activity of Olive Leaf Extract (OLE) and Modulation of Host Cell Gene Expression by HIV-1 Infection and OLE Treatment' *Biochemical and Biophysical Research Communications*, **2003**, 307, 1029-1037.

Leonardis A., Aretini A., Alfano G., 'Macciola V., Ranalli G., 'Isolation of a hydroxytyrosol-rich extract from olive leaves (Olea Europaea L.) and evaluation of its antioxidant properties and bioactivity', *European Food Research and Technology*, **2008**, 226, 653-659.

Li J., Chase H.A., 'Use of Expanded Bed Adsorption to Purify Flavonoids from Ginkgo Biloba L.' Journal of Chromatography A, **2009**, 1216, 8759–8770.

Liu X., Xu Z., Gao Y., Yang B., Zhao J. and Wang L., 'Adsorption Characteristics of Anthocyanins from Purple-fleshed Potato (Solanum tuberosum Jasim) Extract on Macroporous Resins', International Journal of Food Engineering, **2007**, 3-4.

Liu R.H., 'Potential Synergy of Phytochemicals in Cancer Prevention: Mechanism of Action', *The Journal of nutrition*, **2004** , 134, 3479S-3485S.

Lua T., Finkel T., 'Free radicals and senescence', *Experimental Cell Research*, **2008**, 314(9), 1918- 1922.

Madhavi D.L., Deshpande S.S and Salunkhe D.K., 'Food Antioxidants, Technological, Toxicological and Health Perspectives',*Marcel Dekker* ,**1996**.

Mahoney J.R.M., Graf E., 'Role of Alpha-Tocopherol, Ascorbic Acid, Citric Acidand EDTA as Oxidants in Model Systems', *Journal of Food Science*, **1986,** 51(5), 1293-1296.

Malek A. and Farooq S., 'Kinetics of Hydrocarbon Adsorption on Activated Carbon and Silica Gel', *Biochemical and Biophysical Research Communications*, **1997**, 354(4), 872-878.

Markin D., Duek L. and Berdicevsky I., 'In vitro antimicrobial activity of olive leaves Antimikrobielle Wirksamkeit von Olivenblattern in vitro', *Mycoses*, **2003**, 46, 132-136.

Micol V., Caturla N., Perez-Fons L., Mas V., Perez L., Estepa A., 'The olive leaf extract exhibits antiviral activity against viral haemorrhagic septicaemia rhabdovirus (VHSV)', *Antiviral Research*, **2005**, 66, 129-136.

Michels A.J., Hagen T.M., and Frei B., 'A New Twist on an Old Vitamin: Human Polymorphisms in The Gene Encoding The Sodium-Dependent Vitamin C Transporter 1', *The American Journal of Clinical Nutrition*, **2010**, 92, 271-272.

Montgomery J.M., 'Water Treatment: Principles and Design, 2nd Edition', *John Wiley & Sons*, **1985**.

Nenadis N., Vervoort J., Boeren S., Tsimidou M.Z., 'Syringa Oblata Lindl Var. Alba as A Source of Oleuropein and Related Compounds', *Journal of the Science of Food and Agriculture,* **2007**, 87, 160–166.

Omar S.H., 'Cardioprotective and neuroprotective roles of oleuropein in olive', *Saudi Pharmaceutical Journal*, **2010**, 18, 111-121.

Omar S.H., 'Oleuropein in Olive and its Pharmacological Effects', *Scientia Pharmaceutica*, **2010**, 78, 133-154.

Pietta P.G., 'Flavonoids as Antioxidants', *Journal of Natural Products*, **2000**, 63, 1035-1042.

Pokorny J., 'Natural antioxidants for food use', *Trends in Food Science & Technology*, **1991**, 2, 223-227.

Puertaa R., Domíngueza E.M., Ruíz-Gutíerrezb V., Flavill J.A., Hoult J.R.S., 'Effects of Virgin Olive Oil Phenolics on Scavenging of Reactive Nitrogen Species and Upon Nitrergic Neurotransmission', *Life Sciences*, **2001**, 69, 1213–1222.

Rajalakshmi, D.; Narasimhan, S., 'Food Antioxidants: Sources and Methods of Evaluation. In Food Antioxidants: Technological,Toxicological and Health Perspecties; Madhavi, D. L., Deshpande, S. S., Salunkhe, D. K., Eds.; *Marcel Dekker: New York*, **1996**; 65-158.

Rao A.V., Rao L.G.,'Carotenoids and human health', *Pharmacological Research*, **2007**, 55, 207–216.

Rice-Evans C.A., Miller N.J. and Paganga G., 'Antioxidant properties of phenolic Compounas' *Trends in Plant Science*, **1997**, 2(4), 152-159.

Rigacci S., Guidotti V., Bucciantini M., Parri M., Nediani C., Cerbai E., Stefani M., Berti A.,'Oleuropein aglycon prevents cytotoxic amyloid aggregation of human amylin', Journal of Nutritional Biochemistry, **2010**, 21, 726-735.

Rodriguez-Amaya D.B., 'Quantitative Analysis, in Vitro Assessment of Bioavailability and Antioxidant Activity of Food Carotenoids—A Review', *Journal of Food Composition and Analysis,* **2010**, 23, 726–740.

Russo M., Spagnuolo C., Tedesco I. and Russo G.L., 'Phytochemicals in Cancer Prevention and Therapy: Truth or Dare?', *Toxins*, **2010**, 2, 517-551.

Rouquerol J., Rouquerol F., Sing K.S.W., 'Adsorption by Powders and Porous Solids', *Academic Press, New York*, **1999**.

Ryan D., Robards K., ' Changes in phenolic content of olive during maturation', *International Journal of Food Science and Technology*, **1999**, 34, 265-274.

Scordino M., Di Mauro A., Passerini A. And Maccarone E., 'Adsorption of Flavonoids on Resins: Cyanidin 3-Glucoside', *Journal of Agricultural and Food Chemistry*, **2004**, 52, 1965-1972.

Seet R.C.S., Lee C.J., Lima E.C.H., Tan J.J.H., Quek A.M.L.,Chong W., Looi W., Huang S., Wang H.,Chan Y., Halliwell B., 'Oxidative Damage in Parkinson Disease: Measurement Using Accurate Biomarkers', *Free Radical Biology and Medicine*, **2010**, 48, 560–566.

Sharma A.T., Mitkare S. S., Moon R.S., 'Multicomponent Herbal Therapy: A Review', *International Journal of Pharmaceutical Sciences Review and Research*, **2011**, 6(2), 185-187.

Sharma V., Zhang C., Pasinetti G.M. and Dixon R.A., 'Fractionation of Grape Seed Proanthocyanidins for Bioactivity Assessment', *The Biological Activity of Phytochemicals*, **2011**, 41, 33-46.

Shılın N.S., 'Oxidative Mechanisms In Haematological Malignancies', *Indian Journal of Medical and Paediatric Oncology* , **2011**, 22, 21-23.

Silva E.M., Pompeu D.R., Larondelle Y., Rogez H., 'Optimisation of The Adsorption of Polyphenols From Inga Edulis Leaves on Macroporous Resins Using an Experimental Design Methodology', *Separation and Purification Technology*, **2007**, 53, 274–280.

Smirnoff N., 'Antioxidants and reactive oxygen species in plants' *Blackwell Publishing*, **2005.**

Smith M.A., Zhu X., Tabaton M., Liu G., McKeel D.W., Cohen M.L., Wang X., Siedlak S.L., Dwyer B.E., Hayashi T., Nakamura M., Nunomura A., Perry G., 'Increased Iron and Free Radical Generation in Preclinical Alzheimer Disease and Mild Cognitive Impairment', *Journal of Alzheimer's Disease*, **2010**, 19(1), 363-372.

Soler-Rivas C., Espin J.C. and Wichers H.J., 'Oleuropein and related compounds', *Journal of the Science of Food and Agriculture*, **2000**, 80, 1013-1023.

SpecialChem, Antioxidant Families, http://www.specialchem4adhesives.com/tc/antioxidants/index.aspx?id=families, **2011**.

Stahl W., 'Flavonoid-Rich Nutrients for the Skin', *Nutrition for Healthy Skin*, **2011**, 2, 85-90.

Subhashini R., Mahadeva R.U.S., Sumathi P. and Gunalan G., 'A Comparative Phytochemical Analysis of Cocoa and Green Tea', *Indian Journal of Science and Technology*, **2010**, 3, 188-192.

Sudjanaa A.N., D'Orazio C., Ryan V., Rasool N., Ng J., Islam N., Rileya T.V., Hammera K.A., 'Antimicrobial activity of commercial *Olea europaea* (olive) leaf extract', *International Journal of Antimicrobial Agents*, **2009**, 33, 461-463.

Suzuki M., 'Adsorption Engineering', *Elsevier, Tokyo*, **1990**.

Süntar I.P., Akkol E.K., Yılmazer D., Baykal T., Kırmızıbekmez H., Alper M., Yesilada E., 'Investigations on The in Vivo Wound Healing Potential of Hypericum Perforatum L.', *Journal of Ethnopharmacology*, **2010**, 127, 468-477.

Svilaas A., Sakhi A.K., Andersen L.F., Svilaas T., Ström E.C., Jacobs D.R., Ose J.L., and Blomhoff R., 'Intakes of Antioxidants in Coffee, Wine, and Vegetables Are Correlated with Plasma Carotenoids in Humans', *The Journal of Nutrition*, **2004**, 134, 562-567.

Telang S., Clem A.L., Eaton J.W and Chesney J., 'Depletion of Ascorbic Acid Restricts Angiogenesis and Retards Tumor Growth in a Mouse Model', *Neoplasia*, **2007**, 47-56.

Tu P.F., Jia C.Q. and Zhang, H.Q., 'Application of Macroporous Adsorption Resins to Study and Production of TCM New Drugs', *World Science and Technology*, **2004**,6(3), 22-28.

Tung Y. and Chang S., 'Inhibition of Xanthine Oxidase by Acacia confusa Extracts and Their Phytochemicals', *Journal of Agricultural and Food Chemistry,* **2010**, 58, 781–786.

Tutornext, Characteristics of Physical and Chemical Adsorption, http://www.tutornext.com/characteristics-physical-chemical-adsorption/2614, **2011**.

Vaquero M.J.R., Serravalle L.R.T., Manca de Nadra M.C., Strasser de Saad A.M., 'Antioxidant Capacity and Antibacterial Activity of Phenolic Compounds from Argentinean Herbs Infusions' *Food Control*, **2010**, 21, 779–785.

Visioli F., Poli A. and Galli C., 'Antioxidant and Other Biological Activities of Phenols from Olives and Olive Oil' *Medicinal Research Reviews*, **2002**, 49, 65-75.

Voutilainen S., Nurmi T., Mursu J., and Rissanen T.H., 'Carotenoids and cardiovascular health', *American Journal of Clinical Nutrition*, **2006,** 83**,** 1265-1271.

Warren L. M., Julian C. S. and Peter H., 'Unit Operations of Chemical Engineering', *Mcgraw Hill*,7th Edition, **2005**.

Wang, J.F., Xue D. and Cang, J., 'The Application of Separation and Purification of Effective Elements in Chinese Herbal Medicine by Macroporous Adsorptive Resin', *Hunan Guiding Journal of TCMP*, **2001**, 7(3), 125-126.

Wiseman H., Halliwell B., 'Damage to DNA by reactive oxygen and nitrogen species: role in inflammatory disease and progression to cancer', *Biochemical Journal*, **1996**, 313, 17-29

Xin S., Kejun Z., Xianjun S., Hongbing L., Yu S., Long-Xi Y., 'Scavenging Effects of Plant Antioxidants on Gas-Phase Free Radicals in Mainstream Cigarette Smoke' *Analytical Letters*, **2010**, 43, 446-454.

Xuan Liu., Zhenghong X., Yangxiang G., Bin Y., Jian Z. and Lijun W., 'Adsorption Characteristics of Anthocyanins from Purple-fleshed Potato (Solanum tuberosum Jasim) Extract on Macroporous Resins', International Journal of Food Engineering, **2007**, 3, 1-16.

Yamada K., Ogawa H., Hara A., Yoshida Y., Yonezawaa Y., Karibe K., Nghia V.B., Yoshimura H., Yamamoto Y., Yamada M., Kuniyasu Nakamura K., Imai K., 'Mechanism of the antiviral effect of hydroxytyrosol on influenza virus appears to involve morphological change of the virus', *Antiviral Research*, **2009**, 83, 35-44.

Yang J., Martinson T.E., Liu R.H., 'Phytochemical profiles and antioxidant activities of wine grapes', *Food Chemistry*, **2009** , 116, 332–339.

Yang R.T., 'Adsorbents:Fundamentals and Applıcations', *John Wiley & Sons*, **2003**.

Ye J., Wang L., Chen H., Dong J., Lu J., Zheng X., Wu M. and Liang Y., 'Preparation of Tea Catechins Using Polyamide' *Journal of Bioscience and Bioengineering*, **2010**, 111, 232-236.

Zhaoa G., Yinb Z., Donga J., 'Antiviral Efficacy Against Hepatitis B Virus Replication of Oleuropein Isolated from Jasminum Officinale L. Var. Grandiflorum', *Journal of Ethnopharmacology*, **2009**, 125, 265-268.

APPENDIX A

CALIBRATIONS CURVES OF OLEUROPEIN AND RUTIN

Calibration methods were required to evaluate the quantity of oleuropein and rutin in olive leaf extract. External calibration methods were applied in this study. In this calibration, a stock solution of rutin and oleuropein were prepared. Oleuropein was dissolved in 50 % acetonitrile-water solution but rutin was dissolved in 70 % ethanol-water solution. Each concentration was injected to HPLC. The amounts of oleuropein and rutin were calculated using peak areas obtained from HPLC analysis results. Construction of a calibration curve and determination of its linear region are very significant parts of this study because the linear calibration curve should be used to determine the oleuropein amount in an unknown solution.

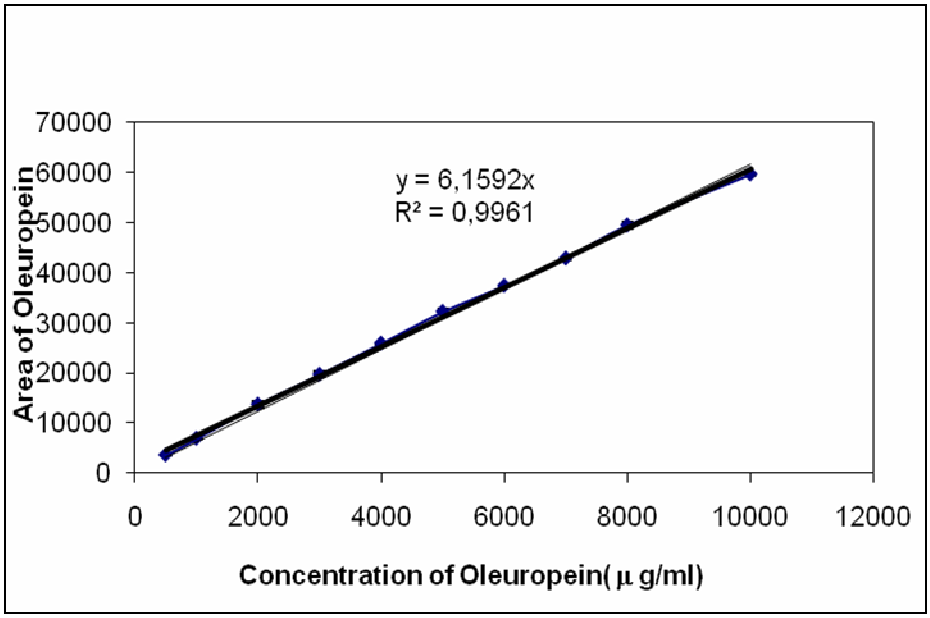

Figure A1. Calibration Curve of Oleuropein.

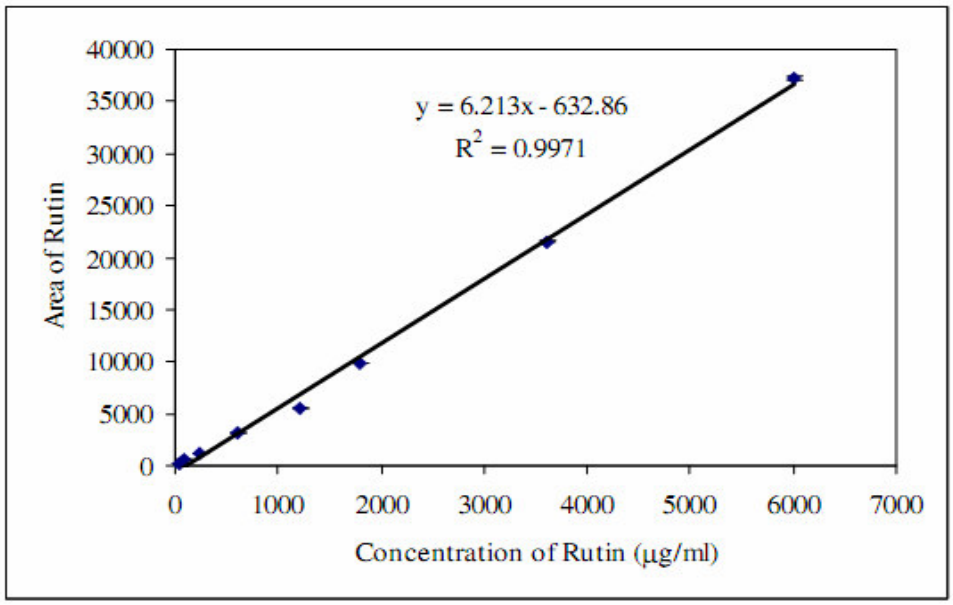

Figure A2. Calibration Curve of Rutin
(Source: Bayçın et al., 2006).

APPENDIX B

CALIBRATION CURVE OF GALLIC ACID

0.5 mg/ml stock standard of gallic acid solution was prepared. Then, this stock solution was prepared by dissolving 250 mg of dry gallic acid in 10 ml of ethanol and diluting to 500 ml with distilled water. The solution was kept at 4 ºC. The standard concentrations that were prepared for calibration curve were 0.01-0.02-0.03-0.04-0.05-0.06-0.07-0.08 and 0.09 mg/ml. Calibration curve of Gallic acid was shown in Figure C1.

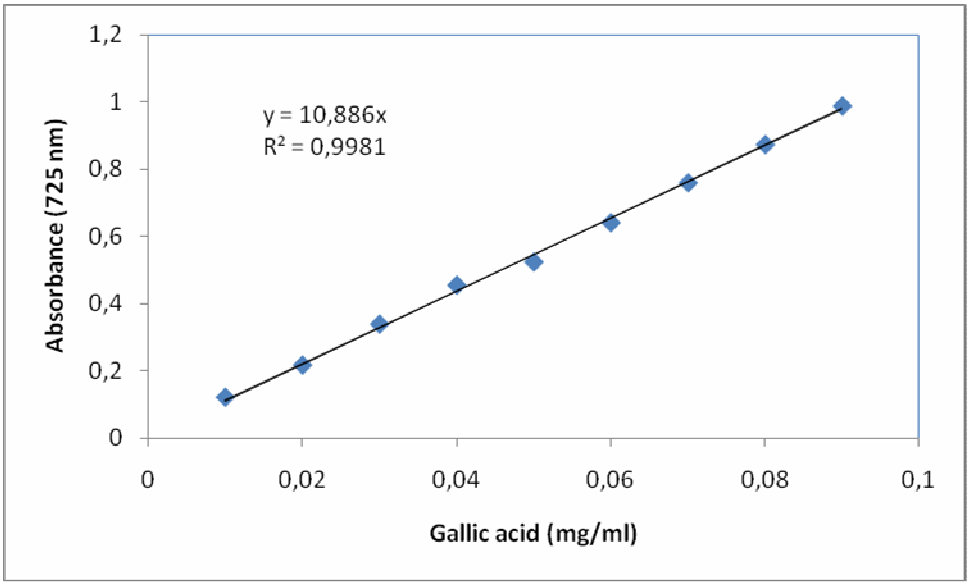

Figure B1. Calibration curve of Gallic acid.

Calculation of Total Phenol Contents in Gallic acid Equivalent (GAEq):

Absorbance value of sample was 0.537. Dilution factor was obtained 50 for this experiment. Solid-liquid ratio of the solution is 0.05 (1/20)

GAEq (mg GA/g sample) = [A*DF*$V_{solvent}$ (ml)]/ [slope of calibration curve*sample amount (g)]

49.32 GAEq (mg GA/g sample) was obtained.

Where,

GA: gallic acid

A: absorbance of working solution

V: solvent volume for dissolving extract

Sample amount: weighted extract

DF: dilution factor

APPENDIX C

CALIBRATION CURVE OF TROLOX AND AND SAMPLE CALCULATION

Total antioxidant activity of the samples was determined by using improved ABTS radical cation decolorization assay. This radical cation exhibit inhibition. This inhibition can be monitored as a decrease in the absorbance values at 734 nm in UV-Visible Spectrophotometer. In the first place, the absorbance of $ABTS^+$ radical cation solutions was measured. It was adjusted to absorbance of 0.7 ± 0.02.Next, sample solution was added to $ABTS^+$ radical cation solution and the absorbance values were taken at each 1 minute during 6 minutes. Average of these 6 data was investigated and its decrease from the absorbance value of $ABTS^+$ radical cation solution was calculated in order to find out inhibition.

After obtain the percentage inhibition value, calibration curve for trolox was used to find the antioxidant capacity for plant extract (Figure B1).

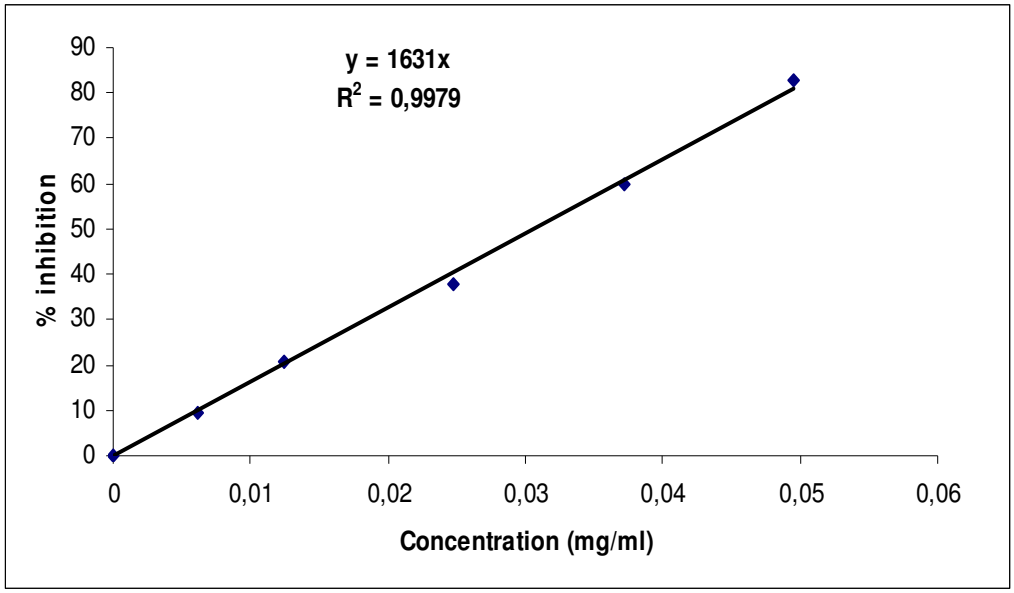

Figure C1. Calibration Curve for Trolox.

Sample Calculation for percentage inhibition:

Initial absorbance value of $ABTS^{+}$ radical cation was 0.712. The six measured absorbance values after adding the olive leaf extract solution were, 0.515, 0,427, 0.396, 0.382, 0.368 and 0.355. The averages of these values were calculated as 0.407. The inhibition percentage is;

[(Initial absorbance value – Average absorbance value) / Initial absorbance value]*100

= 42.83 %.

The inhibition percentage of samples were measured at least three different Concentrations (10-20-30 µl) and at three replicates Figure B2-B10)

Antioxidant Capacity Curves:

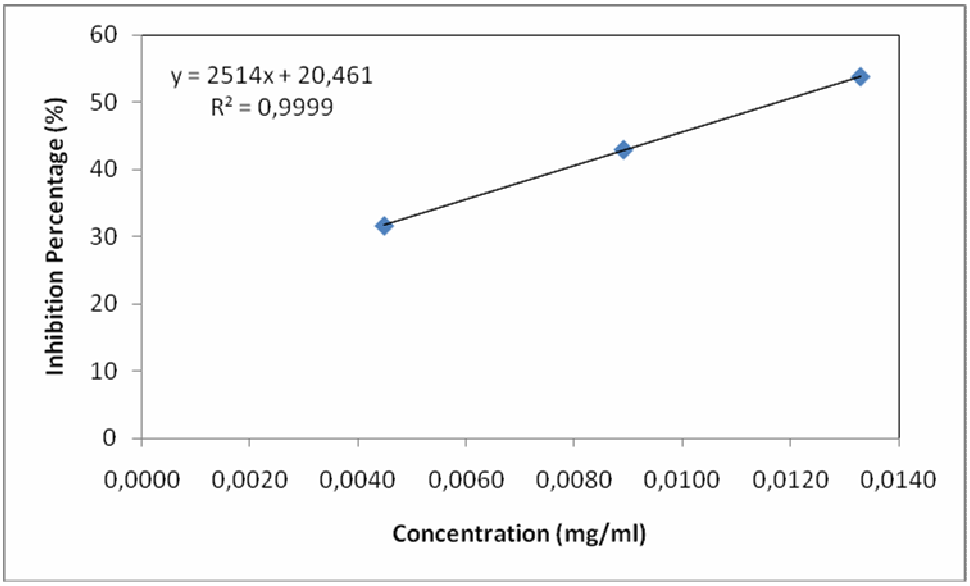

Figure C2. Inhibition percentage of water fraction of desorption study at consist super velocity of 122cm/h.

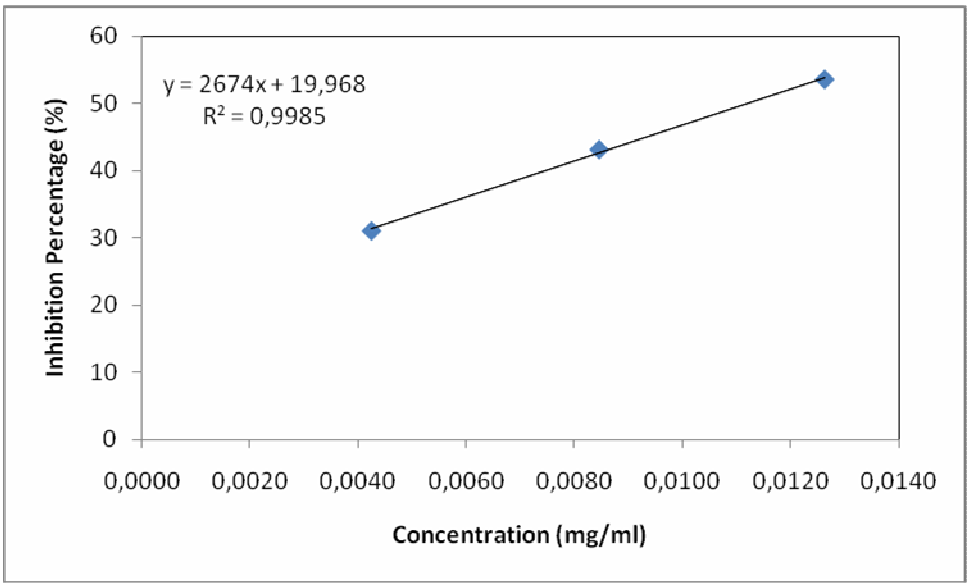

Figure C3. Inhibition percentage of 40 % aqueous alcohol elution fraction for super velocity of 122 cm/h.

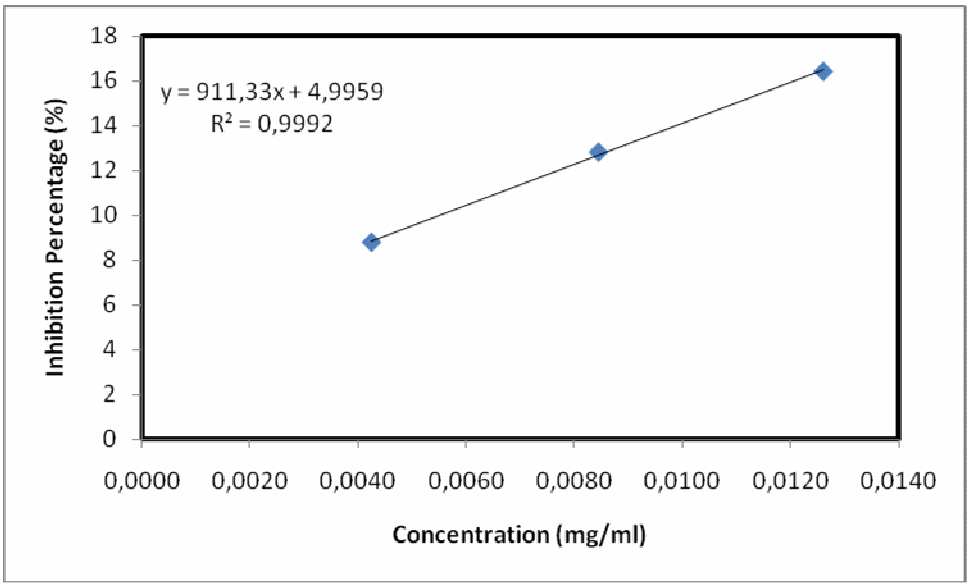

Figure C4. Inhibition percentage of 90 % aqueous alcohol elution fraction for super velocity of 122 cm/h.

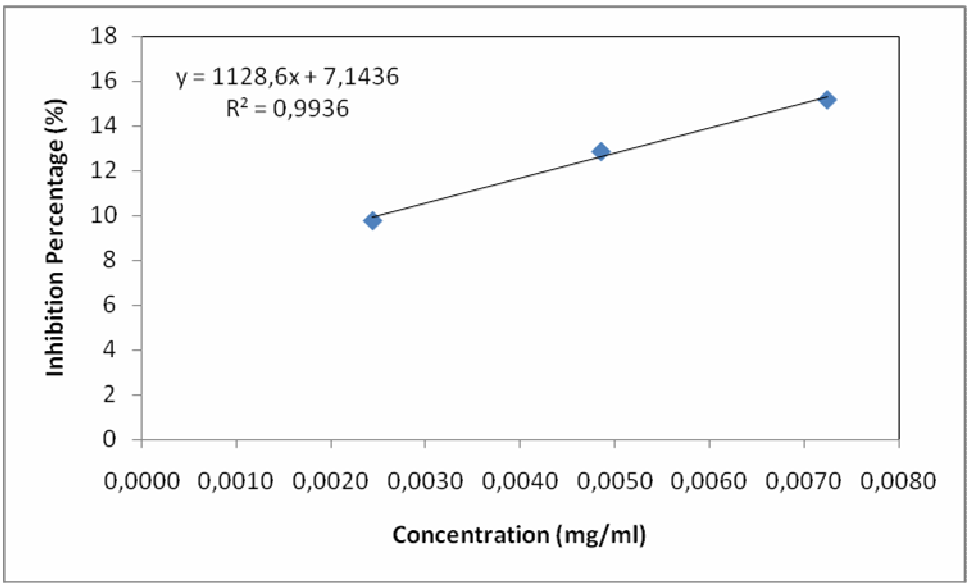

Figure C5. Inhibition percentage of water elution fraction for super velocity of 367 cm/h.

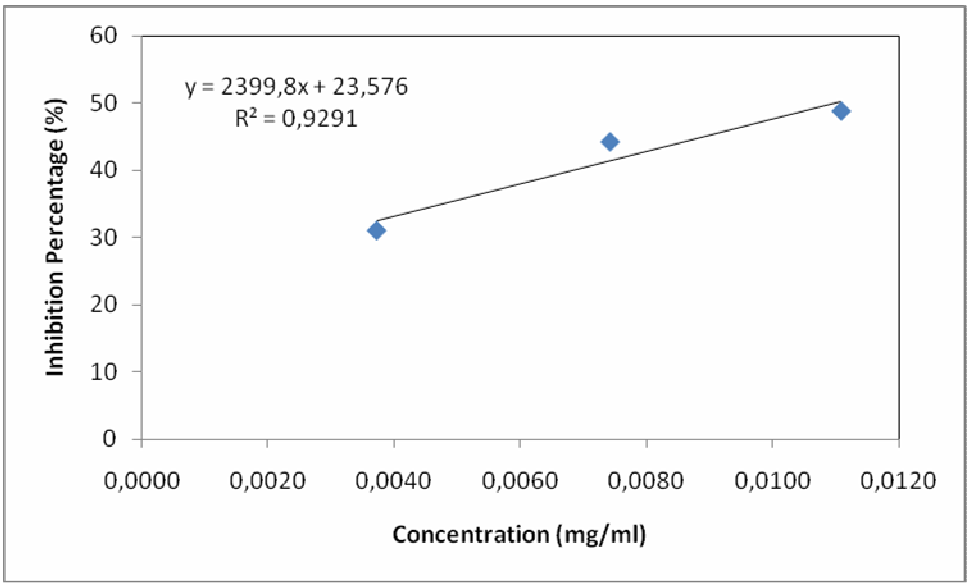

Figure C6. Inhibition percentage of 40 % aqueous alcohol elution fraction for super velocity of 367 cm/h.

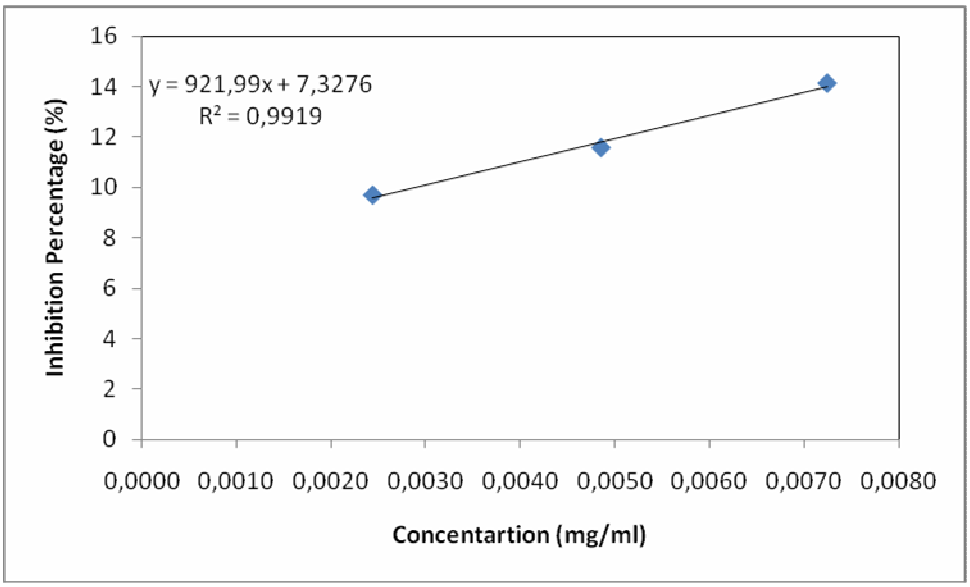

Figure C7. Inhibition percentage of 90 % aqueous alcohol elution fraction for super velocity of 367 cm/h.

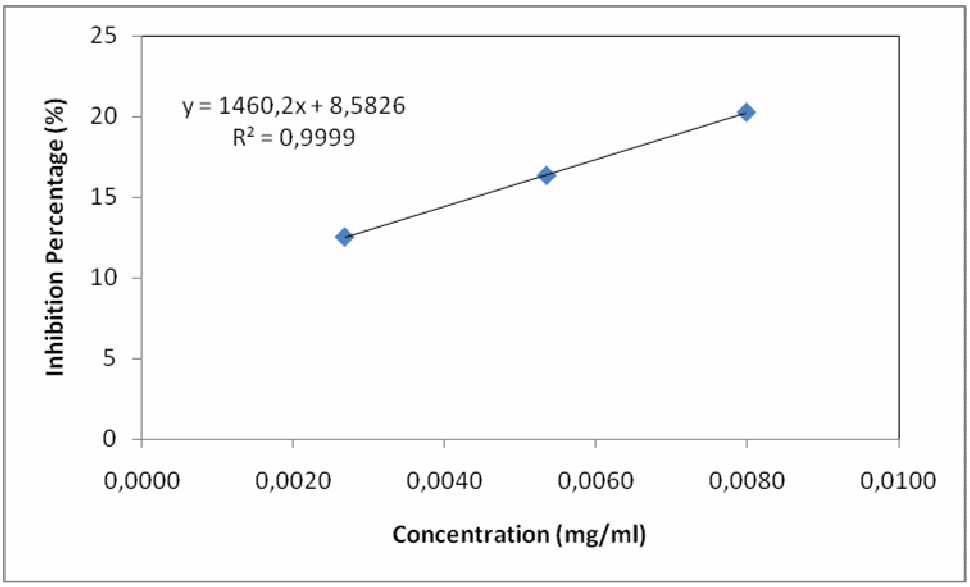

Figure C8. Inhibition percentage of water elution fraction for super velocity of 611 cm/h.

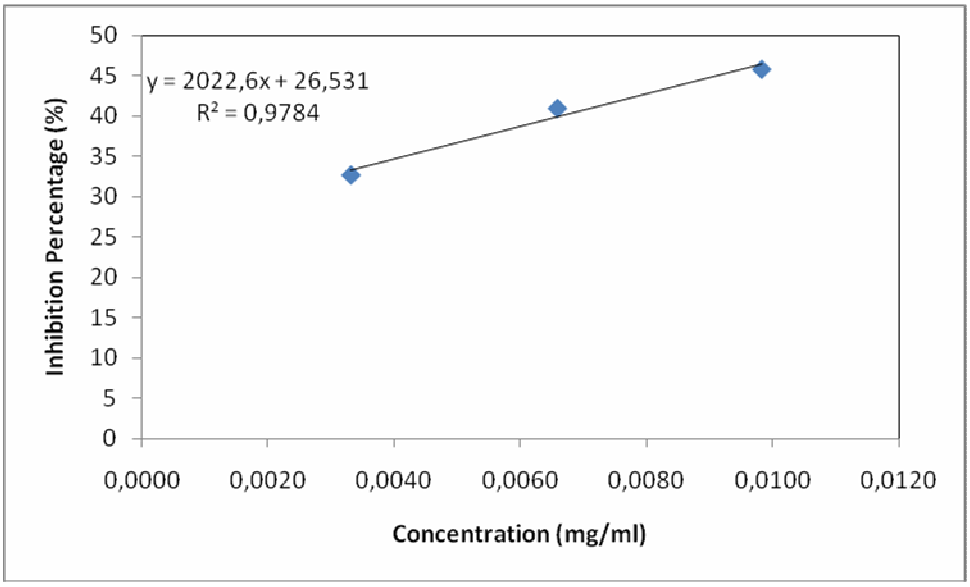

Figure C9. Inhibition percentage of 40% aqueous alcohol elution fraction for super velocity of 611 cm/h.

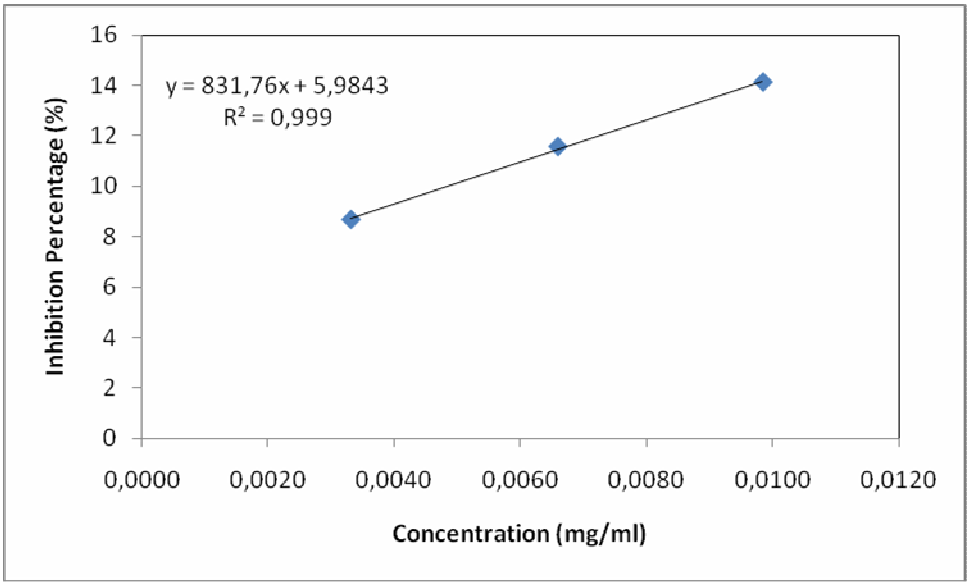

Figure C10. Inhibition percentage of 90% aqueous alcohol elution fraction for Super velocity of 611 cm/h.

APPENDIX D

CALCULATION OF STATIC EXPERIMENTS

XAD7HP was used for the removal of oleuropein and rutin from the crude olive leaf extract. The olive leaf liquid extract was analyzed in HPLC before and after adsorption in order to find out the concentration of oleuropein and rutin and the adsorbed amounts on XAD7HP were calculated from the following equation.

$$Q_c = (C_i - C_e)\frac{V}{W}$$

Where,

Q_e = Equilibrium solute phase concentration, mg polyphenol/g silk fibroin

C_i = Initial liquid phase concentration, mg polyphenol/ml olive leaf extract

C_e = Equilibrium solute concentration in the aqueous phase, mg polyphenols/ml olive leaf extract

V = Volume of liquid phase, ml

W = Mass of the adsorbent, g

When adsorption was performed at room temperature, the solid-liquid ratio was set to 0.05, the initial concentration and equilibrium concentration were determined as 9.94 mg/ml and 5 mg/ml, respectively by using calibration curves. Then the adsorbed amount can be calculated as follows.

Q_e = 98.8 mg oleuropein/ g XAD7HP

APPENDIX E

CALCULATION OF DYNAMIC EXPERIMENTS

Concentrate mass ratio (%) = (fractional mass of concentrate / total mass of concentrate) × 100%.

Recovery ratio (%) = (fractional mass of oleuropein or rutin / total mass of oleuropein or rutin in solution) × 100%.

Purity of oleuropein or rutin (%) = (fractional mass of oleuropein or rutin / fractional mass of concentrate) × 100%.

Concentrate mass ratio (%) = (fractional mass of concentrate / total mass of concentrate) × 100%.

Recovery ratio of oleuropein or rutin (%) = (fractional mass of oleuropein or rutin / total mass of oleuropein or rutin) × 100%.

Purity of oleuropein or rutin (%) = (concentration of oleuropein or rutin ÷concentration of impurities) ×100%.

Overall recovery ratio of oleuropein or rutin (%) = mass of oleuropein or rutin in elution fractions ÷ (concentration of oleuropein or rutin in feedstock × volume of feedstock loaded) ×100%.